CHARACTERIZATION AND MEASUREMENT OF THE HIV-1 LATENT RESERVOIR USING SINGLE GENOME ANALYSIS AND DROPLET DIGITAL PCR

By

Katherine Michelle Bruner

A dissertation submitted to Johns Hopkins University in conformity with the requirements for the degree of Doctor of Philosophy

Baltimore, MD

March 2017

Abstract

Although antiretroviral therapy (ART) suppresses viral replication to clinically undetectable levels, HIV-1 persists in $CD4^+$ T cells in a latent form not targeted by the immune system or ART (Chun et al., 1997b; Finzi et al., 1997; Ruelas and Greene, 2013; Siliciano et al., 2003; Wong et al., 1997a). This latent reservoir is a major barrier to cure. Many individuals initiate ART during chronic infection, and in this setting, most proviruses are defective (Ho et al., 2013a). However, the dynamics of the accumulation and persistence of defective proviruses during acute HIV-1 infection are largely unknown. Here we show that defective proviruses accumulate rapidly within the first few weeks of infection to make up over 93% of all proviruses, regardless of how early ART is initiated. Using an unbiased method to amplify near full-length proviral genomes from HIV-1 infected adults treated at different stages of infection, we demonstrate that early ART initiation limits the size of the reservoir but does not profoundly impact the proviral landscape. This analysis allows us to revise our understanding of the composition of proviral populations and estimate the true reservoir size in individuals treated early vs. late in infection. Additionally, we demonstrate that common assays for measuring the reservoir significantly overestimate or underestimate the size of the latent reservoir and no assay we tested correlates with the number of intact proviruses. Using our analysis of full-genome sequences, we identify regions and features of the HIV-1 genome that, when interrogated simultaneously, specifically distinguish intact HIV from defective genomes. We describe here a novel intact proviral DNA assay (IPDA) using multiplex droplet digital PCR that allows us to accurately quantify the number of intact proviruses, which are likely the closest estimate to the true size of the latent reservoir. In preliminary results from matched patient samples, the IPDA strongly correlates with full-

genome sequencing results. Many defective proviruses contain defects that likely preclude elimination by eradication strategies and could obscure the measurement of real changes in the rarer intact proviruses. By eliminating 90-95% of all defective proviruses and measuring primarily intact proviruses, we anticipate the IDPA will better assess the impact of eradication strategies on the true reservoir of virus that must be eliminated to achieve an HIV-1 cure.

Robert F. Siliciano, MD/PhD – Advisor and Reader

Professor and HHMI Investigator

Department of Medicine

Johns Hopkins University School of Medicine and

Howard Hughes Medical Institute

Joel N. Blankson, MD/PhD – Reader

Associate Professor

Department of Medicine

Johns Hopkins University School of Medicine

Preface

When HIV-1 was first discovered in the United States in the early 1980's, an HIV-1/AIDS diagnosis was a death sentence. In 1987, the first antiretroviral drug to combat the virus, 3'-azido-2',3'-dideoxythymidine (AZT), was approved by the FDA. Unfortunately, AZT had a significant amount of toxicity (Yarchoan and Broder, 1987) and patients frequently developed resistance to single drug antiretroviral regimens. It was only after combination therapy that targeted multiple stages of the viral life cycle was introduced in 1995-1996 that patient outcomes greatly improved (Gulick et al., 1997; Hammer et al., 1997). Instead of a death sentence, HIV-1 became a manageable but chronic disease, requiring daily medication to keep the virus at bay.

When combination therapy was introduced, it was predicted that patients could be cured of HIV-1 after 2 to 3 years on treatment based on the decay rate of the virus in the blood of infected individuals (Perelson et al., 1997). However, our lab along with two other groups proposed that a dormant or latent state of HIV-1 may exist in the memory $CD4^+$ T cells of infected patients that could allow the virus to survive, even in individuals on suppressive combination therapy (Chun et al., 1997b; Finzi et al., 1997; 1999). In 1997, our lab was able to induce and measure latent virus in the resting $CD4^+$ T cells of patients who were fully suppressed on combination ART using an assay called the viral outgrowth assay (VOA). This discovery of residual virus that persisted despite effective treatment eliminated the hope of curing HIV-1 with antiretroviral therapy alone and necessitated that HIV-1 infected individuals remain on antiretroviral therapy for life.

Since that time, we have learned significantly more about this latent reservoir of virus. We know that this reservoir of virus is extremely stable with a half-life of 44 months

and would take the lifetime of an infected individual to fully decay (Siliciano et al., 2003). Additionally, work conducted by Ya-chi Ho in the Siliciano lab recently discovered that the majority of viral genomes are actually defective and only a small number can produce replication-competent virus (Ho et al., 2013a). More importantly, her work highlighted that the gold standard quantitative viral outgrowth assay (QVOA), which measures viral genomes that can produce virions, significantly underestimated the size of the latent reservoir. Thus, it could be even more difficult to cure patients than we originally thought (Ho et al., 2013a).

My research has expanded the scope of Ya-chi Ho's original findings, which only examined patients treated late in infection, to patients treated early in HIV-1 infection. My work has also focused on performing a more comprehensive characterization of the proviral landscape in patients as well as developing a more accurate assay to measure the true size of the latent reservoir in HIV-1 infected individuals. I believe that the work described in this dissertation has contributed to our understanding of what kinds of proviruses are present in patients and determined how early defective proviruses begin to accumulate in the resting $CD4^+$ cells of patients. These results have broad implications to our assessment and understanding of HIV-1 cure strategies. Finally, we have designed and developed an assay that we hope will be a valuable research tool, both in evaluating latency reversal agents in the lab as well as someday in clinical trials in HIV-1 infected patients.

Acknowledgements

The work described here was completed with the help of many talented and dedicated individuals. First and foremost, I thank my mentor, Dr. Robert F. Siliciano. Bob initially conceived of the idea to develop a PCR-based assay that eliminated certain defective proviruses by strategically placing a single PCR amplicon and together we both developed the idea into the IPDA ddPCR. I want to thank him for allowing me the freedom to explore a project I found interesting while at the same time providing guidance and teaching me how to think independently as a scientist. I would also like to thank Dr. Janet Siliciano who has served as my second mentor in the lab and has provided critical guidance in my project. I appreciate all the work Bob and Janet do to ensure the lab has adequate resources. I never had to worry about funding for the project and they constantly made sure I had everything I needed to move the project forward. I also would like to thank my additional committee members, Dr. Stuart Ray, Dr. Joel Blankson and Dr. Sarah Wheelan. Their guidance and direction was critical not only for the science but also for the trajectory of my PhD in general. I am also grateful to the CMM program, including Dr. Rajini Rao, Dr. Robert Casero, Leslie Lichter, Colleen Graham for all of their help and advice.

The Siliciano lab members also played a critical role in both this project and in my development as a scientist. Dr. Ya-chi Ho was instrumental not only in sharing her full-genome sequencing protocol with me but also in being very generous with various lab research tools she created. These reagents were critical in my initial assay development experiments and I would not have gotten the project off the ground without them. Alexandra Murray and Mary Soliman also played a key role in this project through assisting me with the full-genome sequencing protocol. I am thankful for their help in this project as well as their

great company which made the work much more enjoyable. Ross Pollack performed the *in vitro* infection experiments and I am thankful for his enthusiasm and help on this project. I also must thank Jun Lai, Adam Longwich, Subul Beg, and Holly McHugh who were instrumental in the recruitment of both the HIV-1 positive and HIV-1 negative donors.

Additionally, this project was made possible with the help and support of some great collaborators. Dr. Steven Deeks at The University of California, San Francisco suggested we study the proviral pool in patients treated during acute infection and provided all the samples to do so. Dr. Douglas Richman at the University of California, San Diego along with colleagues Dr. Matthew Strain and Steven Lada performed the total DNA ddPCR measurements presented in our Nature Medicine publication. Finally, Dr. Janice Clements of the Retrovirus Laboratory at Johns Hopkins School of Medicine kindly allowed us to use their BioRad droplet digital PCR system used in the development of the IPDA ddPCR.

I must also thank my family who have supported me before and during graduate school. When I married my husband, I also gained a great second family. The Bruner family, particularly my husband's parents, Kurt and Olivia been a wonderful source of wisdom, encouragement and support. I must also thank my parents, Jim and Susan Bierschenk. They have always encouraged me and been my constant supporters. They instilled a love for learning in me at a young age and always encouraged me to give my best to everything I set my mind to and to do everything with integrity and honor. My sister Amanda has been my dear friend and I am so thankful for her love and support. Finally, I thank my husband Kyle who has been my best friend and constant supporter for the past 8 years. I have loved going through high school, college and now graduate school with him and am so grateful for his encouragement, love, support and prayers throughout this process.

Table of Contents

List of Tables

CHAPTER 1.

CHAPTER 2.

CHAPTER 3.

List of Figures

CHAPTER 1.

CHAPTER 2.

CHAPTER 3.

Chapter 1. Measuring the latent reservoir: An overview of current assays

The work presented in this chapter was published in Trends in Microbiology in April 2015, volume 23(4):192-203.

1.1 The establishment of HIV-1 latency

HIV-1 currently infects more than 34 million people worldwide, with over 1.1 million people infected in the United States alone. Although highly active antiretroviral therapy (HAART) is effective in suppressing HIV-1 replication by blocking various stages of the viral life cycle, it is not a curative treatment due to the existence of a latent viral reservoir in resting memory CD4+ T cells (Chun et al., 1997a; Finzi et al., 1997; 1999; Wong et al., 1997b). In addition, the latent reservoir (LR) is extremely stable and has a long half-life of 44 months, requiring an HIV-1-infected patient to be on HAART for the rest of his or her life (Siliciano et al., 2003). The LR is thought to be established when HIV-1 infects activated CD4+ helper T cells that are returning to a memory state, the result of a normal physiological process occurring after a CD4+ T cell has encountered its cognate antigen (Siliciano and Greene, 2011). Since resting memory CD4+ T cells are nonpermissive for viral gene expression, the viral genome persists in a DNA form as an integrated provirus that is not actively transcribed and resides in cells that are not targeted by the host immune system (Ruelas and Greene, 2013). These resting memory CD4+ T cells serve as the main LR of HIV-1 and are a major barrier to eradication of HIV-1 (Josefsson et al., 2013; Katlama et al., 2013).

1.2 Measurement and composition of the latent reservoir

The LR was first measured and characterized in the late 1990's using a culture technique called the viral outgrowth assay (VOA), which is still considered the current gold standard for measuring the number of proviruses in latently infected cells. (Finzi et al., 1997; 1999; Siliciano and Siliciano, 2005). The VOA makes use of phytohemagglutinin (PHA), a strong global T cell mitogen, which induces release and replication of HIV-1 from latently infected cells after one round of maximal activation. Since the development of the VOA, other assays such as PCR-based approaches, which measure total HIV-1 proviral DNA, have been developed as a simpler method to measure the LR (O'Doherty et al., 2002; Rouzioux et al., 2013; Strain et al., 2013). Although both culture and PCR-based methods are commonly used, there is little correlation between the two. According to initial VOA studies, approximately $1/10^6$ resting CD4+ T cells were thought to contain replication-competent virus, but recent studies using PCR-based assays show that $300/10^6$ resting CD4+ T cells contain HIV-1 proviral DNA (Eriksson et al., 2013).

These measurement discrepancies are attributed to the heterogeneous population of proviruses in the LR. This population of proviruses can be divided into two main types: those capable of outgrowth following one round of T cell activation and those that don't replicate, or are noninduced, after one round of T cell activation (**Figure 1.1**). The VOA measures only the former population, whereas PCR-based approaches detect both kinds of proviruses, thus partially explaining the lack of correlation between the two assays. Interestingly, most noninduced proviruses are defective (Ho et al., 2013a), the majority of which contain large internal deletions, which arise by copy choice

recombination between two parental viral RNA strands during reverse transcription (Ho et al., 2013a; Sanchez et al., 1997; Simon-Loriere and Holmes, 2011). Other defective proviruses contain inactivating G to A nucleotide hypermutations by APOBEC3G, a cytidine deaminase of the host innate immune defense system (Kieffer et al., 2005; Stopak et al., 2003; Yu et al., 2004). APOBEC3G is packaged into budding HIV-1 virions and after viral infection of a new cell it causes cytidine to uracil deamination on the HIV-1 minus strand during reverse transcription, resulting in stop codons in most open reading frames. These two types of proviruses are nonfunctional and will not produce infectious virus in the VOA. In addition, a small percentage of proviruses that are noninduced following a single round of T cell activation have genetically intact genomes and have been shown to be replication-competent (Ho et al., 2013a). These proviruses are termed intact, noninduced replication-competent proviruses. In order to achieve a functional HIV-1 cure, all of the induced as well as intact, noninduced replication-competent proviruses must be purged from the LR, since these are the proviruses capable of propagating the infection.

1.3 Accurately measuring changes in the size of latent reservoir

Currently, the most commonly studied strategy to eliminate the latent reservoir is to reverse latency by the shock and kill method (Archin and Margolis, 2014; Deeks, 2012; Margolis, 2014). The rationale is to “shock” and force HIV-1 out of the reservoir by inducing expression of the integrated viral genome. The virus within these cells will subsequently undergo RNA synthesis and viral proteins will be translated and expressed. The released virus particles would cause killing of the infected T cells by cytopathic effects or clearance by the immune system. Histone deacetylase inhibitors (HDACIs)

have been shown to be the most effective in reversing HIV-1 latency to date (Archin et al., 2012a; 2014; Shirakawa et al., 2013; Ylisastigui et al., 2004), but recent studies have shown a discrepancy between the effects of latency reversing agents (LRA) tested on *in vitro* HIV-1 model cell systems and *ex vivo* primary cells from HIV-1 infected patients (Bullen et al., 2014), highlighting a priority in the field to find consistently effective LRA candidates that will reduce the size of the latent reservoir in patients. Furthermore, in order to determine if these LRAs are effective, it is equally important to develop techniques that accurately measure changes in the latent reservoir size.

Significant progress has been made in developing culture and PCR assays since the initial discovery of the latent reservoir of HIV-1 in the 1990's. However, a detailed comparison of all the current assays has shown no precise correlation between the measurements made using the VOA or PCR assays (Eriksson et al., 2013). Since measuring the latent reservoir differs depending on what assay is used, it is urgent to develop a high-throughput and reliable assay that is sensitive and can accurately measure the true size of the latent reservoir. This is especially important in determining the efficacy of pharmacological agents used in current or future clinical trials to decrease or eliminate the latent reservoir and to reliably conclude if a functional or sterile cure has been achieved in HIV-1-infected patients undergoing eradication treatments.

1.4 Culture-based assays to measure the latent reservoir

The LR was initially defined and measured using the viral outgrowth assay (VOA), a culture-based assay that is still considered the gold standard to measure outgrowth of HIV-1 from latently infected resting T cells (Finzi et al., 1997; 1999). To set up a VOA, resting CD4+ T cells are isolated from a patient on HAART and plated in

fivefold serial dilution. Phytohemagglutinin (PHA), a lectin, is combined with irradiated allogeneic PBMCs, called feeders and added to resting CD4+ T cells to induce global T cell activation. The feeders are added to ensure successful activation since they contain macrophage and dendritic cells, which act as antigen-presenting cells (Siliciano and Siliciano, 2005). Initially, CD4+ lymphoblasts from HIV-1-negative donors were used to amplify released virus from the patient cells to detectable levels, but this process can be simplified by using a self-replicating cell line called MOLT-4/CCR5, which expresses high levels of CD4 and CXCR4 and can be stably transfected with CCR5, a co-receptor for HIV-1 viral entry (Laird et al., 2013). The patient cells are co-cultured with lymphoblasts or MOLT4 cells for two to three weeks and then are analyzed for viral outgrowth using a p24 ELISA assay. Alternatively, a highly sensitive RT-PCR can detect viral outgrowth in as early as seven days after activation (Laird et al., 2013). Recent work used a modified culture assay to allow for <1 virus producing cell per well for better quantification of HIV-1 with no need for amplification of the virus before PCR measurement. In addition, it allows for the detection of any provirus that goes on produce unspliced RNA after activation, even if mature virions are not produced (Cillo et al., 2014a). Although the VOA has a number of advantages including the ability to isolate and culture latently infected cells from patients and to detect the outgrowth of replication-competent virus (Finzi et al., 1997; 1999), recent studies have shown that the VOA underestimates the true size of the LR and that the LR is actually larger than the 1 replication-competent provirus per 10^6 resting CD4+ T cells measured by the VOA (Ho et al., 2013a). While the VOA can detect proviruses that are induced after one round of maximal T cell activation, it cannot detect intact, noninduced replication-competent

proviruses, which may pose as a barrier to curing HIV-1. Additionally, the VOA uses large volumes of blood (120-180mL), is expensive and requires 3 weeks of culture in a BSL3 laboratory. These shortcomings need to be kept in mind when using the VOA to measure LR size in patients.

1.5 PCR-based assays to measure the latent reservoir

Complementary approaches to the VOA are PCR-based assays to measure the LR. These methods provide a quicker and easier approach for studying the LR and can be applied to a variety of immune cell types. The most common PCR method for measuring the LR is a quantitative PCR (qPCR) using either resting CD4 T cells (McBride et al., 2013), unfractionated peripheral blood mononuclear cells (PBMCs), (Besson et al., 2012; Gandhi et al., 2012; Hatano et al., 2009; Rouzioux et al., 2013; Zhu et al., 2011) or bulk $CD4^+$ T cells (Chun et al., 2011; Markowitz et al., 2014). All methods involve isolating the desired cell populations from patient blood and subsequently extracting the DNA. A qPCR using primers in conserved regions of the HIV-1 genome is carried out on the DNA extracts. The number of infected cells is calculated using a standard curve of known amounts of DNA from a plasmid standard such as pNL4-3. RNase P, a ribonuclease that is present in two copies per diploid genome, is frequently used to determine the total number of cells in the sample. The standard curve and total cell number estimates the frequency of cells that harbor HIV-1 DNA. These methods have also been adapted to measure proviral DNA in the gut associated lymphoid tissue (GALT) (Chun et al., 2008; Yukl et al., 2010), a region thought to possibly be another reservoir of HIV-1 latency, as well as in CD4+ T cells in the bone marrow (Durand et al., 2012). Other PCR methods take advantage of the highly precise measurements of digital

droplet PCR to measure HIV-1 DNA in CD4 T cells (Eriksson et al., 2013; Strain et al., 2013) as well as PBMCs (Eriksson et al., 2013; Tebas et al., 2014). The DNA is extracted in the same manner as with qPCR, however, the sample is divided into thousands of droplets, allowing for single template amplification and detection. This allows for precise and absolute quantification of HIV-1 DNA rather than relative quantification derived from a standard curve, as with qPCR.

In measuring the LR, it is important to detect only integrated proviruses, not extra-chromosomal HIV-1 DNA resulting from residual viremia or viral blips. Multiple methods have been developed to measure only integrated HIV-1 proviral DNA. The most common method is Alu-PCR which can be applied to either $CD4^+$ T cells or PBMCs (Brady et al., 2013; Liszewski et al., 2009; Mexas et al., 2012; O'Doherty et al., 2002). Alu-PCR amplifies only integrated HIV-1 genomes by using one primer targeted for Alu elements, which are found in high copy numbers in the human genome, and a second primer located in the HIV-1 *gag* gene. Proviruses integrated in proximity to Alu elements are detected while nonintegrated viruses are excluded. A standard curve is used to account for proviral genomes that are too far from an Alu sequence to be detected. Alternative methods for measuring integrated proviruses include linker ligation PCR (Vandegraaff et al., 2001) and inverse PCR (Chun et al., 1997a). When Alu-PCR was compared side by side to methods detecting all proviral DNA in patients on suppressive HAART, there was a strong correlation between the two methods indicating the majority of proviral DNA in HAART patients is integrated (Eriksson et al., 2013). Although unintegrated proviruses are not considered to be part of the LR and are typically found in low levels in patients on HAART (Besson et al., 2012; Gandhi et al., 2012; Mexas et al.,

2012), unintegrated forms such as 2-long terminal repeat (LTR) circles are commonly used as a measure of recent infection or ongoing replication. A number of assays have been developed to study unintegrated forms of HIV-1 including a digital droplet PCR assay on resting CD4+ T cells and PBMCs (Eriksson et al., 2013), as well as a qPCR assay on PBMCs (Butler et al., 2001; Buzón et al., 2010; Zhu et al., 2011). These assays use primers flanking the 2-LTR circle junction, a region unique to 2-LTR circles and not found in integrated proviruses to amplify only unintegrated virus.

PCR-based methods have also been instrumental in shaping our understanding of the LR. While the culture-based VOA is expensive, labor intensive, and requires a large input of blood, PCR assays provide a much quicker, cheaper, and easier alternative. However, when compared to the VOA, PCR assays give infected cell frequencies that are at least two logs higher than those detected by the VOA (Eriksson et al., 2013). While the VOA underestimates the true size of the LR since one round of activation doesn't release all replication-competent proviruses, PCR assays overestimate the latent reservoir because they cannot discriminate between defective and replication-competent proviruses. Both types of assays provide different measures of the LR and highlight the importance of using multiple measurements to give an accurate picture of the LR.

1.6 Measuring Residual Viremia

While HAART is effective in suppressing viremia to below the clinical limit of detection of 50 copies/mL, replication-competent virus can still be detected at low levels in the plasma, indicating persistent residual viremia despite the presence of HAART (Sahu et al., 2010). To measure residual viremia, the highly sensitive single-copy assay (SCA) was developed and can detect down to one copy of HIV-1 RNA per mL of plasma

(Dahl et al., 2013; Palmer, 2013; Palmer et al., 2003). The SCA is a two-step RT-PCR that uses primers against a conserved region of *gag* in the HIV-1 genome. Although the SCA is a useful tool for measuring viral persistence in the plasma, it doesn't measure the size of the LR within resting CD4+ T cells, thus it is not the best measure to quantify changes in the LR on someone receiving eradication treatment. The SCA combined with both culture and PCR-based assays may provide an effective method to quantify the LR in a patient undergoing suppressive HAART.

1.7 Treatment interruption and time to rebound

Initially, it was thought that only a few years of HAART treatment would be necessary to cure a patient. However, the discovery of the LR and its long-term stability has rejected this notion and patients must remain on HAART their entire lives. There is a growing trend in HIV-1 eradication studies and among HIV-1 patients who have undergone bone marrow transplantations (Henrich et al., 2013; Hütter et al., 2009; Yukl et al., 2013) to stop HAART treatment and determine LR size by the time it takes for viral rebound to occur. This was done in the case of the two HIV-1 positive "Boston patients", who had undetectable levels of HIV-1 DNA after undergoing allogeneic stem cell transplantations for cancer treatment (Henrich et al., 2013). However, these patients had a rebound of viremia months after stopping HAART treatment (Henrich et al., 2014). Although taking a patient off of HAART is ultimately the only way to determine if a patient is cured, there are precautions and ethical issues to consider when using "time to rebound" as a measurement of LR size. Studies have shown that drug resistance can occur as a result of patient non-adherence to medication or as a result of treatment interruption (Arnedo-Valero et al., 2005; Luebbert et al., 2012). Additional difficulties

with this approach include the uncertainty of if or when rebound will occur. If the LR is reduced significantly in size but not entirely eliminated, it could take months or years to determine whether or not the patient was actually cured.

1.8 Current Measurements in Eradication Clinical Trials

Since latency-reversing agents (LRAs) seek to reactivate HIV-1 by inducing transcription of the latent provirus into RNA, it is important to have methods to detect changes in HIV-1 RNA production. Thus, in addition to the VOA, qPCR-based methods have been developed for measuring HIV-1 RNA production in PBMCs (Hatano et al., 2009; Yukl et al., 2010), resting CD4+ T cells (Archin et al., 2012a), and in the GALT (Eriksson et al., 2013; Yukl et al., 2010) as well as measuring HIV-1 mRNA in resting CD4+ T cells (Bullen et al., 2014). Digital droplet PCR has also been to quantify HIV-1 RNA (Jones et al., 2014). In addition to determining whether or not a LRA has been effective in "shocking" the virus to produce RNA, it is also important to determine whether or not the infected cells have been "killed" and eliminated from the reservoir. In order to do this, an accurate measure of the LR before and after treatment(s) is necessary. **Table 1.1** summarizes the different assays used in measuring the LR. Current eradication trials involve the administration of monoclonal antibodies, cytokines, HDAC inhibitors (Archin et al., 2012a; Rasmussen et al., 2014b), gene therapies (Tebas et al., 2014), and intensification treatments (Puertas et al., 2014). Most current and future trials will measure LRA efficacy by either outgrowth of virus with the VOA, cell-associated RNA, plasma RNA, and total and integrated HIV-1 DNA, or a combination of multiple measures as is shown in **Table 1.2**. The outcomes of these trials will vary since measuring the latent reservoir differs depending on what assay is used.

1.9 Discussion

Following the discovery of the LR in resting memory T cells and its long-term stability, it has become an urgent task to identify ways to eliminate this major barrier to eradication. Currently, the predominant strategy to eliminate the LR is the "shock and kill" method which aims to "shock" HIV-1 out of the LR by inducing HIV-1 gene expression and "kill" infected host cells by way of cytotoxic and immune clearance. It has also become a high priority in the field to develop better ways to measure the LR (International AIDS Society Scientific Working Group on HIV Cure et al., 2012), since current eradication trials lack a universal measure to assess whether or not a decrease in the LR has been achieved. Although many assays have been developed to quantify the LR, there is little correlation between the methods (Eriksson et al., 2013). The only correlation that has been observed between culture and PCR assays is between an Alu PCR specific for integrated DNA in PBMCs and the VOA. Despite a correlation between methods, the Alu PCR still gave infected cell frequencies at least two logs higher than those detected by the VOA (Eriksson et al., 2013).

In addition to a lack of correlation between methods, there are also drawbacks to both PCR-based and culture assays that need to be considered when using them to measure the LR or evaluate eradication therapies. The VOA is still considered the gold standard for measuring the LR, however it underestimates the true size of the LR since it cannot detect all latently infected cells that may pose a barrier to an HIV-1 cure (Ho et al., 2013a). Underestimating the size of the LR may cause a patient to appear "cured", however the patient may still contain latent HIV-1, and if taken off of HAART treatment, viral rebound may occur. PCR-based assays are also commonly used to quantify proviral

DNA, but they cannot distinguish between replication-competent and defective proviruses. An additional concern in using PCR-based assays arises from the fact that many defective proviruses such as those containing lethal hypermutations or large deletions would be unable to produce viral proteins even if latency was successfully reversed. Elimination of infected cells is likely dependent upon viral protein production, thus cells containing defective proviruses may not be eliminated even by successful strategies. In this situation, large numbers of defective viruses could potentially mask successful clearance of latently infected cells resulting from latency reversal therapy. Using PCR assays to measure the efficacy of eradiation agents could possibly lead to the rejection of a successful strategy. Since PCR-based measurements detect defective proviruses as well, it would also be impossible to know when the true latent reservoir has been successfully cleared and when patients can safely be removed from therapy.

Since there are no current assays available that can accurately detect whether or not a patient is "cured" or whether or not a decrease in the LR has been achieved, treatment interruption of HAART in patients is also used to measure reduction in reservoir size in eradication trials. Although treatment interruption is the only definitive way to know whether or not a functional cure has been achieved, there are many concerns with this approach. In 2006, the SMART study compared prolonged HAART treatment, which is now considered the standard treatment of care today, to episodic treatment with antiretrovirals followed by treatment interruption until CD4+ T cell levels dropped below a predetermined threshold (Strategies for Management of Antiretroviral Therapy (SMART) Study Group et al., 2006). The patients with treatment interruption experienced higher levels of morbidity, opportunistic diseases, and malignancies

compared to those on continued treatment (Pace and Frater, 2014; Routy et al., 2012; Silverberg et al., 2007; Strategies for Management of Antiretroviral Therapy (SMART) Study Group et al., 2006). Considering the precautions and ethical considerations in removing patients from treatment, it remains necessary to have assays that can measure the effects of therapeutic interventions on reservoir size without the need for treatment interruption.

The main goal in eradication clinical trials is to identify agents that cause a decrease in the LR in HIV-1-infected patients. The current assays available do not correlate well with one another and none measure the true size of the LR (**Figure 1.2**), which prevent accurate identification of successful agents proposed to eliminate the LR as well as comparisons between different eradication trials. In the absence of a universal method of measurement, many clinical trials are using a combination of culture and PCR methods to identify and measure changes in the LR as shown in **Table 1.2**. However, the conclusions drawn from these trials will vary depending on the specific measurements used. In order to reliably conclude if an agent is effective or if a cure has been achieved, an assay is needed that can measure latently infected cells that have the potential to produce replication-competent virus *in vivo*, since these are the only proviruses that may pose a threat to eradication. A high throughput, sensitive, and well-validated assay would be ideal and would aid researchers in the field in their efforts to eradicate HIV-1.

1.10 Tables: Chapter 1

Table 1.1 Comparison of assays for measuring the HIV-1 latent reservoir

Assay	What it measures	What it excludes	Detection Method	Advantages	Disadvantages
Viral outgrowth assay (VOA)	Replication-competent virus induced by single round of T cell activation. Can in principle detect linear unintegrated HIV-1 DNA in recently infected cells. For this reason, the VOA is only useful as a measure of the LR in patients who have had prolonged suppression of viral replication on ART.	Defective proviruses, noninduced replication-competent proviruses (INPs), 1- and 2-LTR circles	p24 ELISA or RT-PCR	Allows for quantification of induced replication-competent proviruses without detection of defective proviruses	-Expensive and requires a large blood volume (120-180 mL) -Time consuming (requires 2-3 weeks tissue culture in a BSL3 laboratory) -Limited dynamic range because levels in most patient on ART are close to the limit of detection with the standard sample volume (180 mL blood) -Does not detect all proviruses that potentially pose a barrier to a cure
T cell activation assays with viral RNA readout	Fraction of proviruses that can be induced to make either cell associated unspliced or multiply spliced HIV-1 RNA or full length HIV-1 mRNA released into the culture supernatant (presumably as virions)	Some defective proviruses, intact proviruses not induced to make HIV-1 RNA after a single round of activation (INPs)	RT-qPCR	-No need for growth of virus before measurement -Less culture time is required than the VOA	-Requires 2-7 days of culture in a BSL3 laboratory -Does not detect all proviruses that potentially pose a barrier to a cure -May detect some defective proviruses
qPCR for HIV-1 DNA	Total proviral DNA including replication-competent proviruses, defective proviruses, and unintegrated forms of HIV-1 DNA	Proviruses with deletions in amplified regions	qPCR	Easy, quick, and does not require any extended culture time in a BSL3 laboratory	-Detects many proviruses that do not pose a barrier to an HIV-1 cure -Provides quantitation relative to a standard curve, but not an absolute value. Different qPCR assays use different standards
Droplet digital PCR (ddPCR) for HIV-1 DNA	Total proviral DNA including replication-competent proviruses, defective proviruses, and unintegrated forms of HIV-1 DNA	Proviruses with deletions in amplified regions	ddPCR	Highly precise; provides an absolute quantitation rather than a relative one	Detects many proviruses that do not pose a barrier to an HIV-1 cure
Alu PCR for Integrated HIV-1 DNA	Integrated proviral DNA	Unintegrated proviral DNA including 1- and 2-LTR circles, and linear unintegrated HIV-1 DNA	qPCR	Useful in measuring integrated proviruses in untreated patients, in which large amounts of unintegrated DNA can confound total proviral DNA measurements	Does not detect proviruses that are too far from an Alu sequence to be amplified, but uses a correction factor to account for these; also detects defective proviruses
qPCR for 2-LTR circles	2-LTR circles	Integrated proviral DNA	qPCR	Used to measure ongoing replication based on the controversial assumption that the circles are labile	Does not detect integrated provirus, which is the only form that can contribute to latency
Droplet digital PCR for 2-LTR circles	2-LTR circles	Integrated proviral DNA	ddPCR	Highly precise; provides an absolute quantitation rather than a relative one; used to measure ongoing replication	Does not detect integrated provirus, which is the only form that can contribute to latency
Single-copy assay (SCA)	Residual viremia	Proviral DNA within cells or compartments	RT-PCR	Valuable as a measure of ongoing virus production in the setting of ART	-Time consuming and does not directly measure the LR as the residual viremia may also originate from other reservoirs. -Limited dynamic range because levels in most patients on ART are close to the limit of detection with the standard sample volume (8 ml plasma).

Table 1.2 Measurements used in select recent and future HIV-1 eradication clinical trials

Name	Clinical Trial ID	Sponsor	Category	Measures	Estimated completion
Lisinopril	NCT01535235	University of California, San Francisco	Angiotensin-converting-enzyme inhibitor	Change in RNA in total CD4s and in GALT, and DNA in total CD4s and GALT	August 2014
Disulfiram	NCT01944371	University of California, San Francisco/Monash University/American Foundation for AIDS Research (amfAR)	Acetaldehyde dehydrogenase inhibitor	Cell-associated RNA in total and resting CD4s, plasma RNA by SCA, proviral DNA, mRNA expression	August 2014
Romidepsin	NCT01933594	AIDS Clinical Trials Group/National Institute of Allergy and Infectious Diseases (NIAID)/Gilead	HDAC inhibitor	Cell-associated RNA in total and resting CD4s, plasma RNA by SCA, total and 2-LTR DNA circles in resting and total CD4s	January 2015
GTU-multiHIV + LIPO-5	NCT01492985	French National Institute for Health and Medical Research-French National Agency for Research on AIDS and Viral Hepatitis (Inserm-ANRS)	DNA + lipopeptide vaccines	Plasma RNA by SCA during and after stopping treatment, and proviral DNA	January 2015
Vacc-4x + Romidepsin	NCT02092116	Bionor Immuno AS/Celgene	Vaccine + HDAC inhibitor, stopping HAART treatment	VOA, total and integrated DNA in CD4s, cell-associated unspliced RNA in CD4s, and plasma RNA	December 2015
CD4-ZETA +/- IL-2	NCT01013415	University of Pennsylvania	Modified T cells with or without IL-2	Plasma RNA by SCA, tissue RNA, frequency of latent replication-competent HIV-1 in PBMCs	December 2015
ULTRASTOP	NCT01876862	Objectif Recherche VACcin Sida (ORVACS)/Fondation Bettencourt Schueller	Highly active antiretroviral therapy (HAART) interruption	DNA in sorted CD4 subsets, plasma RNA by SCA, HIV-1 DNA in PBMCs and total CD4s, defective DNA sequences and presence of stop codons	December 2015
AGS-004	NCT02042248	University of North Carolina at Chapel Hill/Argos Therapeutics/U.S. National Institutes of Health (NIH)	Autologous dendritic cells and HIV strain	Plasma RNA by SCA and VOA	January 2016
Vorinostat	NCT01365065	Bayside/Merck	HDAC inhibitor	Plasma RNA by SCA and unspliced RNA in CD4s	March 2016
BMS-936559	NCT02018510	NIAID	Anti-PD1 antibody	Plasma RNA by SCA, total DNA, 2LTR circle DNA, cell-associated RNA, RNA/DNA ratios in total CD4s	April 2016
Peg-Interferon-a2b	NCT01935089	University of Pennsylvania	Cytokine	Alu-HIV *gag* PCR to detect change in HIV-1 DNA in total CD4s	July 2016
Poly-ICLC	NCT02071095	Campbell Foundation/Oncovir, Inc.	Toll-like receptor (TLR)-3 agonist	Cell-associated RNA, plasma RNA by SCA, and proviral DNA	June 2017
New Era Study	NCT00908544	MUC Research GmbH	2 Nucleoside Reverse Transcriptase Inhibitors (NRTI) + 1 protease inhibitor (PI)/Ritonavir + Maraviroc + Raltegravir	Cell-associated proviral DNA in PBMCs and total CD4s, plasma RNA by SCA	November 2019

1.11 Figures: Chapter 1

Figure 1.1 Profile of different types of HIV-1 proviruses in resting CD4+ T cells

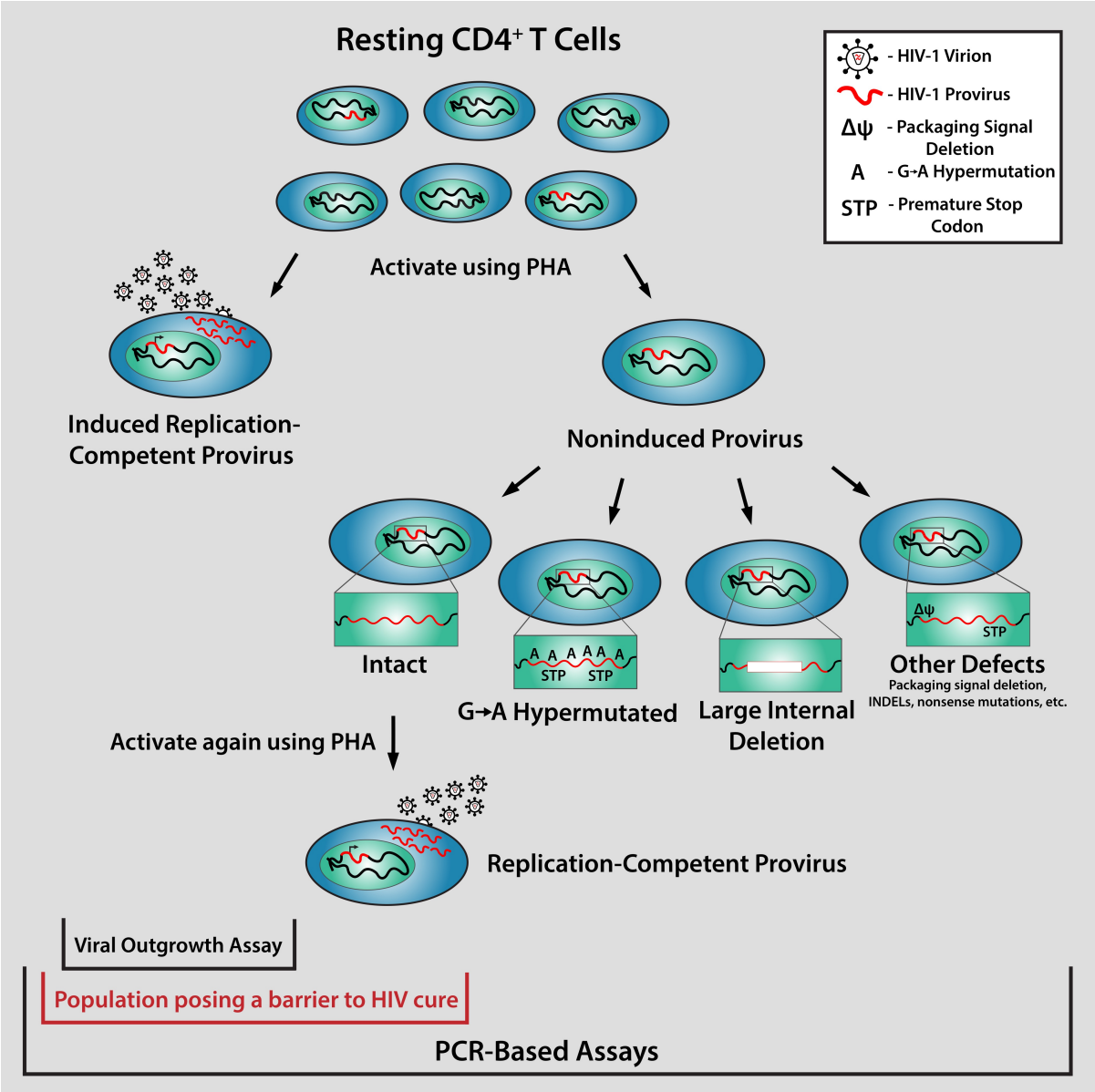

The major types of proviruses are shown, including those that pose a barrier to an HIV-1 cure and those that do not. Following a single round of T cell activation, some proviruses are induced to produce virions, which can infect other cells (induced, replication-competent proviruses). Proviruses that are not induced to produce replication-competent

virions following a single round of T cell activation are termed noninduced proviruses. Many of these noninduced proviruses are defective and contain large internal deletions, G to A hypermutations, or other inactivating defects. However, some noninduced proviruses have fully intact genomes and, on subsequent rounds of cellular activation, can produce virions. These proviruses are termed intact, noninduced proviruses (INPs). Culture-based assays detect induced replication-competent proviruses only, while PCR-based assays detect all types of proviruses. Only induced replication-competent proviruses and INPs pose a barrier to an HIV-1 cure.

Figure 1.2 Venn diagram comparison of proviral populations measured by different methods of assessing the latent reservoir (LR)

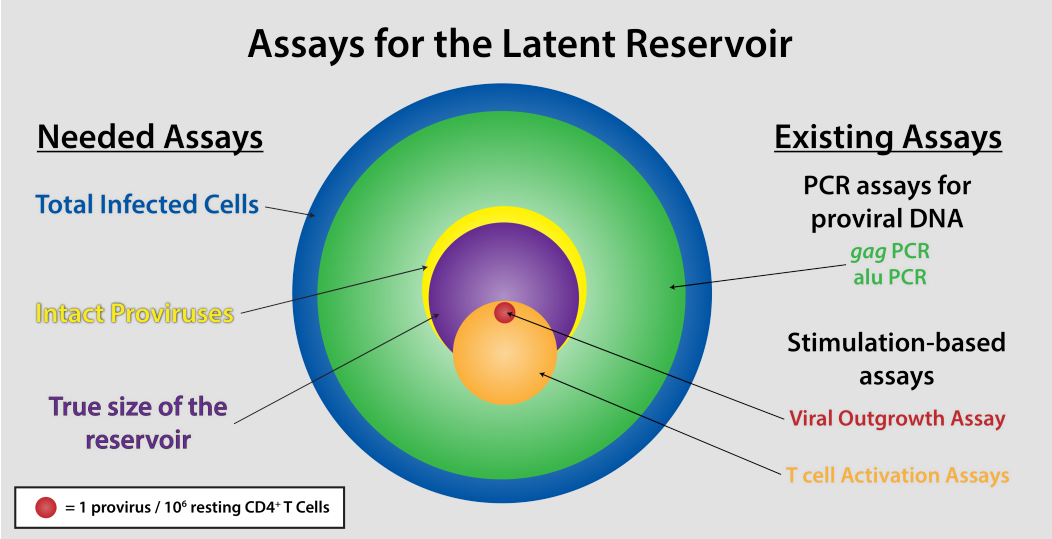

Typical or estimated results from various PCR- and culture-based assays are shown relative to a prediction of the true LR size. The frequency of infected cells detected by the different assays is represented by the area of each circle. PCR-based assays overestimate the LR since most of the templates amplified represent defective viruses (Ho et al., 2013b; Eriksson et al., 2013). Additionally, some proviruses are likely to be deleted in the primer binding sites for the PCR, so PCR-based assays are likely to underestimate the total number of infected cells. The viral outgrowth assay (VOA) underestimates the LR size because not every replication-competent virus is induced by a single round of T cell activation (Ho et al., 2013a). Assays involving T cell activation with a viral RNA readout give intermediate values but suffer from both of the problems mentioned above: some of the viral RNA detected is derived from defective proviruses and not all of the replication-competent proviruses are induced by a single round of activation (Cillo et al., 2014b; Laird et al., 2013). There is a need for assays that measure only those proviruses that pose a threat to an HIV-1 cure.

Chapter 2. Defective proviruses rapidly accumulate during acute HIV-1 infection

The work presented in this chapter was published in Nature Medicine in September 2016, volume 22(9):1043-9.

2.1 Introduction

HIV-1 establishes infection in $CD4^+$ T cells (Chun et al., 1997b; Finzi et al., 1997; 1999), generating a latent reservoir with an extremely long half-life (44 months) that necessitates life-long treatment (Crooks et al., 2015; Siliciano et al., 2003). Efforts to eradicate this reservoir include the "shock-and-kill" approach in which latent proviruses are induced so that infected cells can be eliminated (Archin and Margolis, 2014; Deeks, 2012; Archin et al., 2012a). The latent reservoir was initially defined using a quantitative viral outgrowth assay (QVOA) (Crooks et al., 2015; Finzi et al., 1997; Laird et al., 2013; Siliciano and Siliciano, 2005). PCR can also detect proviral DNA (Henrich et al., 2012; Rouzioux et al., 2013; Strain et al., 2013). However, the QVOA and PCR assays correlate poorly (Eriksson et al., 2013). We recently examined discrepancies between the assays by sequencing gag^+ proviruses from QVOA wells negative for viral outgrowth (Ho et al., 2013a). Most proviruses were defective, but 12% were intact, and some of these could be reactivated following a second round of T cell activation (Ho et al., 2013a). However, these studies were limited to individuals who initiated ART late in the course of infection and only analyzed gag^+ proviruses in cells that had been expanded for weeks in culture (Ho et al., 2013a). As immediate ART is now recommended for all infected individuals (Günthard et al., 2014), and since the size and perhaps other characteristics of the

reservoir differ in individuals treated early versus late in infection (Archin et al., 2012b; Deng et al., 2015; Jain et al., 2013), we sought to define the composition of proviral populations in individuals treated during acute infection. As cure efforts advance, it is essential to understand how defective proviruses accumulate, persist in individuals and affect reservoir assay measurements. Therefore, we conducted a proviral analysis in unmanipulated samples from HIV-1 infected adults treated at different stages of infection.

2.2 Results

We developed a novel, unbiased single genome amplification method that captures intact and defective proviruses. Since deletions likely occur during minus strand synthesis before the second strand transfer event of reverse transcription, primers were designed to capture deletions arising during this process (**Fig. 2.1a**) (Delviks-Frankenberry et al., 2011; Jetzt et al., 2000; Yu et al., 1998). PCRs were performed at limiting dilution to prevent *in vitro* recombination and competition between short and long templates. Following the near full length outer PCR, *gag* and *env* inner PCRs were used to confirm clonality, and six overlapping inner PCRs were performed on all wells at limiting dilution (**Fig 2.1b**). PCR products were directly sequenced to minimize PCR-induced error.

We examined proviral DNA in purified resting $CD4^+$ T cells from ten subjects initiating ART during the chronic phase of infection (CP; ART started >180 days after infection) (**Table 2.1**). Analysis was performed on freshly isolated cells to prevent bias from *in vitro* expansion. Strikingly, 98% of proviruses were defective (**Fig. 2.2 a,b** and **Fig. 2.3**). The most common defects were internal deletions (80%), which varied in size

(15 bp to ~8 kb) and in location in the genome. Some proviruses had 3' deletions affecting the *env*, *tat*, *rev* and *nef* genes. We also identified proviruses with 5' deletions affecting *gag* and *pol* and others with very large deletions (>6 kb) encompassing most HIV-1 genes (**Fig. 2.2 a,b**). The 5' deletions and very large deletions, representing 40% of all sequences, were not identified in a previous screen because they contain deletions in the *gag* gene (Ho et al., 2013a). Proviruses with small (15-97bp) deletions at the packaging signal and major splice donor site represented 5% of sequences (**Fig. 2.2b**). These proviruses are likely replication-defective due to failure to correctly make spliced HIV-1 RNAs or to package genomes into virions (Ho et al., 2013a). Some clones contained multiple deletions suggesting multiple template switching events during reverse transcription (**Fig. 2.2a**) and others contained sequence inversions or insertions (**Fig. 2.2b**). For each type of deletion, proviruses with sequence homology at the deletion junctions were found (**Fig. 2.2c**), consistent with template switching during reverse transcription (Hwang et al., 2001). In control experiments, plasmids containing reference (NL4-3) or patient-derived proviruses were diluted into human genomic DNA and amplified by the same procedure with no defects observed (data not shown). Additionally, deletions showed nonrandom distribution within the HIV-1 genome with distinct hotspots (**Fig. 2.4**) and we observed identical deletions in independent amplifications from the same subject, reflecting clonal expansion of infected cells (see below). Taken together, these results indicate that the deletions we observe occurred *in vivo* and do not result from PCR recombination. We also identified 7% of proviruses with APOBEC3F/G-induced hypermutation and an additional 8% with both deletions and hypermutation, indicating that these processes can occur together during reverse

transcription (**Fig. 2.2b**). Almost all hypermutated proviruses contained mutated start codons for the *gag*, *gag-pol* and *nef* ORFs due to the presence of an obligatory position 2 glycine codon which creates the APOBEC3G consensus site, ATGGGT (Kieffer et al., 2005; Yu et al., 2004). Additionally, all hypermutated sequences had multiple internal stop codons in the larger ORFs (*gag*, *gag-pol*, *env*, *nef*) and only a small fraction could make functional gene products (**Fig. 2.5**). These defects and common deletions affecting key viral ORFs (**Fig. 2.2a,b**) likely prevent many defective proviruses from being eliminated by eradication strategies that depend on viral protein expression. All subjects had undetectable viral loads (<50copies/mL) for >8 months prior to sampling and all but one had low frequencies of 2LTR circles in cells (< 25 copies/10^6 resting $CD4^+$ T cells), which represented less than 8% of the total number of infected cells (**Fig. 2.6**). The labile nature of linear unintegrated HIV-1 DNA and the low level of 2LTR circles suggest the majority of the sequences examined were integrated proviruses (Pierson et al., 2002). Of 152 near full-length sequences examined, only 3 sequences were intact (2%). These data indicate that defective proviruses are much more common than previously shown (**Fig. 2.2b**).

Since the dynamics of proviral accumulation remain unclear, we sought to determine how rapidly defective proviruses accumulate. We examined the proviral populations in subjects treated during the acute/early phase of infection (AP; ART started within 100 days in all subjects and within 60 days in 8 of 9 subjects) (**Table 2.1**). Surprisingly, only 7% of proviruses were intact, even in subjects 2453, 2454, 3693, and 2443 who initiated ART within the first few weeks of infection (**Fig. 2.7a,d** and **Fig. 2.8**). Although, the number of individuals subjected to this extensive analysis was small, the

results were very consistent between subjects. The remaining proviral sequences contained defects similar to those in CP-treated subjects (**Fig. 2.7a,d**) and there was no significant difference in the fraction of intact proviruses compared to CP-treated subjects (**Fig. 2.9a**). AP-treated subjects had a higher fraction of hypermutated sequences (35% vs. 14%, $P = 0.0036$, **Fig. 2.9b**) and a significantly lower fraction of deleted sequences (57% vs. 82%, $P = 0.0028$, **Fig. 2.9c**) suggesting that hypermutation is particularly important during acute infection, perhaps due to upregulation of APOBEC3G/F by type I interferons (Harper et al., 2015; Pillai et al., 2012; Stacey et al., 2009). Interestingly, defects are even detectable in a single round of *in vitro* infection (41% of sequences, **Fig. 2.7b,d**). Consistent with this result, we readily detected defective proviruses in unfractionated $CD4^+$ T cells from viremic subjects in the chronic phase of infection, representing 65% of sequences (**Fig. 2.7c,d**). In these subjects, the provirus populations include both proviruses in newly infected cells and archived proviruses in the reservoir. These results indicate that defective proviruses are likely generated during the initial rounds of replication after transmission, as defective proviruses are generated at a high frequency from the process of reverse transcription (**Fig. 2.7b**). Since many of the proviruses identified have defects that would preclude high-level expression of viral genes, cells carrying these proviruses would likely be less susceptible to elimination through viral cytopathic effects or lysis by cytotoxic T lymphocytes. Thus even individuals treated very early have large numbers of defective proviruses. Together, these results demonstrate that defective proviruses arise commonly, accumulate rapidly within two to three weeks after infection, and persist *in vivo*.

Proliferation of cells carrying replication-competent proviruses could be a major barrier to eradication (Kearney et al., 2015; Maldarelli et al., 2014; Wagner et al., 2014). Integration-site analysis, pioneered by Schröder et al. (Schröder et al., 2002), has provided important evidence for proliferation of infected cells *in vivo* but does not reveal whether the proviruses are replication-competent (Cohn et al., 2015; Maldarelli et al., 2014; Wagner et al., 2014). Our unbiased analysis allowed us to detect expanded cellular clones *in vivo* and evaluate the presence of defects. Among 312 sequences from 9 AP- (**Fig. 2.10a**) and 10 CP-treated subjects (**Fig 2.10b**), 38 were from expanded cellular clones identified as identical sequences arising from independent amplifications. Importantly, all contained gross defects that preclude replication (**Fig. 2.11a,b**). In subjects 2529, 2609, CP03, CP05, and CP10, expanded clones represented over 25% of all the sequences (**Fig. 2.10a,b**). Subject 2521 contained an expanded clone representing 11% of all proviral sequences (**Fig. 2.10a, 2.11a**) after just 17 months of infection and 8 months on suppressive ART, indicating expanded clones do not require years to accumulate to large proportions. Our results indicate the majority of expanded clones are defective. However, considering that <7% of proviruses are intact, rare expanded clones may carry replication-competent virus and contribute to HIV-1 persistence, as was seen in a recent clinical case study (Kim and Siliciano, 2016; Simonetti et al., 2016). Although cells harboring defective proviruses can undergo clonal expansion with minimal consequences to the host cells, cells harboring replication-competent viruses could likely expand through either activation of the cell but not the provirus (Bosque et al., 2011) or possibly proliferation and survival of the cells despite viral gene expression and virion production.

Our analyses show that the fraction of intact proviruses is much lower than originally thought even in individuals treated early. We have previously shown that intact proviruses replicate well *in vitro* when reconstructed (Ho et al., 2013a). Furthermore, when wells that were negative for viral outgrowth in the VOA were reactivated, additional replication competent virus was isolated (Ho et al., 2013a). These data taken together suggest that some if not all of these intact proviruses are competent for viral replication and that the number of intact proviruses is likely the closest estimate to the true size of the latent reservoir. Given these results, we sought to more accurately estimate the true reservoir size in AP- and CP- treated individuals, as defined by the number of intact proviruses, and compare that result to current assays such as the QVOA and DNA PCR. We used a validated droplet digital method for proviral DNA with *gag* primers (Massanella et al., 2015; Strain et al., 2013) (gag^+ proviruses) and corrected for proviruses deleted in *gag* (total number of infected cells). The DNA PCR assay gave infected cell frequencies dramatically higher than the frequency of cells with intact proviruses ($P < 0.0001$ for CP-treated; $P < 0.0001$ for AP-treated subjects). The QVOA gave infected cell frequencies that were dramatically lower than the frequency of cells with intact proviruses ($P < 0.001$ for CP-treated; $P < 0.01$ for AP-treated subjects) (**Fig. 2.12a,b**). We found that the QVOA potentially underestimates the latent reservoir by a median of 27-fold in CP-treated subjects and 25-fold in AP-treated subjects (**Fig. 2.12c**). However, DNA PCR overestimated the reservoir size by a median of 188-fold in CP-treated subjects and 13-fold in AP-treated subjects (**Fig. 2.12c**). Importantly, there was no correlation between the number of intact proviruses and either the QVOA or DNA PCR results (**Fig 2.13a-c**). Additionally, the relationships between the QVOA, intact

proviruses, and proviral DNA varied greatly from person to person in both CP-(**Fig. 2.12d** and **Fig. 2.14a**) and AP-treated subjects (**Fig. 2.12e** and **Fig. 2.14b**). This precludes the use of either the QVOA or DNA PCR as a surrogate marker for the number of intact proviruses, which is likely the closest estimate of the true size of the latent reservoir.

2.3 Discussion

This unbiased screen demonstrates that the fraction of intact proviruses is considerably smaller than previously shown and that defects accumulate as early as two to three weeks after infection. Although surprising, the rapid accumulation is consistent with the observation that defects can be observed in 40% of proviruses generated in a single round *in vitro* infection (**Fig. 2.7d**) and the fact that cells harboring defective proviruses may be less susceptible to immune clearance or cytopathic effects. With these new data, we were able to revise our estimates of the reservoir size in both CP- and AP-treated individuals. If all intact proviruses can be induced *in vivo*, the true size of the latent reservoir would be on average 12 infectious proviruses (median of AP-treated) in acute/early treated individuals and 37 infectious proviruses (median of CP-treated) per million resting $CD4^+$ T cells in chronically treated individuals, with substantial person-to-person variation. Furthermore, our results change our understanding of the impact of early ART on the proviral landscape. While early ART initiation limits the size of the latent reservoir, it does not have a profound impact on the composition of proviral populations, with the vast majority of proviruses in both CP- and AP-treated adults containing defects. Finally, these results have implications for assessing HIV-1 cure strategies. Since there is no correlation between the QVOA or DNA PCR and the number of intact proviruses, these assays cannot be used to accurately predict the true reservoir

size, even in individuals treated early in infection. Indeed any analysis of subgenomic regions of proviruses to evaluate viral evolution or reservoir reduction must be reconsidered in this context, since the majority of sequences studied will be from defective proviruses (Lorenzo-Redondo et al., 2016). Importantly, since the nature of the defects described here indicates that many defective proviruses may not be eliminated by eradication strategies, defective proviruses could obscure the measurement of real changes in the rarer intact proviruses that must be eliminated to achieve a cure.

2.4 Materials and Methods

Study subjects

The Johns Hopkins Institutional Review Board and the UCSF Committee on Human Research approved this study. All participants provided written consent prior to enrollment. Nineteen HIV-1 infected individuals who met the criteria of suppressive ART and undetectable plasma HIV-1 RNA level (< 50 copies per mL) for a minimum of 8 months were enrolled. Ten of these participants were recruited from the SCOPE and OPTIONS cohorts at the University of California, San Francisco. CP-treated subjects are defined as subjects starting ART >180 days from the estimated date of infection. AP-treated subjects started ART < 100 days after the estimated date of infection. Viremic subjects were either untreated or had viral loads > 4000 copies/ml on ART. Table 2.1 details the characteristics of study participants.

Isolation of resting CD4+ T lymphocytes

Peripheral blood mononuclear cells (PBMCs) were isolated using density centrifugation on a Ficoll-Hypaque gradient. CD4+ T cells were isolated from PBMCs

using a negative selection method (CD4+ T cell Isolation Kit II, Miltenyi Biotec). Resting CD4+ lymphocytes (CD4+, CD69–, CD25– and HLA-DR–) were enriched by a second negative depletion (CD25-Biotin; Anti-Biotin MicroBeads; CD69 MicroBead Kit II; Anti–HLA-DR MicroBeads, all from Miltenyi Biotec). Resting CD4+ cell purity was consistently >95% as assessed using flow cytometry.

DNA extraction and limiting dilution PCR

DNA was extracted from 2 x 10^6 resting CD4+ cells using the Qiagen Gentra Purgene Cell Kit A, which allows for extraction of large fragments of ~200kb in size so as to minimize fragmentation of HIV-1 genomes. DNA was subjected to a nested limiting dilution PCR protocol modified from Ho et al. using Platinum Taq HiFi Polymerase (Life Technologies) (Ho et al., 2013a). The outer PCR was nearly full-length from HXB2 coordinates 623 to coordinates 9,686 and employed a touchdown PCR protocol. The outer PCR wells were diluted 1:3 with DI water and 1μL of outer PCR DNA was used for nested amplification of both gag and env to determine clonality. Clonality was determined using Poisson statistics and at dilutions giving a high probability of clonality ($P > 0.85$), all outer PCR wells, including those that were negative for gag and env, were subjected to six inner PCRs. 1μL of outer PCR DNA was used for each nested PCR reaction. A detailed PCR protocol and primer sequences and locations can be found in Table 2.2. PCR products were visualized on 1% agarose gels. The products were directly sequenced to minimize PCR-induced error using the QIAquick Gel Extraction Kit followed by Sanger sequencing. Sequencing reads from the six overlapping nested PCRs were aligned and compared to the reference genome HXB2 using CodonCode Aligner software to reconstruct near full-length sequences and identify defects. Hypermutation

was determined using the full-length sequence for each clone and the Los Alamos hypermut algorithm (Rose and Korber, 2000). Some hypermutated clones had extensive hypermutation that prevented full sequencing of the entire genome. Since the PCR products were correctly sized on an agarose gel, the sequences were inferred to be full-length hypermutated. We were able to directly map the majority of deletions by direct sequencing of PCR products generated with primers flanking the deletion junction. Some very large internal deletions were identified despite deletion of some inner primer binding sites. Observed bands likely resulted from exponential amplification in the outer PCR and linear amplification in inner PCRs. These deletions were confirmed through sequencing bands from multiple inner PCRs, all of which showed the exact same deletion product.

In vitro infections

HIV-1 negative donor CD4+ T cells were isolated as above and activated with phytohaemagglutinin (PHA) (0.5μg/mL) for 3 days in IL2-containing medium (Kim et al., 2014). Cells were infected with replication-competent HIV-1 Ba-L virus (300 ng p24/10^6 cells) by spinoculation (2 hrs, 37°C, 1200 x *g*). Cells were then suspended at 3 x 10^6/mL in IL2-containing medium and incubated for 6 days at 37°C. Following the incubation, supernatant was collected, and stored at -80°C. 25 x 10^6 HIV-1 negative donor CD4+ T cells were activated by αCD3/αCD28 stimulation for 72 hours in IL-2-containing medium as previously described (Kim et al., 2014). Activated cells were suspended in 2.5mL of IL-2-containing medium and distributed in 100μL aliquots into a 96-well v-bottom plate. A 500ng inoculum of HIV-1 Ba-L was added to each well and cells were infected by spinoculation (2hrs, 37°C, 1200 x *g*). Following the spinoculation, cells were suspended in 40mL of IL2-containing medium supplemented with enfuvirtide

(10uM) to prevent additional rounds of viral replication. Following a two day incubation at 37°C, genomic DNA was isolated and analyzed as above.

Quantitative viral outgrowth assay

The QVOAs were performed as previously described (Finzi et al., 1997; Laird et al., 2013; Siliciano and Siliciano, 2005). MOLT-4/CCR5 cells were added on Day 2 of the culture (Laird et al., 2013) and the culture supernatants were examined using the standard protocol, which involves an ELISA for the p24 viral capsid protein (PerkinElmer) after 21 days. HIV-1 RNA in the culture supernatant was not measured. MOLT-4/CCR5 cells were obtained from NIH AIDS reagent program, were negative for mycoplasma contamination, and were stained to verify expression of CD4, CXCR4, and CCR5. Infectious units per million cells (IUPM) values were calculated using IUPMStats (Rosenbloom et al., 2015). If all culture wells were negative for viral outgrowth, the median posterior estimate of infection frequency was used.

Droplet digital PCR

DNA was extracted from 5-10 x 10^6 resting CD4+ T cells using the QIAamp DNA Blood Mini Kit. DNA was fragmented and a duplex droplet digital PCR was performed with primers in the *gag* gene as well as primers for 2LTR circles as previously described (Massanella et al., 2015; Strain et al., 2013). For pt. 2609, primers in the pol gene were used instead as the *gag* PCR primers and probes contained multiple mismatches with the patient sequence and did not amplify (Massanella et al., 2015). Measurements of the cellular gene RPP30 in a replicate well by ddPCR were used to calculate the frequency of resting $CD4^+$ T cells. The frequency of gag^+ DNA and 2LTR

circles were plotted as a frequency per 10^6 resting $CD4^+$ T cells. In the case of a negative 2LTR circle measurement, the lower limit of detection was determined using the total cellular input for that sample. Since many of the proviruses examined were *gag* negative, we also estimated the total number of infected cells in study subject resting $CD4^+$ T cells as the copies of gag^+ proviral DNA divided by the fraction of proviruses detected that were gag^+. For Pt. 2609 the total number of infected cells was estimated as the copies of pol^+ proviral DNA divided by the fraction of proviruses detected that were pol^+ since the *gag* PCR primers did not amplify.

Bayesian analysis to calculate number of intact proviruses

The proportion of intact genomes for each subject was estimated using an Empirical Bayesian analysis, with prior distributions generated separately for the acute and chronic subject cohorts. The proportion of clones identified as intact was calculated for each subject, and the mean and variance of this measurement were used to generate beta prior distributions with the same mean and variance. The proviral genome sequences were treated as Bernoulli trials, with intact clones counted as successes. The final estimate for the percent of intact genomes for each subject was calculated as the expected value of the posterior distribution. The number of intact proviruses was calculated as the frequency of cells with total HIV-1 DNA times the frequency of intact proviruses estimated for each subject using an empirical Bayesian model.

Correlation plots

All data sets except the percent of intact proviruses followed a log distribution and were log transformed. The log transformed data met the D'Agostino-Pearson test for

normal distribution, and Pearson correlations were performed on log transformed data. For the QVOA data in which one of the samples was below the limit of detection, the median posterior estimate of infection frequency was plotted instead. $P < 0.05$ was considered statistically significant. GraphPad Prism software was used to perform all statistical tests and correlation plots.

2.5 Tables: Chapter 2

Table 2.1 Study Participant Characteristics

Pt. ID	Age	Sex	Race[a]	ART regimen	Infection duration (months)	Time on ART (months)	Time on suppressive ART (months)[b]	Treatment start time after infection (days)[c]	Viral load (copies/ mL)[d]
2453	59	M	W	TDF/FTC, NVP	134	133	130	24	<50
2454	34	M	W	TDF/FTC/RPV	85	84	77	17	<50
2443	52	M	W	TDF/FTC/EVG/COBI	80	79	70	29	<50
2529	32	M	AS	TDF/FTC/RPV	29	26	25	97	<50
2521[e]	47	M	W	TDF/FTC, DGV	17	15	8	53	<50
3693	46	M	W	TDF/FTC, DGV	11	10	9	25	<50
2286	49	M	W	TDF/FTC/RPV	147	145	142	39	<50
2609	33	M	W	ABC/3TC/DTG	26	24	20	50	<50
2531	40	M	W/LA	TDF/FTC, RAL	34	32	28	57	<50
CP01	64	M	LA	TDF, 3TC, ETR	>179	130	127	>180	<50
CP02	61	M	AA	ABC/3TC, DRV/r, RAL	131	89	58	>180	<50
CP03[f]	76	M	W	ABC/3TC, ATV/r	>194	192	191	>180	<50
CP04	49	F	AA	TDF/FTC/EFV, DRV/r	322	210	129	>180	<50
CP05	56	F	AA	ABC, FTC, ETR, RAL	>214	>187	31	>180	<50
CP06	64	M	W	ABC, FTC, ETR	>263	>203	103	>180	<50
CP07	36	M	N/A	TDF/FTC/EFV	>124	65	55	>180	<50
CP08	45	M	AA	ETR, MVC, RAL	>131	>53	16	>180	<50
CP09	45	M	AA	3TC, DRV/r, RAL	311	132	103	>180	<50
CP10	58	M	AA	ETR, DRV/r, RAL	261	>189	91	>180	<50
VM01	33	M	AA	TDF/FTC/EFV	137	106	-	>180	4,719
VM02	20	M	AA	-	unknown	-	-	-	101,484

[a]AA, African-American; W, Caucasian; AS, Asian; LA, Latino; N/A, Not reported. Race was self-reported by study participants.

[b]Time of continuous suppression of plasma HIV-1 RNA to <50 copies/mL prior to enrollment.

[c]Treatment initiated within the first 3 months of infection is considered to be treated in the acute phase of infection.

[d]Plasma HIV-1 RNA levels for all patients were <50 copies/mL for at least 8 months before this study.

[e]Subject had a blip (~1000 copies/mL) 4 months before sampling. Proviral sequences from this individual are shown but were excluded from any analyses of reservoir size.

[f]Subject may have initiated treatment early in the course of infection but records are unclear and there is no prior negative HIV-1 test. Thus this individual is included as a chronically-treated subject.

Drug abbreviations ABC, abacavir; ATV, atazanavir; COBI, cobicistat; DRV, darunavir; DTG, dolutegravir; EFV, efavirenz; EVG, elvitegravir; ETR, etravirine; FTC, emtricitabine; MVC, maraviroc; NVP, nevirapine; RAL, raltegravir; RPV, rilpivirine; TDF, tenofovir disoproxil fumarate; 3TC, lamivudine; /r, boosted with ritonavir.

Table 2.2 PCR Primers and conditions

PCR	Length	Primer Name	HXB2 position	Primer sequence	Extension time
Outer PCR	9,064	BLOuterF	623 – 649	AAATCTCTAGCAGTGGCGCCCGAACAG	10 m
		BLOuterR	9,662 – 9,686	TGAGGGATCTCTAGTTACCAGAGTC	
Inner PCRs					
gag	1,448	5GagIn	836 – 857	GGGAAAAAATTCGGTTAAGGCC	1 m 30 s
		3GagIn	2,264 – 2,283	CGAGGGGTCGTTGCCAAAGA	
env	2,841	5EnvIn	6201-6231	GAGAAAGAGCAGAAGACAGTGGCAATGAGAG	3 m 30 s
		3EnvIn	9007-9042	CTTGTAAGTCATTGGTCTTAAAGGTACCTGAGGTCTG	
A	4,449	275F	646 – 666	ACAGGGACCTGAAAGCGAAAG	5 m
		3INOut	5,072 – 5,094	AATCCTCATCCTGTCTACTTGCC	
B	5,793	263F	651 – 672	GACCTGAAAGCGAAAGGGAAAC	6 m
		3AccOut	6,421 – 6,443	GGCATGTGTGGCCCARAYATTAT	
C	6,385	5INOut	3,248 – 3,270	ACTCCATCCTGATAAATGGACAG	6 m 30 s
		BLInnerR	9,604 – 9,632	GCACTCAAGGCAAGCTTTATTGAGGCTTA	
D	4,778	5AccOut	4,899 – 4,922	CGGGTTTATTACAGGGACARCARA	5 m
		280R	9,650 – 9,676	CTAGTTACCAGAGTCACACAACAGACG	

Outer PCR cycling conditions:
94°C for 2 m; then 94°C for 30 s, 64°C for 30 s, 68°C for 10 m for 3 cycles; 94°C for 30 s, 61°C for 30 s, 68°C for 10 m for 3 cycle; 94°C for 30 s, 58°C for 30 s, 68°C for 10 m for 3 cycle; 94°C for 30 s, 55°C for 30 s, 68°C for 10 m for 21 cycle; then 68°C for 10 m. (30 total cycles)

Inner PCR cycling conditions: (**X** = extension time from the table above)
94°C for 2 m; then 94°C for 30 s, 64°C for 30 s, 68°C for **X m** for 3 cycles; 94°C for 30 s, 61°C for 30 s, 68°C for **X m** for 3 cycle; 94°C for 30 s, 58°C for 30 s, 68°C for **X m** for 3 cycle; 94°C for 30 s, 55°C for 30 s, 68°C for **X m** for 36 cycle; then 68°C for **X m**. (45 total cycles)

2.6 Figures: Chapter 2

Figure 2.1 Full Genome Sequencing Method for Proviral DNA

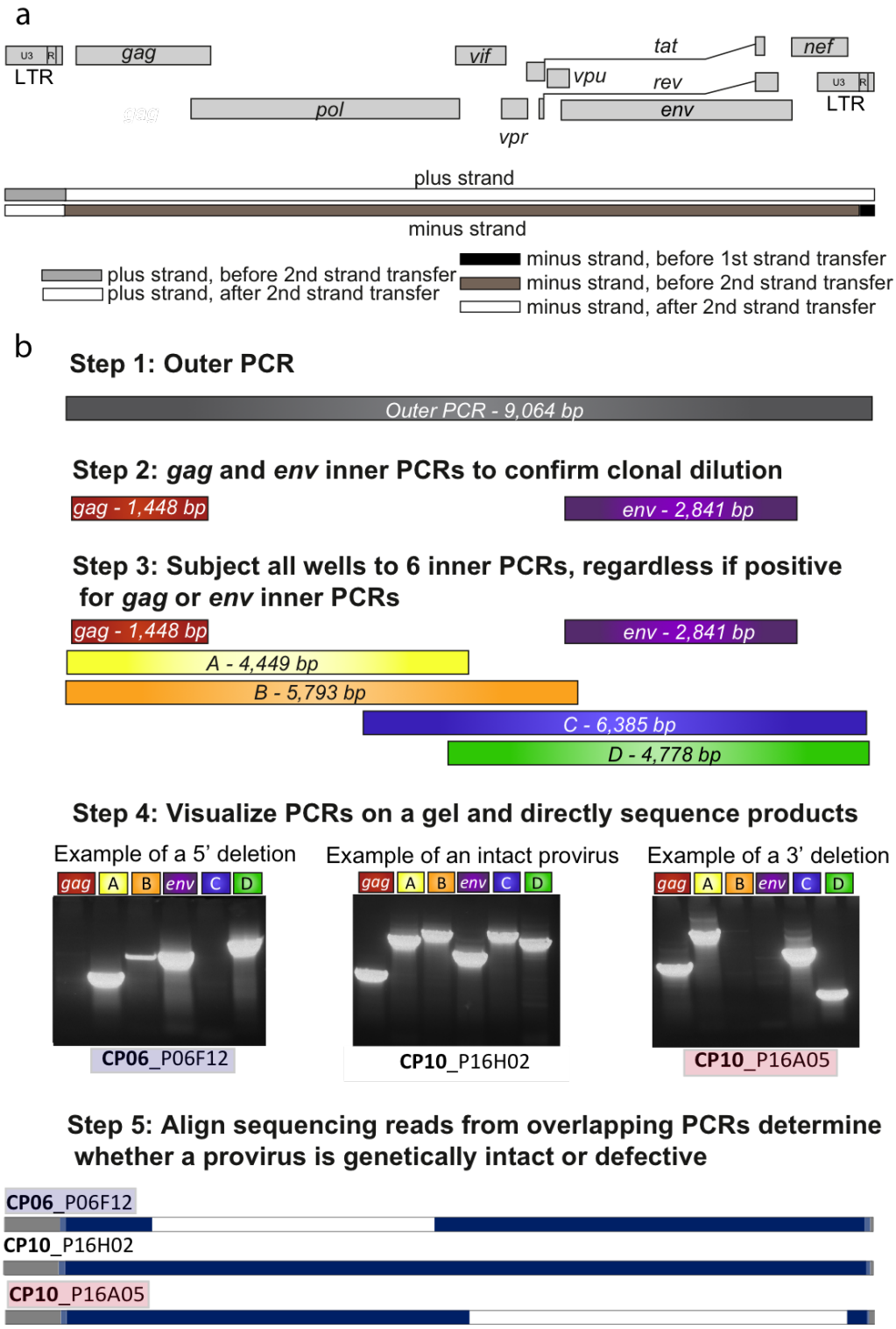

(**a**) Schematic of strand transfer events during reverse transcription relative to the HIV-1 genome. Deletions occur during minus strand synthesis before the second strand transfer event by the same copy choice mechanism that leads to recombination (Hwang et al., 2001). **(b)** Unbiased full genome sequencing strategy based on mechanistic considerations in (a) to capture the majority of defective proviruses. Bands from representative proviruses with a 5' deletion, an intact sequence, and a 3' deletion are shown.

Figure 2.2 Proviral sequences in chronically-treated subjects are highly defective

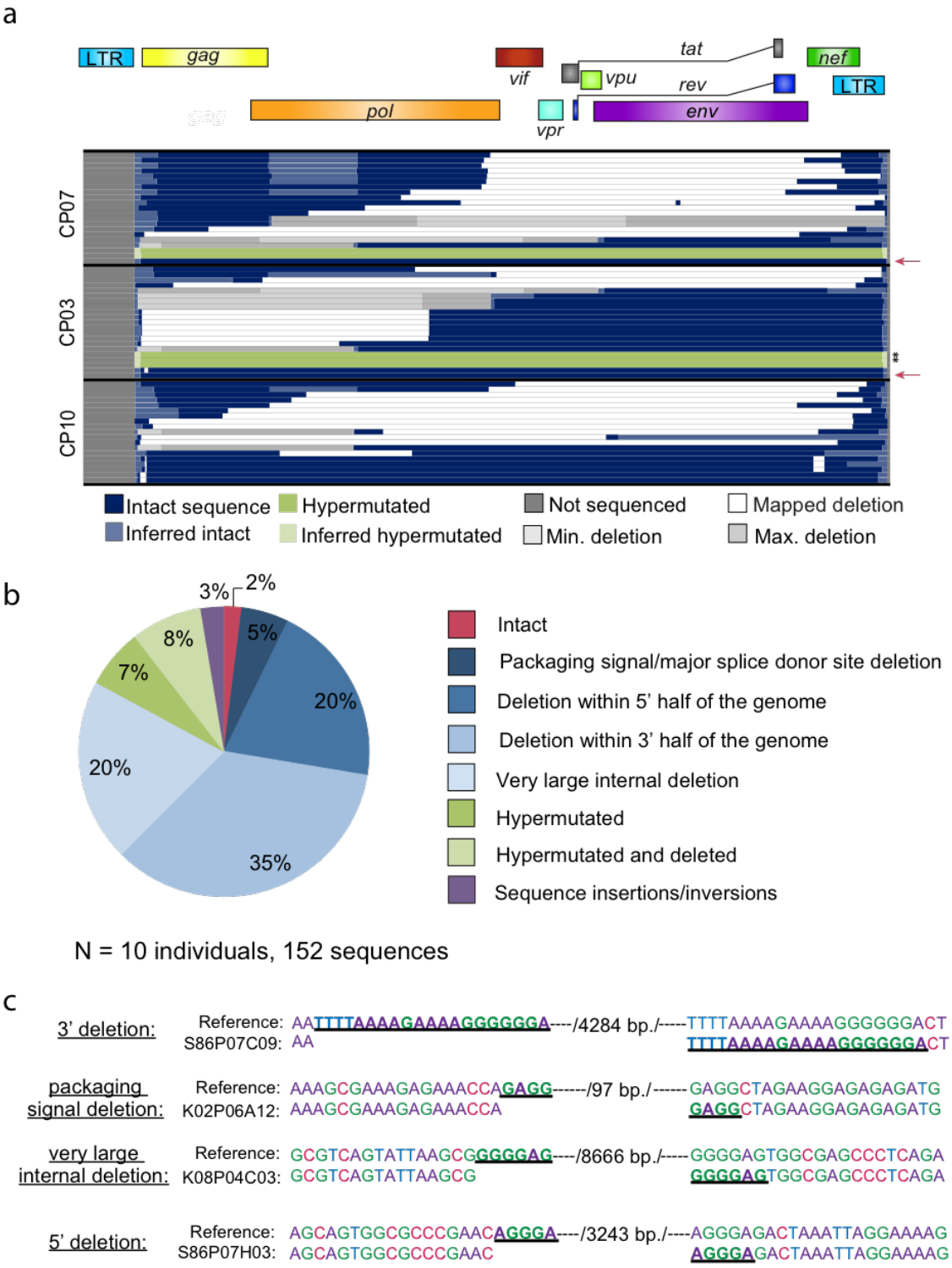

(**a**) Maps of proviral clones from three representative subjects treated during the chronic phase of infection. Each horizontal bar represents an individual clone identified through full genome sequencing. In cases where a deletion could not be precisely mapped due to a deletion encompassing multiple forward or reverse primer binding sites, the possible maximum and minimum deletions sizes are plotted (in grey). If sequencing data shows a mapped deletion that removes primer-binding sites for other amplicons, the resulting missing sequence was inferred to be present (light blue or green). A pink arrow denotes full-length, genetically intact sequences. Black asterisks indicate likely full-length hypermutated proviruses that were not fully sequenced due to extreme hypermutation. See **Figure 2.3** for maps of proviruses from seven additional subjects. (**b**) Summary of 152 proviral sequences. (**c**) Short repeats (underlined) identified on both ends of the deletion junctions are consistent with a copy choice mechanism of recombination resulting in deletion of the intervening sequence and one homology region (/number of basepairs deleted/).

Figure 2.3 Characterization of proviral sequences in subjects initiating ART during chronic infection

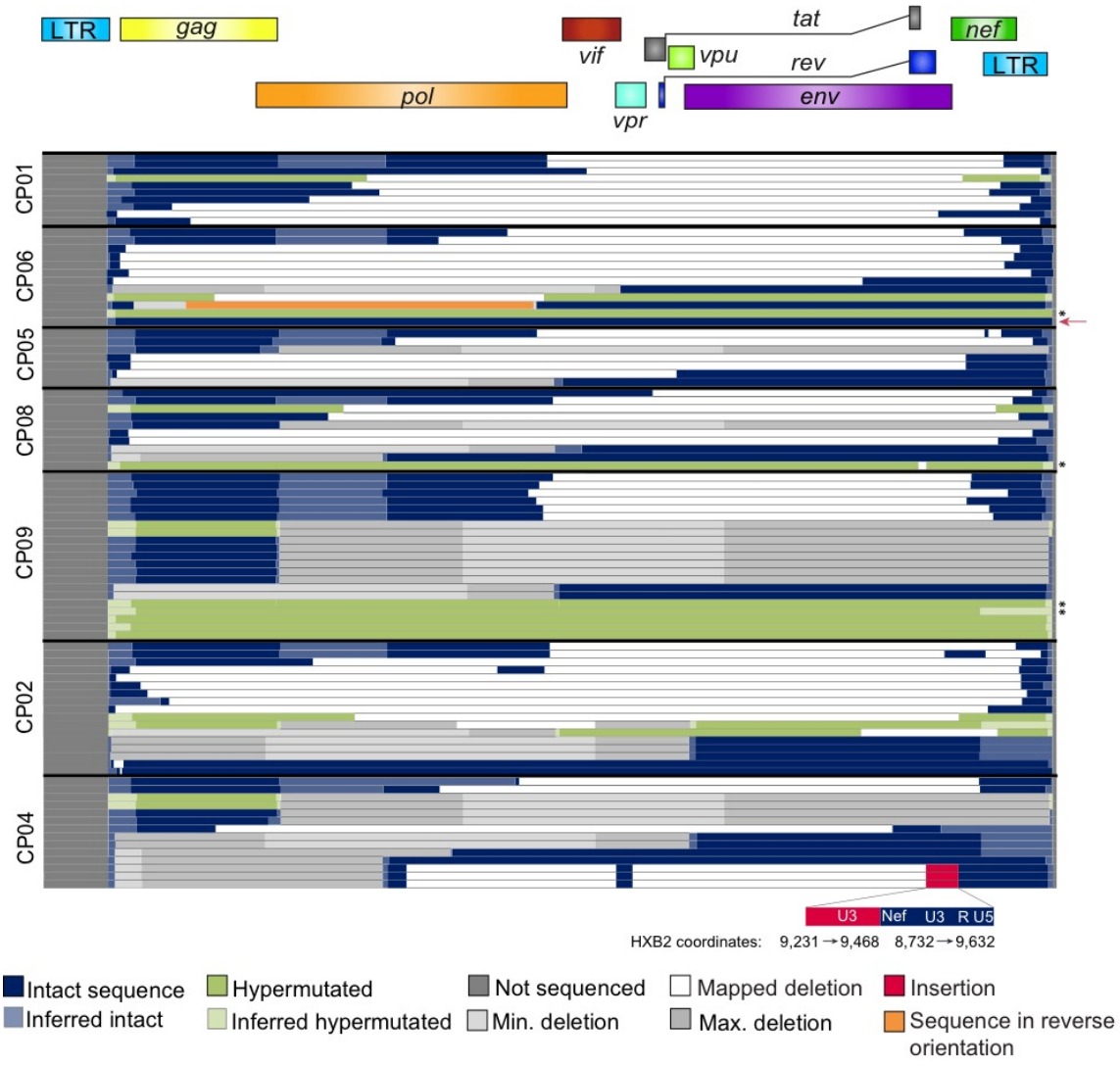

Sequence maps of proviral clones from seven additional subjects treated during the chronic phase of infection. Each horizontal bar represents an individual clone identified through full genome sequencing. In cases where a deletion could not be precisely mapped, likely due to a deletion encompassing multiple forward or reverse primer binding sites, the maximum and minimum deletions sizes are plotted (in grey). If

sequencing data shows a mapped deletion that removes primer-binding sites for other amplicons, the resulting missing sequence was inferred to be present (light blue or green). A pink arrow denotes full-length, genetically intact sequences. Black asterisks indicate likely full-length hypermutated proviruses that were not fully sequenced due to extreme hypermutation.

Figure 2.4 Deletions are nonrandom and occur at hotspots in the HIV-1 genome

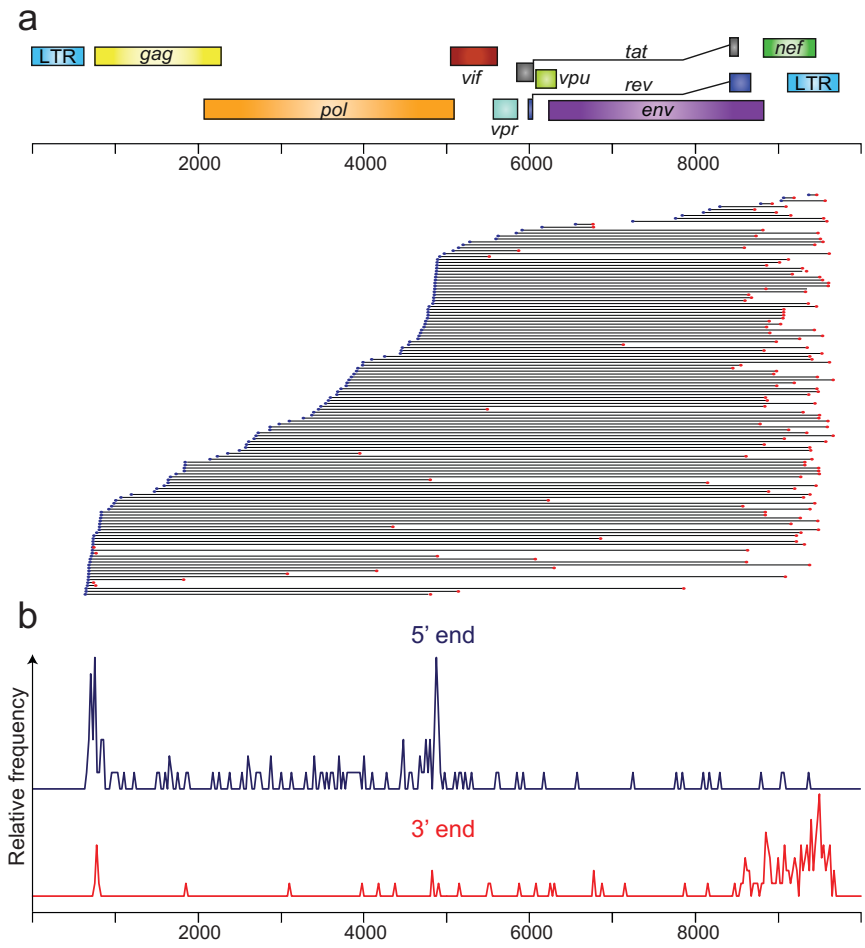

(a) Distribution of deletions in subject sequences. Each horizontal line indicates a unique proviral deletion from a clone identified by near full-length genome sequencing. Sequences from all treated subjects (acute/early and chronic phase) are included. In cases of identical (expanded) clones, only one clone was included in this analysis. For proviral clones with multiple deletions, one horizontal bar is shown for each deletion. Blue and red circles indicate the 5' and 3' ends of the deletion, respectively. **(b)** Distribution of the 5' (blue) and 3' (red) ends of the deletions. Hotspots for deletions, indicated by spikes in the frequency distributions, may be related to structural features in the RNA genome.

Figure 2.5 High proportion of hypermutated sequences contain mutated start codons and premature stop codons

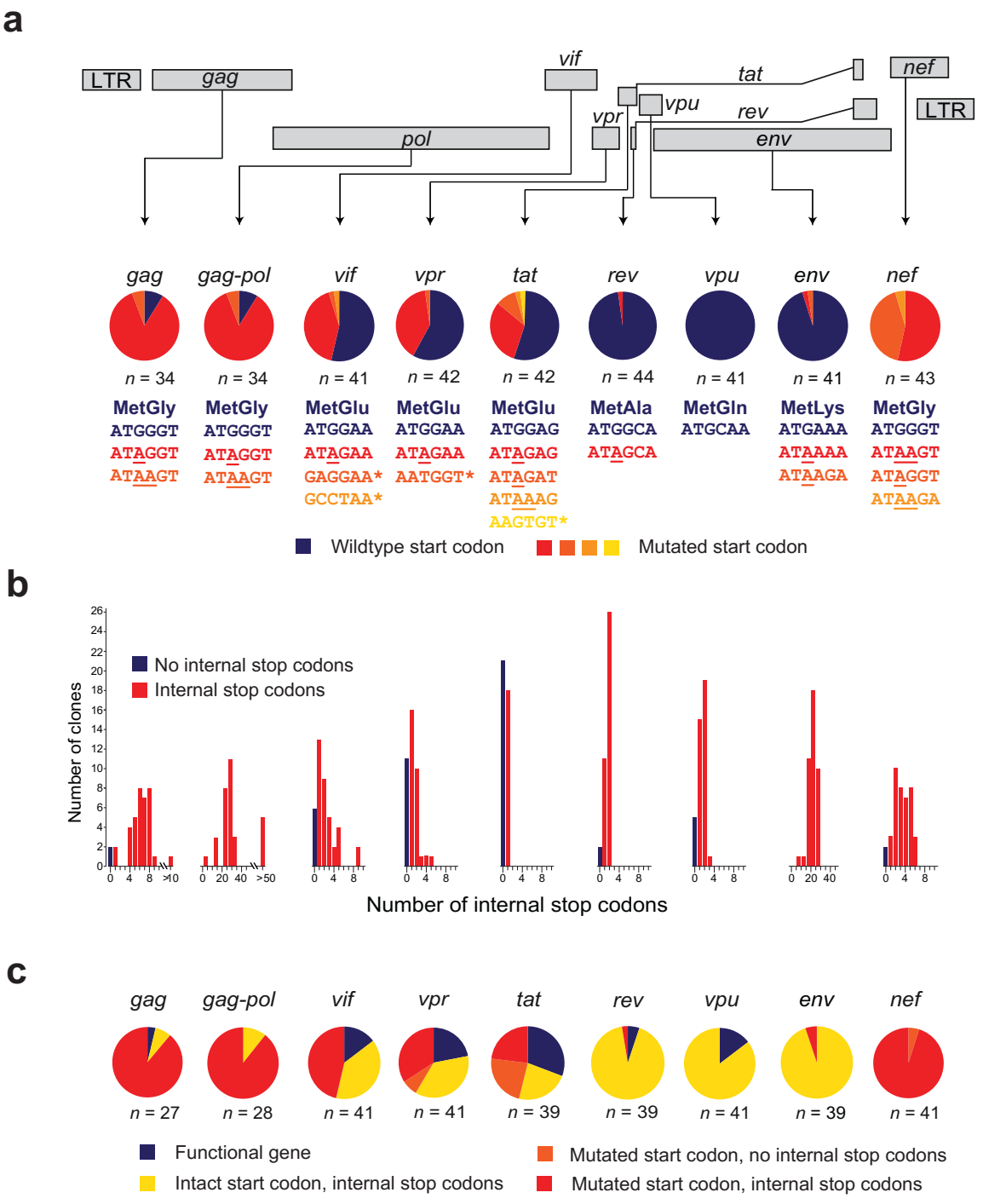

(a) Fraction of hypermutated sequences that contain a functional start codon for each HIV-1 gene. The ATG and second codon as well as the translated amino acid sequence are shown in blue. Sequences with G to A hypermutation by APOBEC3F/G affecting the ATG start codon are shown in red and orange with hypermutated nucleotides underlined. An asterisk denotes other types of mutations affecting the start codon (frameshift mutation, etc). Hypermutated sequences were identified using the Los Alamos hypermut algorithm (Rose and Korber, 2000). This analysis was performed on all unique hypermutated sequences from acute and chronic phase subjects for which the relevant start codon was present. n indicates the number of sequences analyzed. **(b)** Frequency of hypermutated sequences that contain internal, premature stop codons in each HIV-1 gene. Wild type (blue) sequences contained no premature stop codons, and mutated (red) sequences contained 1-50 premature stop codons per gene. **(c)** Frequency of hypermutated sequences that contain functional or defective copies of each HIV-1 gene. Proviruses with both an intact start codon and no internal stop codons were relatively rare and were considered to make a functional copy of a given gene (blue). The remaining proviruses contained defective copies of a given gene and had a functional start codon but contained internal stop codons (yellow), a mutated start codon but no internal stop codons (orange) or contained both a mutated start codon and internal stop codons (red).

Figure 2.6 2-LTR circles are present at low levels in resting CD4$^+$ T cells of subjects treated during acute or chronic infection

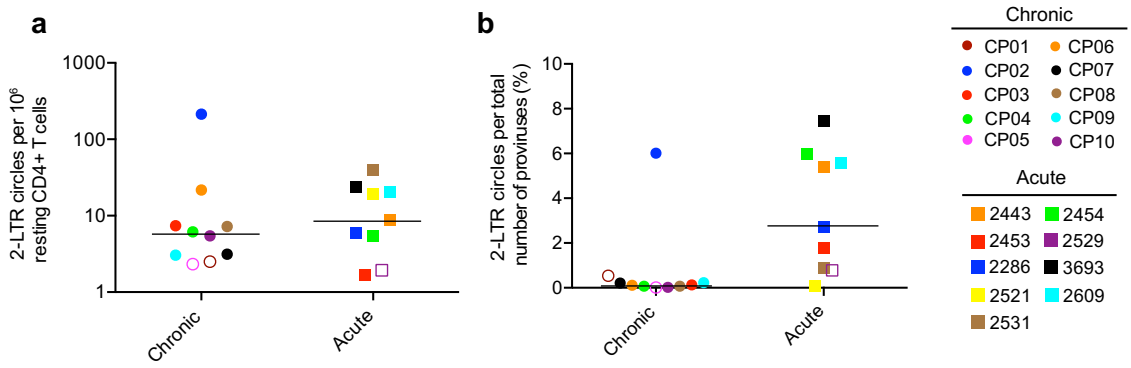

(a) 2-LTR circles were measured by ddPCR (Massanella et al., 2015; Strain et al., 2013). The cellular gene RPP30 was measured in a replicate well by ddPCR and used to calculate the total number of cells. Levels of 2-LTR circles were expressed as a frequency per 10^6 resting CD4+ T cells. In cases where no 2-LTR circles were detected (represented by an open symbol), the limit of detection is plotted as determined by the cellular input for that sample. **(b)** Frequency of 2-LTR circles relative to the total number of proviruses. The number of 2-LTR circles was measured as in (a) and was normalized to the total number of proviruses per 10^6 resting CD4+ T cells. The predicted total number of proviruses was calculated for each subject by correcting the gag ddPCR result (see **Fig. 2.12**) for the fraction of proviruses with deletions in gag.

Figure 2.7 Defective proviruses accumulate rapidly during the course of HIV-1 infection

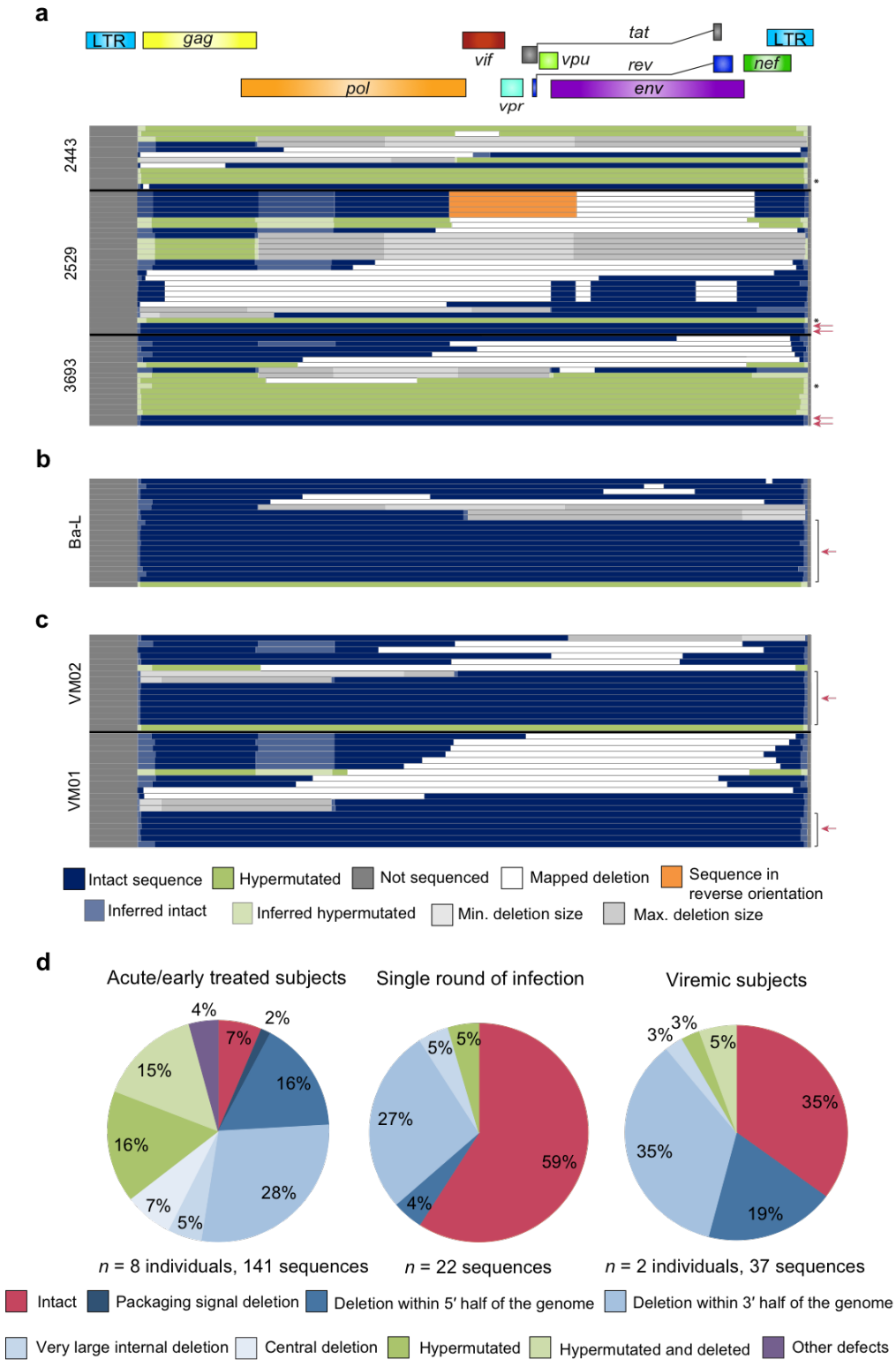

(**a—c**) Maps of independent proviral clones. Each horizontal bar represents an individual clone identified through full genome sequencing. In cases where a deletion could not be precisely mapped, likely due to a deletion encompassing multiple forward or reverse primer binding sites, the maximum and minimum deletions sizes are plotted (in grey). If sequencing data shows a mapped deletion that removes primer-binding sites for other amplicons, the resulting missing sequence was inferred to be present (light blue or green). A pink arrow denotes full-length, genetically intact sequences. Black asterisks indicate likely full-length hypermutated proviruses that were not fully sequenced due to extreme hypermutation. (**a**) Sequences from resting $CD4^+$ T cells of three representative subjects treated during acute/early infection (9 subjects total studied). For additional acute/early subject sequences, see **Fig. 2.8**. (**b**) Sequences identified following a single round of *in vitro* infection of healthy donor $CD4^+$ T lymphoblasts with HIV-1 (Ba-L isolate). (**c**) Sequences from $CD4^+$ T cells from viremic subjects in the chronic phase of infection. (**d**) Summary of all proviral sequences identified from each study population.

Figure 2.8 Characterization of proviral sequences in subjects initiating ART during acute/early infection

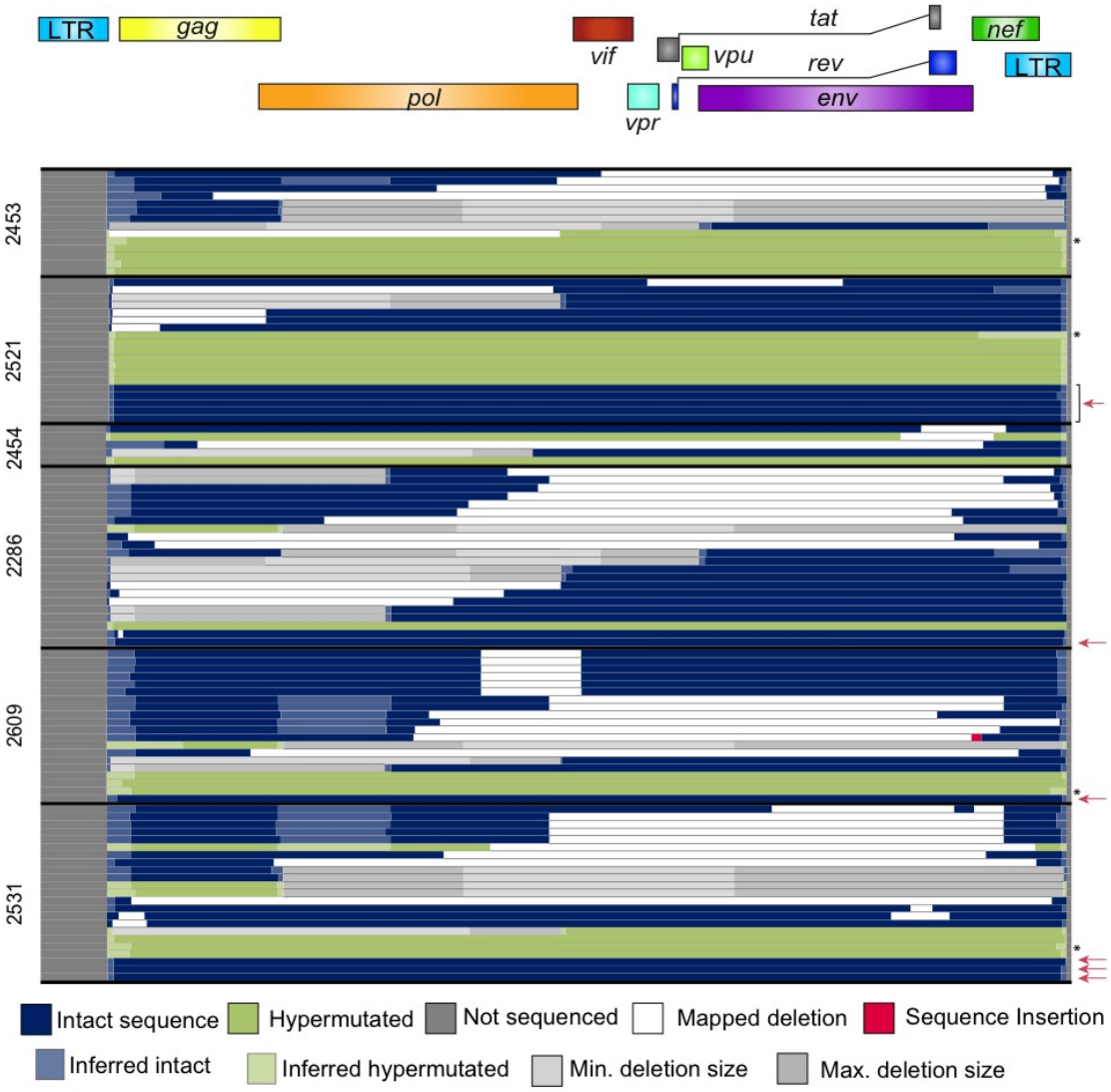

Sequence maps of proviral clones from six additional subjects treated during the acute/early phase of infection. Each horizontal bar represents an individual clone identified through full genome sequencing. In cases where a deletion could not be precisely mapped, likely due to a deletion encompassing multiple forward or reverse primer binding sites, the maximum and minimum deletions sizes are plotted (in grey). If sequencing data shows a mapped deletion that removes primer-binding sites for other

amplicons, the resulting missing sequence was inferred to be present (light blue or green). A pink arrow denotes full-length, genetically intact sequences. Black asterisks indicate likely full-length hypermutated proviruses that were not fully sequenced due to extreme hypermutation.

Figure 2.9 Acutely-treated subjects have a higher fraction of hypermutated proviruses and a lower fraction of deleted proviruses than chronically-treated subjects.

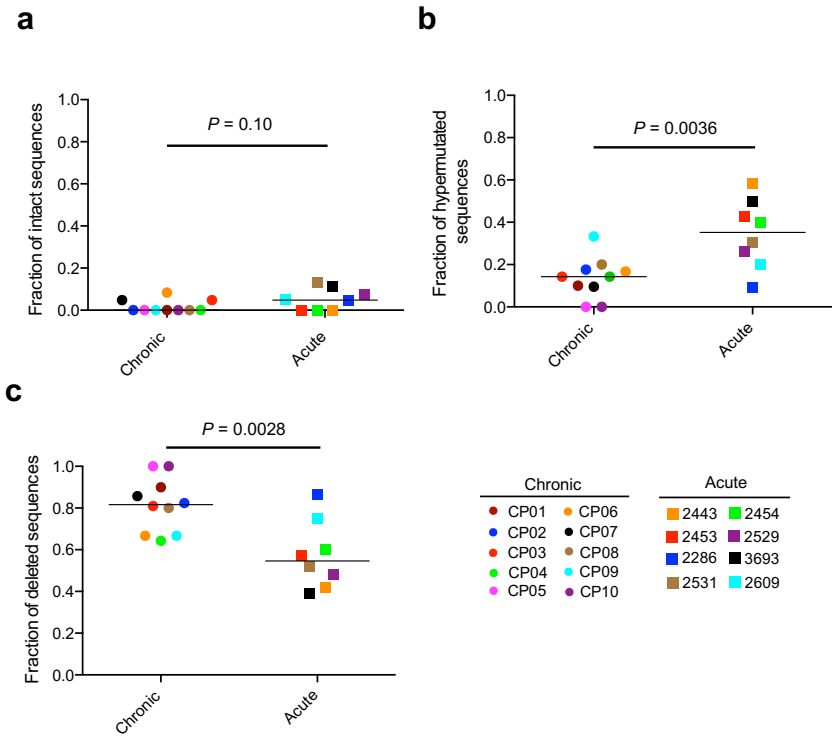

(**a,b,c**) Sequences were obtained by near full-length genome sequencing performed at limiting dilution. Horizontal bars indicate median values. Statistical significance was determined using a two-tailed unpaired t-test. The variance between groups was not statistically different. (**a**) The fraction of intact sequences was calculated by dividing the number of intact clones by the total number of clones observed for each subject. (**b**) The fraction of hypermutated sequences was calculated as described in (a) but using the number of hypermutated clones instead of the number of intact clones. Hypermutation was determined for each sequence by the Los Alamos hypermut algorithm (Rose and Korber, 2000). (**c**) The fraction of deleted sequences was calculated as described in (a) but using the number of deleted clones instead of the number of intact clones.

Figure 2.10 Expanded clones are present in many chronically or acutely treated individuals

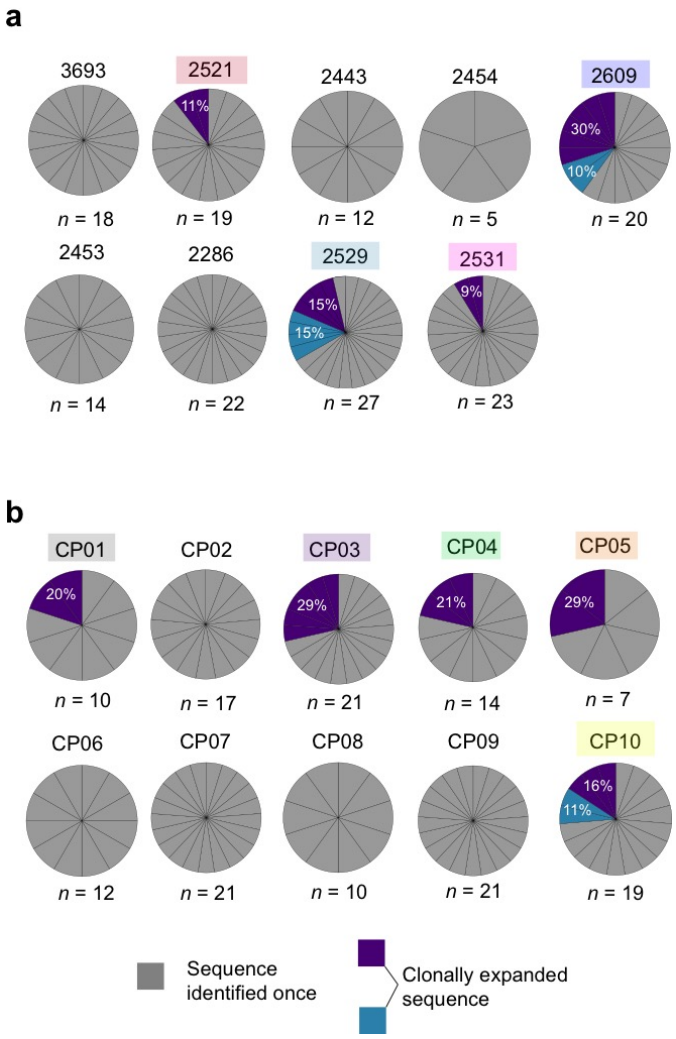

(**a,b**) Proportion of sequences from subjects treated during acute (**a**) or chronic (**b**) infection that are expanded clones. The number of sequences examined for each subject (n) is noted. Expanded clones (purple/blue) are shown as a percentage of total sequences from the relevant subject. Colored boxes denote the subject in which each expanded clone was identified (see **Fig. 2.11a,b**).

Figure 2.11 Expanded clones identified in chronically and acutely treated subjects are grossly defective

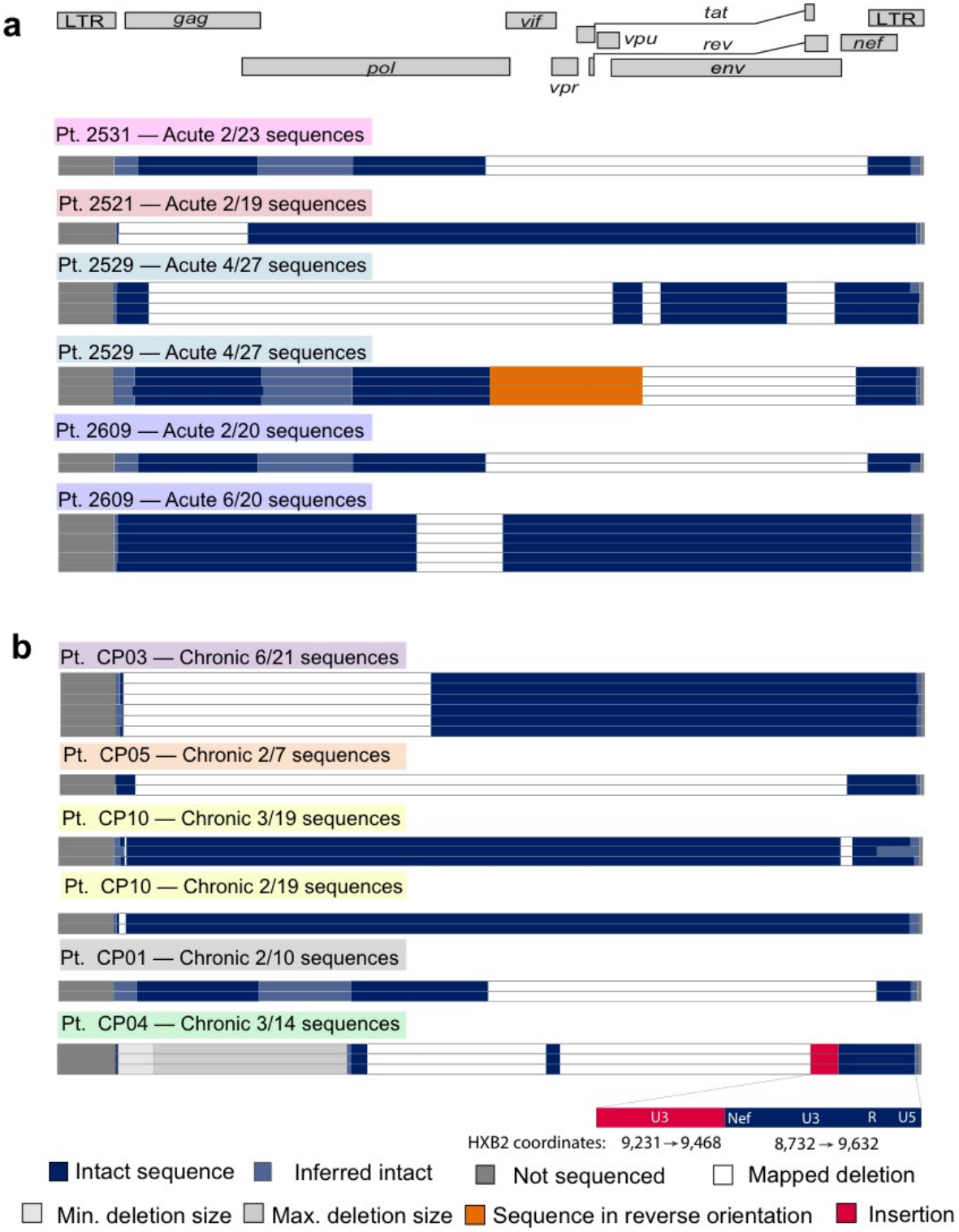

(**a,b**) Maps of expanded HIV-1 clones identified in resting $CD4^+$ T cells from subjects treated in acute (**a**) or chronic (**b**) infection. Expanded clones are defined as clones amplified in completely independent PCR reactions from a single subject that are identical at every nucleotide. The frequency of each clone is shown relative to the total number of clones identified in that subject. Colored boxes denote the subject in which each expanded clone was identified (see **Fig. 2.10a,b**).

Figure 2.12 Current assays significantly underestimate or overestimate the size of the latent reservoir

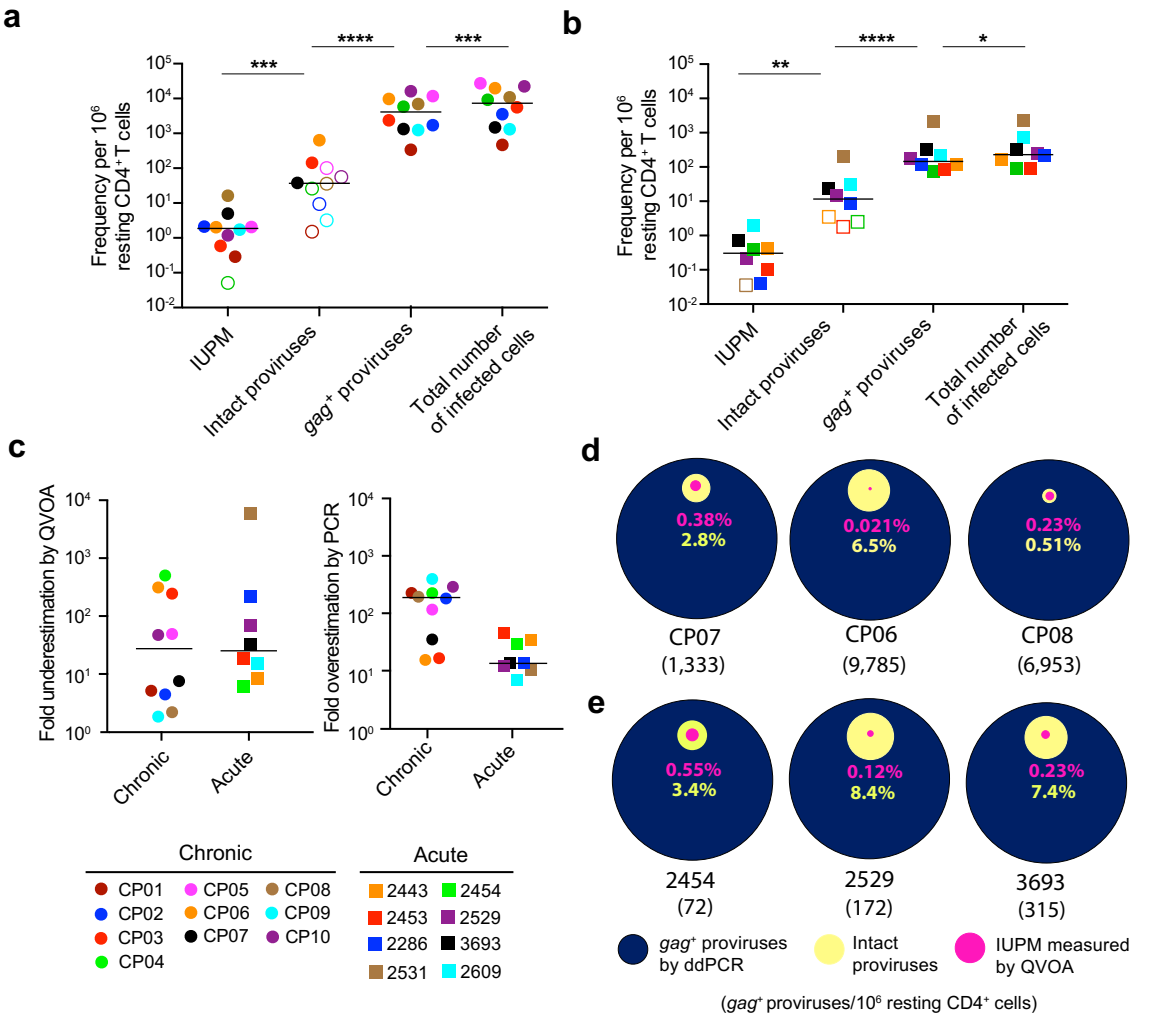

(**a**,**b**) Comparison of different reservoir measurements in resting $CD4^+$ T cells from subjects starting ART during chronic (**a**) or acute (**b**) infection. The frequency of infected cells was measured by QVOA, which detects cells that release infectious virus after one round of T cell activation and is reported as the number of infectious units per million resting $CD4^+$ T cells (IUPM). For individuals in whom the IUPM was below the limit of detection, the median posterior estimate of infection frequency was plotted instead (open symbols). The predicted total number of infected cells was calculated for each subject by

correcting the ddPCR result (gag^+ proviruses) for the fraction of proviruses with deletions in *gag*. The frequency of cells with intact proviruses was calculated as the frequency of infected cells times the fraction of intact proviruses estimated for each subject using an empirical Bayesian model. Open symbols indicate subjects in which no intact proviruses were detected. Horizontal bars indicate median values. Statistical significance was determined using a two-tailed paired t-test and the variance was similar between groups. *$P < 0.05$; ** $P < 0.01$; *** $P < 0.001$; **** $P < 0.0001$. (**c**) Underestimation of the latent reservoir size by the QVOA was calculated by dividing the number of intact proviruses by the QVOA result for each subject. Overestimation of the latent reservoir size by DNA PCR was calculated by dividing the gag^+ provirus PCR values by the number of intact proviruses. Horizontal bars indicate median values. (**d,e**) Comparison of infected cell frequencies as determined by QVOA (pink), analysis of intact proviruses (yellow), and ddPCR for gag^+ proviral DNA (blue) for three representative CP- (**d**) and AP- treated (**e**) subjects. All values are plotted as a percentage of the frequency of cells with gag^+ proviral DNA. The number of gag^+ proviruses per million resting $CD4^+$ T cells as measured by ddPCR is indicated in parenthesis for each subject. For additional subject comparison plots, see **Fig. 2.14**.

Figure 2.13 The number of intact proviruses does not correlate well with current assays

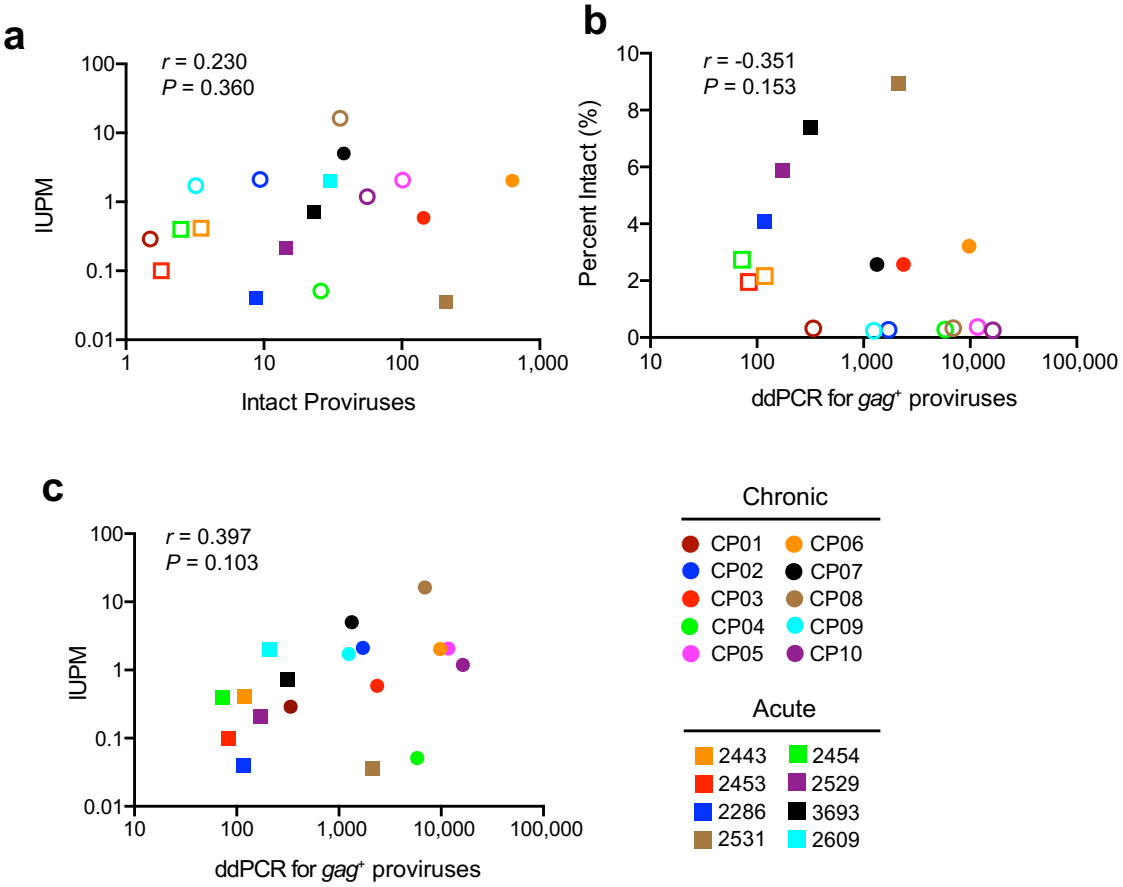

(**a**) Pearson correlation between the number of intact proviruses and the frequency of infected cells as measured by the QVOA (IUPM). The number of intact proviruses was calculated as the frequency of infected cells times the fraction of intact proviruses estimated for each subject using an empirical Bayesian model. Open symbols indicate subjects in which no intact proviruses were detected. (**b**) Pearson correlation between the fraction of intact proviruses and the frequency of cells with gag^+ proviruses as determined by ddPCR (Massanella et al., 2015; Strain et al., 2013). (**c**) Pearson correlation between the IUPM and frequency of cells with gag^+ proviruses as measured in (b).

Figure 2.14 Current HIV-1 reservoir assays exhibit substantial person-person variability

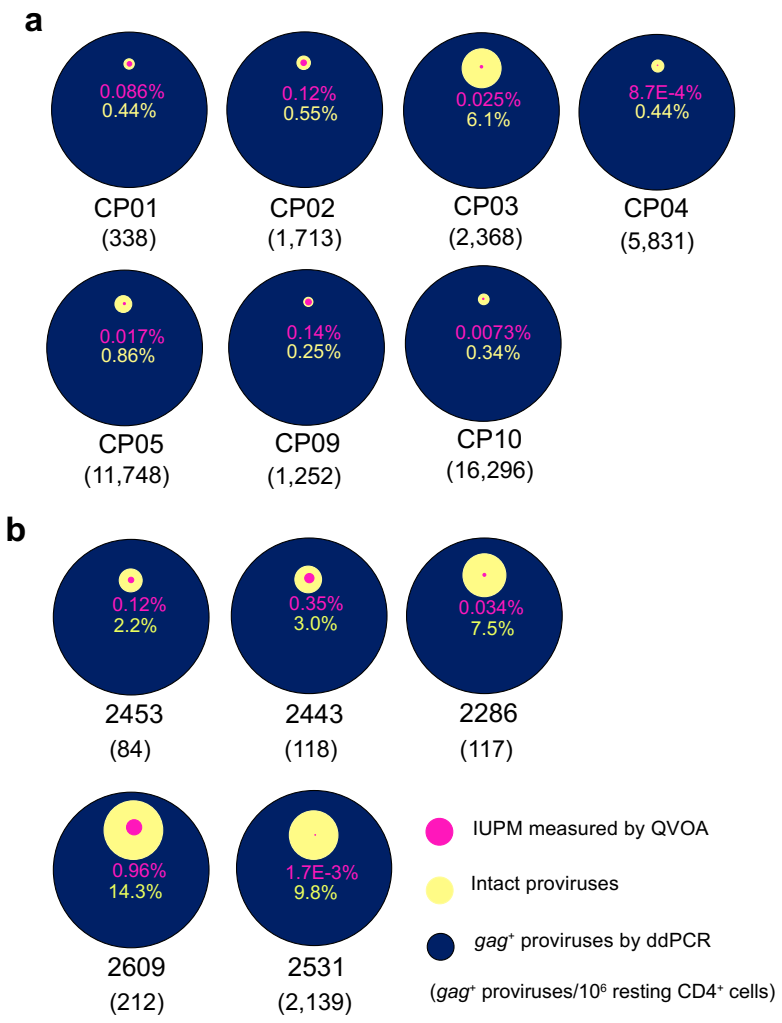

(**a,b**) Comparison of IUPM (pink), number of intact proviruses (yellow), and *gag*$^{+}$ proviral DNA (blue). All values are plotted as a percentage of the frequency of cells with *gag*$^{+}$ proviral DNA. The number of *gag*$^{+}$ proviruses per million resting CD4^{+} T cells as measured by ddPCR is indicated in parenthesis for each subject. (**a**) Comparison for subjects treated during chronic infection (**b**) Comparison for subjects treated during acute/early infection.

Chapter 3. A novel droplet digital PCR-based assay for quantifying genetically intact HIV-1 proviruses

3.1 Introduction

HIV-1 preferentially infects activated $CD4^+$ T cells, most of which die via viral cytopathic effects or are cleared by the adaptive immune response. A small fraction of activated $CD4^+$ T cells transition from an activated state to a resting memory state, generating long-lived adaptive immunologic memory. When activated $CD4^+$ T cells that are HIV-1 infected undergo this transition, HIV-1 gene expression largely ceases and the integrated, infectious virus persists as silent integrated genome (Chun et al., 1997a; Finzi et al., 1997; 1999; Wong et al., 1997b). Latently infected cells are present in all infected patients, are not targeted by antiretroviral therapy (ART) (Chun et al., 1997a; Finzi et al., 1997; 1999; Wong et al., 1997b), and persist for the lifetime of infected individuals (Crooks et al., 2015; Finzi et al., 1999; Siliciano and Siliciano, 2005). Because these latently infected cells act as a long-term reservoir for infectious virus, patients must remain on lifelong ART to prevent rebound in viral replication and disease progression, which typically occurs within weeks of stopping therapy (Crooks et al., 2015; Finzi et al., 1999; Siliciano and Siliciano, 2005). The latent HIV-1 reservoir is recognized as the primary barrier to curing HIV-1 infection.

An international effort is underway to eliminate latent HIV-1 and cure the infection (International AIDS Society Scientific Working Group on HIV Cure et al., 2012). A number of drug candidates targeting latent HIV-1 have been tested in Phase I clinical trials (Archin et al., 2012a; 2014; Rasmussen et al., 2014a; Søgaard et al., 2015;

Wei et al., 2014), and many more are in development (Xing and Siliciano, 2013). However, therapeutic development is severely hindered by the lack of an accurate, rapid, and scalable test to measure latent HIV-1 in a clinical setting (Crooks et al., 2015).

The measurement of latent HIV-1 is technically challenging. The Siliciano Lab originally developed the first method for detecting latent HIV-1 using the quantitative viral outgrowth assay (QVOA) (Finzi et al., 1997; Siliciano and Siliciano, 2005). This assay requires 180 mL of patient blood and relies on two to three weeks of expansion of infectious HIV-1 in tissue culture to detect latent HIV-1. A more rapid version of the QVOA, requiring only a single week of HIV-1 expansion has also been developed (Laird et al., 2013), however neither version of the QVOA is scalable for clinical use. Recent studies have further shown that the QVOA underestimates the true size of the latent reservoir by 25 to 62 fold (Bruner et al., 2016; Ho et al., 2013a). The design of an accurate PCR-based molecular assay to measure latent HIV-1 is also technically challenging, primarily due to the abundance of defective HIV-1 DNA present in memory $CD4^+$ T cells (Bruner et al., 2016; Ho et al., 2013a), obscuring the measurement of intact, latent HIV-1. As such, current PCR-based assays measuring total HIV-1 DNA overestimate the size of the LR by approximately 188-fold and cannot specifically measure latent HIV-1 (Bruner et al., 2016).

To overcome the critical technical hurdles of standard DNA PCR we designed the intact proviral DNA assay (IPDA). In this assay, we use multiplex digital droplet PCR to specifically detect and quantify genetically intact, latent HIV-1. We analyzed hundreds of full genome sequences from multiple well characterized cohorts (Bruner et al., 2016; Ho et al., 2013a; Imamichi et al., 2016). Through this analysis we identified regions and

features of the HIV-1 genome that, when interrogated simultaneously, specifically distinguish intact HIV from defective genomes.

3.2 Results

We first analyzed full genome sequences from 22 individuals on suppressive ART to determine if a single, strategically placed PCR amplicon could provide discrimination between genetically intact and defective HIV-1 genomes. We performed a sliding window analysis across the HIV-1 genome and determined that defective genomes made up greater than 85% of all the sequences measured by any given amplicon, regardless of where the primers were placed in the genome (**Fig. 3.1a**). Since proviruses with large internal deletions comprise 58-80% of all proviruses and deletions cluster in specific regions of the HIV-1 genome (Bruner et al., 2016), we assessed whether two strategically placed amplicons interrogated simultaneously could provide substantially better discrimination between genetically intact and defective HIV-1 genomes than a single amplicon alone. Our analysis indicated that there were many possible two amplicon combinations that when interrogated simultaneously would correctly identify greater than 80% deleted proviruses as defective (**Fig. 3.1b**). However, we found that an assay with primers in the packaging signal and a second set placed in certain regions of the *env* gene would identify 90% of deleted proviruses as defective (**Fig. 3.1b**).

Proviruses containing G to A hypermutation comprise 15-31% of all proviruses (Bruner et al., 2016). These inactivating G to A mutations result from cytidine deamination on the HIV-1 minus strand by APOBEC3F or 3G during reverse transcription and can result in in-frame stop codons in viral ORFs (Yu et al., 2004).

Hypermutation frequency directly correlates with HIV reverse transcription dynamics and regions that remain single stranded the longest have the highest rates of hypermutation. This occurs upstream of the HIV-1 poly purine tracts (PPT) and portions of the *env* and the *nef* genes have particularly high levels of hypermutation (Kieffer et al., 2005). Since there was relative flexibility in the placement of the 3' amplicon (**Fig. 3.1b**), we chose the rev response element (RRE), a highly conserved region of the *env* gene, to place our second amplicon of the IPDA. To discriminate hypermutated from intact proviruses in the IPDA, we employ two hydrolysis probes targeting the same position in the HIV-1 genome. One probe is designed against the non-hypermutated sequence and is labeled, producing a fluorescent signal when an intact sequence is present. The other probe is designed against the hypermutated sequence and is labeled with a fluorophore that is not detectable by ddPCR. It binds to hypermutated sequences to prevent labeled probe binding and thus prevent fluorescent signal **(Fig. 3.2a).**

To maximize effective hypermutation discrimination and optimize placement of the second IPDA amplicon, we performed an analysis of hypermutated genomes from HIV-1 infected individuals on suppressive ART. We identified 21% of proviruses with APOBEC3F, 14% with APOBEC3G, and 65% with both APOBEC3F and 3G hypermutation signatures (**Fig. 3.2b**). Since none of the non-deleted hypermutated sequences we examined contained only APOBEC3F hypermutation (**Fig. 3.2b**), we chose to focus on APOBEC3G hypermutation for our hypermutation discriminating probes, which was found in 79% of hypermutated genomes (**Fig 3.2b**). We identified three potential regions in the RRE of *env* that contained two APOBEC3G consensus sites within the length of a standard hydrolysis probe (**Fig. 3.2c**). One of these regions was

consistently hypermutated at both APOBEC3G consensus sites in 95% of hypermutated sequences and had a favorable G/C content for suitable probe design. Thus this region was selected for the second amplicon of the IPDA (**Fig. 3.2c**).

We next examined the probe binding region for the second amplicon of the IPDA in 67 hypermutated sequences obtained through full genome sequencing from 15 donors (Bruner et al., 2016). We also performed additional in-depth sequencing of the *env* gene in 4 additional patients to include multiple hypermutated sequences from the same individual. We found that the specific nucleotides that were mutated varied from sequence to sequence. The most common hypermutation variant, present in 36% of hypermutated sequences, was a single G to A mutation at the first G of each of the TGGG sites, CCTTAGGTTCTTAGGA (**Table 3.1**). An additional 23% of hypermutated sequences contained two G to A mutations at the first two G nucleotides in the TGGG sites CCTTAAGTTCTTAAGA. Other variations of one to three G to A mutations at each APOBEC3G consensus sites were also observed and the sequences and relative frequencies are summarized in **Table 3.1**. To test how our hypermutation discrimination probes performed on these different hypermutation patterns found in HIV-1 infected individuals, we performed site directed mutagenesis of NL4-3 or a patient derived plasmid (Ho et al., 2013a) to create the different hypermutated sequence patterns shown in **Table 3.1**. We performed qPCR on all the constructs using the hypermutation discrimination probes and looked for the signal or absence of signal from the intact and hypermutated probes. The wildtype (intact) probe bound to and fluoresced in less than 5% of the hypermutated sequences. These hypermutated sequences either contained a single mutation at only one of the APOBEC3G consensus sites or were not mutated at

either APOBEC3G site in the probe binding region and were an exact match to the probe sequence (**Table 3.1**), thus it is not surprising that the intact probe bound. We also determined that the hypermutated probe bound to the hypermutated sequences that were an exact match in sequence, CCTTAGGTTCTTAGGA as well as the sequences that were different by a single mutation, either by an addition of another APOBEC3G G to A mutation, CCTTAAGTTCTTAGGA or CCTTAGGTTCTTAAGA or by one fewer G to A mutation, CCTTGGGTTCTTAGGA or CCTTAGGTTCTTGGGA. For sequences that were negative for both probe signals, we ran the qPCR products on a gel to verify the presence of a band. This was to confirm that the PCR reaction itself was successful and that lack of fluorescence was due to probe/template mismatches (data not shown). In the IPDA ddPCR reaction, the hypermutated probe is unlabeled thus only sequences that bind to an intact probe will fluoresce. We determined that the IPDA ddPCR will incorrectly identify, at most, only 5% of hypermutated sequence as intact (**Table 3.1**).

Additionally, we verified the sequence conservation of the primer and probe sets selected for the IPDA. Both sets were highly conserved, as determined by analysis against the Los Alamos National Laboratories HIV Sequence Database. The individual reactions are equivalent in amplicon size, G/C content, and required melt temperature. Primer entropy analysis did not reveal a risk of primer or probe dimerization. NCBI BLAST analysis was performed and showed no risk of non-specific amplification. This was confirmed by the absence of amplification by either primer set when genomic DNA from uninfected donors was used as template. Based on these analyses, we are confident we have optimized the IPDA primers and probes.

In the IPDA, $CD4^+$ T cells are isolated from PBMCs from a standard blood draw of 30 mL (**Fig. 3.3**). The next step in sample processing is the isolation of human genomic DNA (gDNA). The isolation of gDNA causes shearing of intact chromosomal DNA into fragments, and the size and distribution of these fragments depends upon the isolation procedure employed. In the IPDA, individual HIV-1 proviruses are partitioned into individual droplets using ddPCR and are analyzed simultaneously at two regions of the genome via multiplex PCR (**Fig. 3.3**). Droplets containing intact proviruses are identified by successful PCR amplification at both regions (**Fig. 3.4**). The size and distribution of gDNA fragmentation can therefore significantly impact the performance of the IPDA. With increasing amounts of gDNA fragmentation, the probability of shearing intact proviruses during isolation increases, thus leading to increased numbers of false-negative droplets and artificial lower counts of intact HIV-1 proviruses. Conversely, droplet formation and DNA loading per reaction is hindered by high molecular weight gDNA with minimal fragmentation. Thus, we sought to optimize the balance between DNA fragmentation and shearing of proviruses while maximizing DNA loading per reaction well for ddPCR.

The likelihood of shearing an intact provirus using a gDNA isolation protocol which produces a set size and distribution of gDNA fragments can be defined using Poisson statistics. The distance between the two amplicons in the IPDA ddPCR reaction is 7,159bp. We therefore used Poisson statistics to determine the proportion of intact proviruses that would survive gDNA isolation without shearing between these regions (**Fig. 3.5a**). Given an average DNA extraction fragment size of 20-30kb with fragments up to 50kb in size from the QIAamp DNA mini extraction kit, these statistical predictions

predict that 75-80% of the genomes will remain intact and unfragmented. To validate these statistical predictions, we designed two control primer/probes sets in the RPP30 gene spaced approximately the same distance as the packaging signal and *env* HIV-1 sets (**Fig. 3.5b**). We extracted gDNA from uninfected donors using the QIAamp DNA mini extraction kit and performed the multiplex RPP30 assay on the cells. We found that on average 74% of the genomes remained unsheared following DNA extraction and PCR amplification in the ddPCR reaction. This result was reproducible in 3 technical replicates from 4 donors indicating that the amount of fragmentation per gDNA extraction is consistent (**Fig. 3.5c**). We are in the process of optimizing the DNA extraction process to minimize shearing to the HIV-1 genomes in the IPDA.

We validated the specificity of the IPDA ddPCR using plasmid controls containing patient-derived proviral sequence from previous studies (Bruner et al., 2016; Ho et al., 2013a). We used plasmids containing a 5' deletion, 3' deletion, hypermutated genome or intact genome and measured them alone or in combination using the IPDA. The plasmid controls showed the specificity of the IPDA reaction. The 5' deletion plasmid was single positive for the *env* amplicon (**Fig. 3.6a**) and the 3' deletion plasmid (**Fig. 3.6b**) and the hypermutated plasmid (**Fig. 3.6c**) were single positive for the 5' amplicon. The intact NL4-3 plasmid showed mostly double positive droplets (**Fig. 3.6d**). Approximately 5% of the reaction droplets were single positive instead of double positive, most likely due to degradation of the plasmid over time. Additionally, we tested the plasmids in combination by diluting the NL4-3 intact plasmid into mixtures of defective plasmids to mimic a patient sample. We held the amounts of 5' and 3' deletion plasmids constant at 1,000 copies each and diluted 1,000 copies (**Fig. 3.7a**), 100 copies

(**Fig. 3.7b**) and 10 copies (**Fig. 3.7c**) of NL4-3 into the mixture of defective plasmids. In each case, we observed the expected ratio of defective to intact sequence.

We next experimentally assessed the linearity, specificity, and limit of detection of the IPDA on ddPCR. IPDA reactions were performed using either NL4-3 plasmid alone, or NL4-3 spiked into healthy donor gDNA isolated with our optimized protocol. To mimic the range of intact provirus quantities typical of HIV-1 infected patient samples, we spiked NL4-3 in a half-log dilution series ranging from 10,000 copies to 3 copies. We observed strong agreement between the predicted and observed NL4-3 copy numbers detected across the entirety of the dilution series in both the plasmid only and plasmid in healthy donor gDNA reactions (**Fig. 3.8a**). Additionally, we tested an HIV-1 cell line (5b5) that contained one provirus per cell in the same dilution series, with and without additional gDNA added (**Fig. 3.8b)**. Linear regression analysis of both dilution curves indicate that the reactions were linear. A lack of amplification in negative control wells along with the concordance of NL4-3 or HIV-1 cell line copy numbers measured in both the presence and absence of healthy donor gDNA clearly demonstrate that our ddPCR reaction is specific (**Fig. 3.8a,b**). We were able to detect 3 copies per reaction, which was our lowest spiked template concentration, suggesting that our limit of detection is approximately 3 copies. These data clearly demonstrate that our optimized IPDA reaction performs well and is reproducible and linear.

Using the banked samples from HIV-1 infected individuals we had previously characterized using full-genome sequencing and/or the QVOA (Bruner et al., 2016), we performed pilot IPDA measurements on 14 HIV-1 infected patients on ART (**Fig. 3.9**). The majority of these pilot experiments were performed using an older version of the

IPDA with primers in the *gag* gene instead of the packaging signal. The percent of intact sequences observed in these individuals is consistent with previously observed levels from full-genome sequencing (Bruner et al., 2016). For 8 of the 14 HIV-1 infected patients, we were able to assess the correlation between the IPDA and in-depth sequencing we had previously performed (Bruner et al., 2016) and found a statistically significant correlation (Pearson r=0.942, P=0.0005). It is important to note that we were able to detect intact proviruses in both chronic and acutely treated individuals. This indicates that the assay can be used in patients who initiated treatment early in infection and typically have smaller and more difficult to measure reservoirs. This initial correlation indicates that the IPDA effectively distinguishes and quantifies intact HIV-1 proviruses and warrants further studies with additional patient samples.

3.3 Discussion

Despite an international effort to eliminate latent HIV-1 and cure individuals infected with HIV-1, therapeutic development is currently hindered by the lack of an accurate and rapid test to measure latent HIV-1. An accurate measurement of intact HIV-1 proviruses, currently the closest estimate to the true size of the latent reservoir, would be beneficial to both researchers and clinicians alike. While research assays currently exist, they either significantly underestimate or overestimate the size of the latent reservoir and are not scalable for clinical use.

To address this critical need, we developed the intact proviral DNA assay (IPDA), a multiplex digital droplet PCR test capable of quantifying the amount of latent HIV-1 in infected patients. Through an in-depth analysis of over 450 full-genome sequences of

latent HIV-1 from infected individuals, we identified specific HIV-1 genome features that, when interrogated simultaneously, specifically distinguish latent HIV-1 with intact genomes from defective ones. Preliminary results are highly encouraging. The percent of proviruses that are intact in patient samples is consistent with levels reported in previous studies. Preliminary data from eight patients for whom we also have full genome sequencing results shows a strong correlation between the IPDA readout and the percentage of genomes that are intact from full-genome sequencing. Currently, the IPDA reports the percentage of intact genomes relative to the proportions of defective genomes. Ongoing work consists of measuring a cellular gene in a replicate ddPCR reaction. This additional measurement will enable us to report the number of intact genomes per million resting $CD4^+$ T cells, data which would be required to assess changes in the intact population of proviruses that would result from a therapeutic intervention.

We have banked samples from ten patients treated during chronic infection and from eight patients treated during acute infection and have previously performed full genome sequencing, total HIV-1 DNA measurement by ddPCR and the QVOA on these banked samples (Bruner et al., 2016). We plan to compare this data to the final, optimized version of the IPDA, which will allow us to compare our new assay with the existing QVOA and total HIV-1 DNA PCR. Additionally, we can then determine whether there is a correlation between the IPDA and the number of intact proviruses observed from full-genome sequencing, which is likely the best benchmark in the absence of an accurate gold standard assay.

Currently, standard single region PCR-based assays detect primarily defective proviruses with intact proviruses comprising less than 10% of what is measured with a

standard PCR in the *gag* gene, the most commonly used gene for DNA PCR measurements (**Fig. 3.10**). In contrast, the IPDA eliminates 90-95% of the defective proviruses and we predict that 70% of what is detected in the IPDA will be from intact proviruses (**Fig. 3.10**). Thus, by eliminating the majority of defective proviruses, which vastly outnumber intact proviruses (Bruner et al., 2016; Ho et al., 2013a; Imamichi et al., 2016), our assay more accurately measures the true size of the latent reservoir present in an infected individual. Many defective proviruses contain defects that likely preclude elimination by eradication strategies and could obscure the measurement of real changes in the rarer intact proviruses. By measuring primarily intact proviruses, we anticipate our assay will better assess the impact of eradication strategies on the true reservoir of virus that must be eliminated to achieve an HIV-1 cure.

3.4 Materials and Methods

Study subjects

The Johns Hopkins Institutional Review Board and the UCSF Committee on Human Research approved this study. All participants provided written consent prior to enrollment. Eight HIV-1 infected individuals who met the criteria of suppressive ART and undetectable plasma HIV-1 RNA level (< 50 copies per mL) for a minimum of months were enrolled. Two of these participants were recruited from the SCOPE and OPTIONS cohorts at the University of California, San Francisco. CP-treated subjects are defined as subjects starting ART >180 days from the estimated date of infection. AP-treated subjects started ART < 100 days after the estimated date of infection. Table 2.1

details the characteristics of study participants, a subset of whom were used in these experiments.

DNA extractions:

DNA was extracted from $5x10^6$ resting $CD4^+$ T cells using the QIAamp DNA extraction kit following the manufacturer protocol (Qiagen). The DNA was eluted using 100µL of AE buffer to concentrate DNA. The DNA concentration was estimated from the A260/A280 absorptivity ratio using a NanoDrop 2000 spectrophotometer (Thermo Scientific). Where specified, control templates were thoroughly mixed with 500ng of human genomic DNA. This DNA was obtained by identical extraction methods from the PBMCs of HIV negative donors. The DNA was not digested prior to ddPCR. A maximum of 750ng of DNA was loaded per ddPCR reaction well.

Droplet digital PCR preparation and conditions:

The hydrolysis probes used in the ddPCR reactions are very sensitive to freeze thaw and too many freeze thaw cycles impair assay performance. Probes were dispensed into 10uL aliquots immediately upon arrival and stored at -20C. Once a given aliquot was thawed, it was not refrozen or reused for later experiments. A sample volume of 20µL was used for all reactions and contained 10µL of 2x ddPCR supermix for probes (BioRad), primers, probes and template DNA. Primers were each used at a final concentration of 750nM and probes were each used at a final concentration of 250nM. The 20µL PCR reaction mix was loaded into the Bio-Rad QX-100 cartridge with 70µL of oil and droplets were formed following the manufacturer's instructions. The droplets were

carefully transferred to a 96 well plate and sealed for 5 sec using the PX1 PCR Plate Sealer (BioRad). The plate was immediately transferred to the thermocycler and run.

PCR conditions

PCR primers and probe sequences are shown in detail in Table 3.2. The fluorophores and quenchers used for each of the probes are also described. Cycling conditions were as follows: 10 minutes at 95°C, 45 cycles each consisting of a 30 second denaturation at 94°C followed by a 59°C extension for 60 seconds, and a final 10 minutes at 98°C. The ramp rate of the thermocycler was adjusted to 2°C/second. After cycling droplets were analyzed immediately.

Standard curve and plasmid controls

Plasmid concentration was estimated from the A260/A280 absorptivity ratio using a NanoDrop 2000 spectrophotometer (Thermo Scientific) and copy number was calculated using the size of the plasmid and a DNA copy number calculator, http://cels.uri.edu/gsc/cndna.html. A 5' deletion plasmid containing the proviral sequence CP03P22E11, which contains a 5' deletion removing the packaging signal, *gag* gene and the first part of *pol* (Bruner et al., 2016) was used as a negative control for the packaging signal primer/probe set. The 4F11 plasmid containing a 3' deletion removing the *env* gene (Ho et al., 2013a) was used as a negative control for the *env* primer/probe set. The 19CB3 plasmid containing a full-length patient derived hypermutated sequence (Ho et al., 2013a) was used as a negative control for the hypermutation discriminating probes. NL4-3 full length plasmid (AIDS reagent) was used as a positive control for both reactions.

Data analysis

Samples were analyzed using the BioRad QuantaLife software v.1.0.596 using the probe mix triplex assay feature. A positive control HIV-1 cell line was used for gating each population. The software automatically calculates a concentration per μL of reaction mixture as well as a copy number per 20μL well. The total copy number per 20μL well values were reported from the software for all populations, packaging signal$^+$ only, *env*$^+$ only, and packaging signal$^+$ and *env*$^+$ double positive. The percent intact from ddPCR was calculated by taking the number of double positive copies/well and dividing by the total number of positive droplets/well (double positive divided by double positive plus both single positive populations). GraphPad Prism software was used to perform all statistical tests and correlation plots. When Pearson correlations were performed, $P < 0.05$ was considered statistically significant.

3.5 Tables: Chapter 3

Table 3.1 Only 5% of patient-derived hypermutated proviruses are predicted to be incorrectly identified as genetically intact by IPDA.

		Wildtype probe	Hypermutated probe	
Sequence	**% hypermutated sequences**	**qPCR**	**qPCR**	**ddPCR**
CCTTGGGTTCTTGGGA*	HXB2 reference genome	✓	×	✓
CCTTAGGTTCTTAGGA	36%	×	✓	×
CCTTAAGTTCTTAAGA	23%	×	×	×
CCTTAGGTTCTTAAGA	13%	×	✓	×
CCTTAAGTTCTTAGGA	11%	×	✓	×
CCTTGGGTTCTTGGGA	3%	✓	×	✓
CCTTGGGTTCTTAGGA	1%	✓	✓	✓
CCTTAGGTTCTTAGAA	2%	×	?	×
CCTTAGGTTCTTGAAA	2%	×	?	×
CCTTAGGTTCTTGAGA	2%	×	?	×
CCTTAAGTTCTTAAAA	1%	×	?	×
CCTTAAGTTCTTAGAA	1%	×	?	×
CCTTGAGTTCTTAGGA	1%	×	?	×
CCTTAGGTTCTTGGGA	1%	✓	✓	✓

* APOBEC3G consensus sites in HXB2 are underlined.

× - Did not fluoresce in qPCR/ddPCR

× - predicted not to fluoresce based on tested hypermutation variants.

✓- produced a fluorescent signal in qPCR/ddPCR

✓- predicted to fluoresce based on tested hypermutation variants.

? - fluorescent signal could not be predicted.

Table 3.2 IPDA Primers and Probes

Primer Name	HXB2 coordinates or Gene	Fluorophore, Quencher	Sequence (5'-3')
Psi_F	692-711		CAGGACTCGGCTTGCTGAAG
Psi_R	797-775*		GCACCCATCTCTCTCCTTCTAGC
Psi Probe	758-740*	FAM, MGB	TTTTGGCGTACTCACCAGT
Env_F	7736-7759		AGTGGTGCAGAGAGAAAAAAGAGC
Env_R	7851-7832*		GTCTGGCCTGTACCGTCAGC
Env_intact	7781-7796	VIC, MGB	CCTTGGGTTCTTGGGA
Env_hypermut	7781-7798	NED, MGB	CCTTAGGTTCTTAGGAGC
RPP30-878-F	RPP30		GACACAATGTTTGGTACATGGTTAAAG
RPP30-878-R	RPP30		CTTTGCTTTGTATGTTGGCAGAAA
RPP30-878-Probe	RPP30	FAM, ZEN/IBFQ	CCATCTCACCAATCATTCTCCTTCCTTC
RPP30-872-F[a]	RPP30		GATTTGGACCTGCGAGCG
RPP30-872-R[a]	RPP30		GCGGCTGTCTCCACAAGT
RPP30-878-Probe[a]	RPP30	VIC, MGB	CTGACCTGAAGGCTCT

*Reverse compliment

[a] modified from Massanella et al. Bio-protocol 5(11): e1492

3.6 Figures: Chapter 3

Figure 3.1 Two amplicons performed in duplex are required to distinguish intact proviruses from deleted ones.

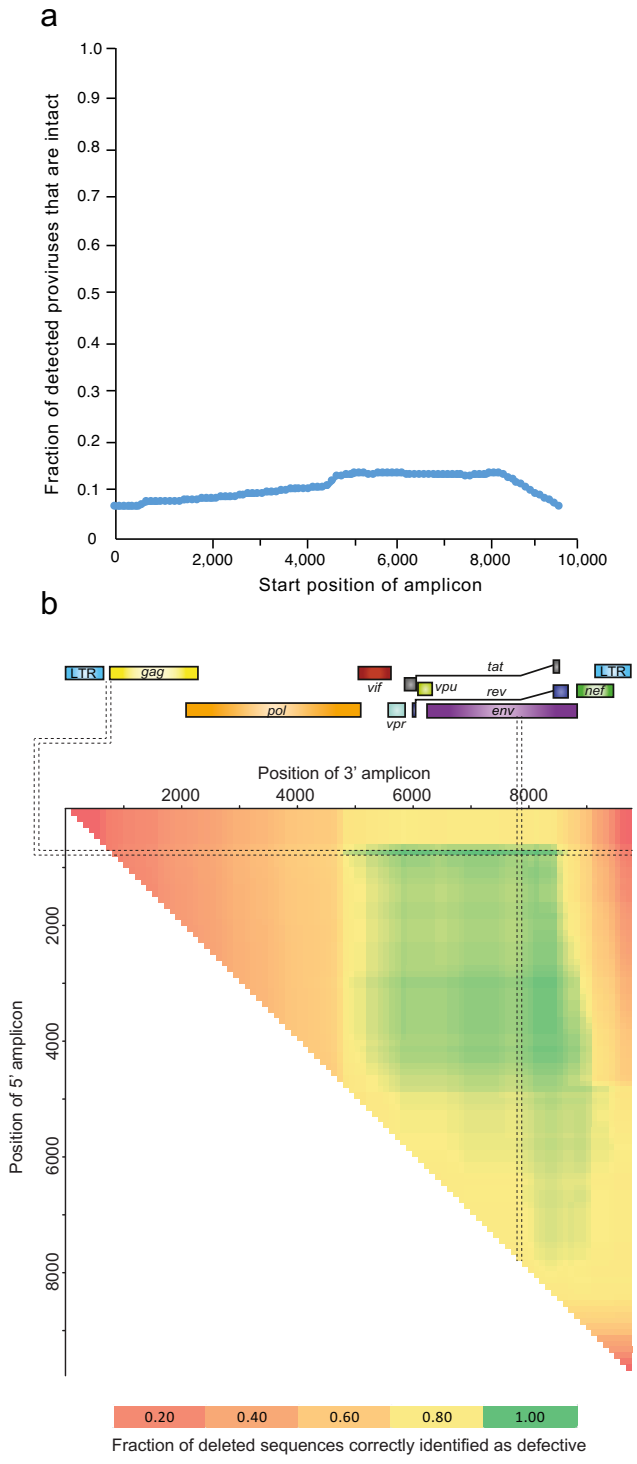

(**a**) Sliding window analysis of theoretical single region PCR amplicons across the HIV genome using 260 full genome sequences from 22 individuals from previously published cohorts (Bruner et al., 2016; Imamichi et al., 2016). Sequences that contained unmapped deletions from the Bruner et al. cohort were excluded from this analysis. Analysis was performed with 100bp increments. The start site of the theoretical amplicons are shown in HXB2 coordinates (x axis) and the proportion of proviruses detected by each amplicon that are actually intact is shown (y axis). (**b**) Sliding window analysis of potential primer locations for a two amplicon, duplex ddPCR assay using 258 full genome sequences from 22 individuals that contained deletions from previously published cohorts (Bruner et al., 2016; Imamichi et al., 2016). Amplicons selected for the ddPCR assay are shown by dotted lines and correctly identify deleted sequences as defective greater than 90% of the time.

Figure 3.2 Hypermutation discriminating probes in the RRE of env should correctly identify 95% of hypermutated sequences as defective.

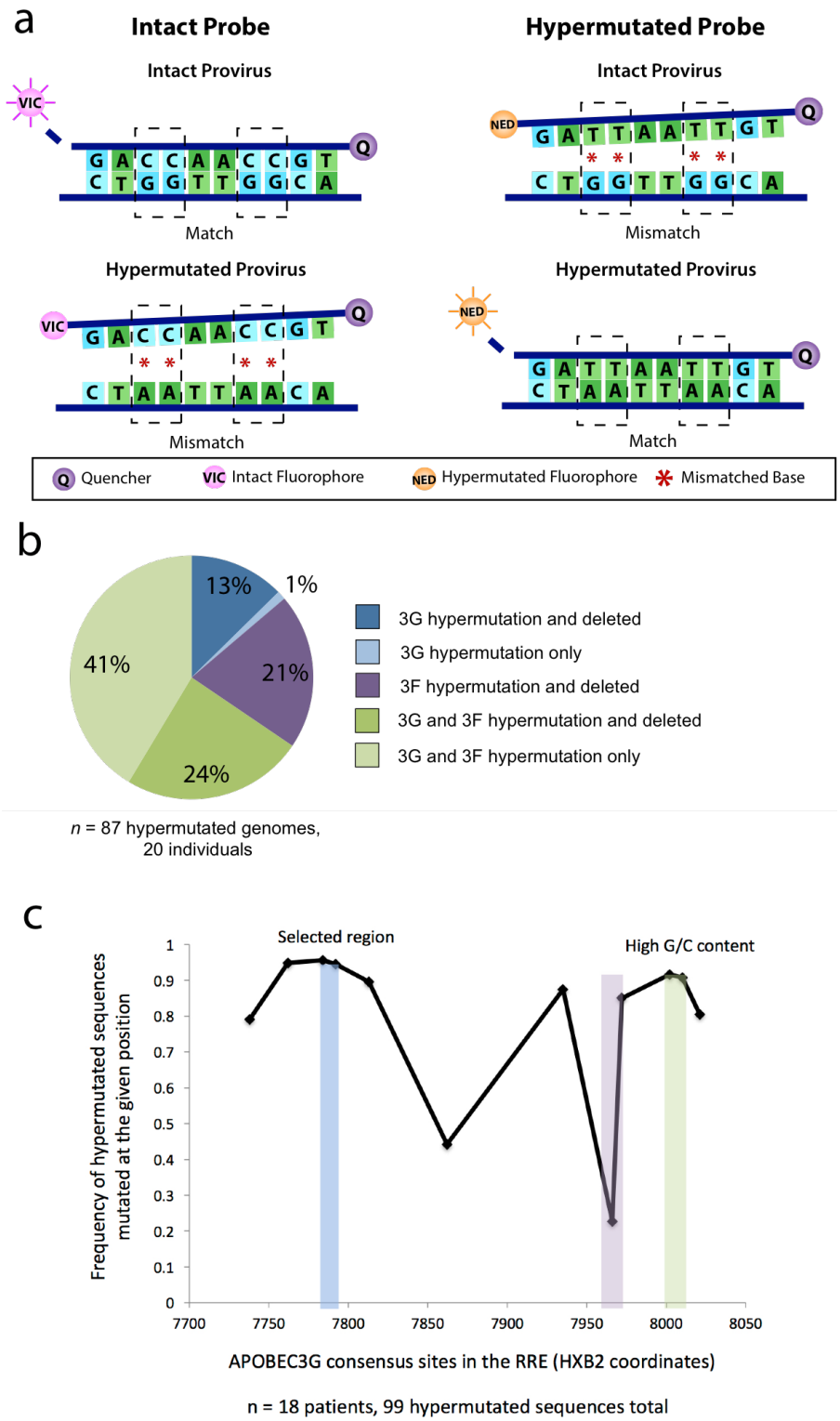

(**a**) Schematic of hypermutation discriminating probes in a hypothetical region of the HIV-1 genome (actual sequence not shown). The intact probe is designed over two APOBEC3G consensus sites (dashed boxes) and directly compliments the nonhypermutated or intact sequence, TGG. The probe will bind and fluoresce when bound to the intact sequence (top left) but will not bind to a hypermutated sequence due to multiple mismatches between the probe and sequence (bottom left). The hypermutated probe is designed over the same two APOBEC3G consensus sites but is designed to match the hypermutated sequence, TAA (top right). The probe will only fluoresce when it binds to a hypermutated sequence and not an intact sequence (bottom right). The hypermutated probe is labeled with a NED fluorophore which is detectable by qPCR but not by the ddPCR. Only the intact probe will produce detectable fluorescence in the IPDA ddPCR. (**b**) Analysis of APOBEC3F and 3G hypermutation in HIV-1 infected individuals. Sequences from existing cohorts (Bruner et al., 2016; Imamichi et al., 2016) were analyzed for APOBEC3F or 3G signatures using the using the full-length sequence for each clone and the Los Alamos hypermut algorithm (Rose and Korber, 2000). (**c**) Analysis of APOBEC3G consensus sites in the RRE of the HIV-1 *env* gene. Each point represents a single APOBEC3G consensus site in the HXB2 reference genome. Three regions (shaded boxes) were identified as having two APOBEC3G sites within the length of a standard hydrolysis probe. One region was excluded for use an IPDA amplicon due to low levels of APOBEC3G at a single site (purple box) and another was excluded because the G/C content of the region was too high for proper probe design (green). The selected region for an IPDA amplicon (blue box) is hypermutated in 95% of hypermutated sequences.

Figure 3.3 Schematic of IPDA workflow and analysis.

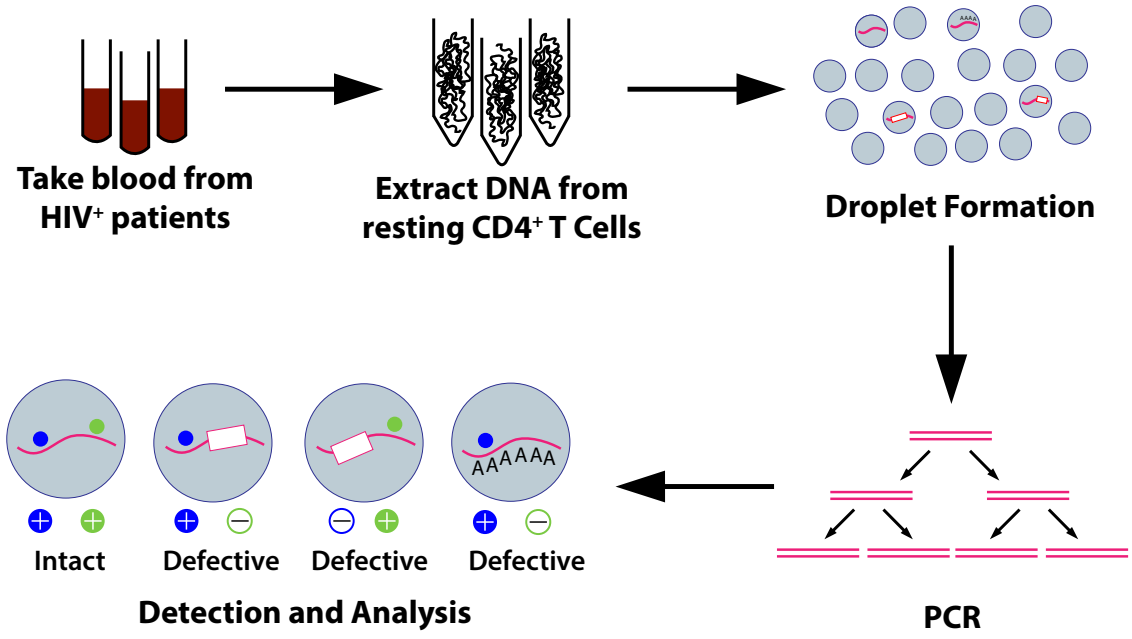

The IDPA workflow begins with a blood draw of ~30mL from an HIV-1 positive individual. Resting cells are purified from whole blood and DNA is extracted and put into the droplet generator of the BioRad QX100 instrument. The sample is partitioned into 20,000 nanoliter droplets which contain the primers and probes for an HIV-1 duplex PCR reaction. The droplets are cycled and then read by the droplet reader as positive or negative for one or both fluorophores. Droplets that are positive for both amplicons are considered to contain an intact provirus.

Figure 3.4 Proposed assay readout for a duplex droplet digital PCR targeting the packaging signal and env regions of the HIV-1 genome.

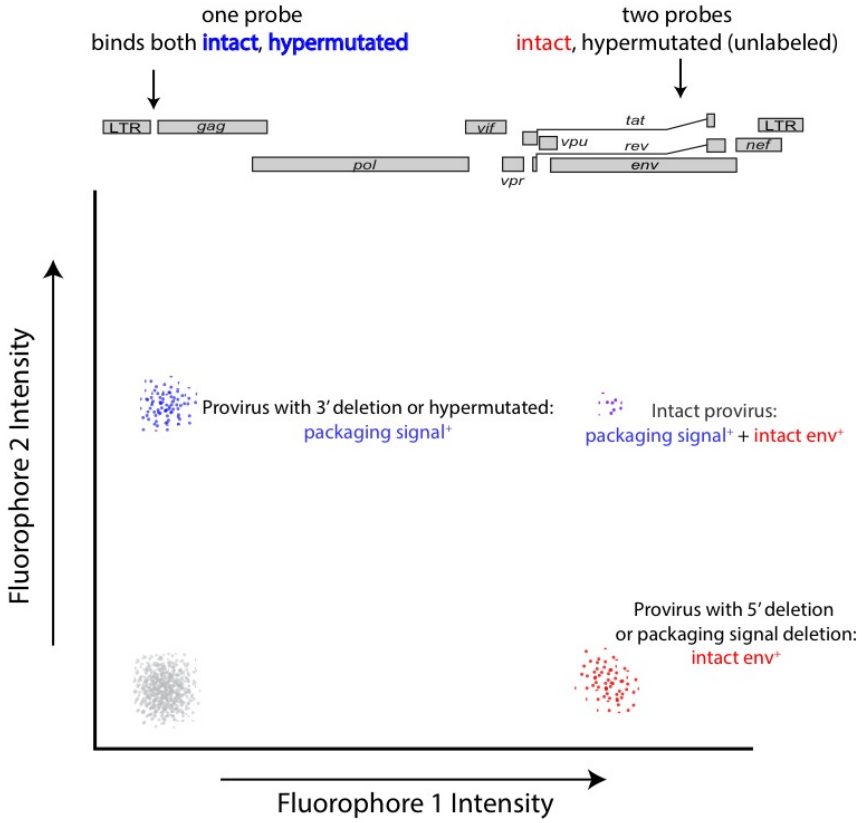

Assay schematic for droplet digital PCR with two amplicons, one in the packaging signal and one in the RRE of the HIV-1 genome. Each amplicon has a probe labeled with a unique fluorophore. The packaging signal amplicon, labeled with fluorophore 2 will detect any proviruses that have a genetically intact packaging signal, including hypermutated proviruses. The *env* amplicon incorporates two probes that can distinguish between hypermutated and non hypermutated (intact) sequence. The probe that binds to hypermutated sequences is unlabeled and the intact probe is labeled (fluorophore 1). Only proviruses that are not hypermutated and not deleted in the region of the probe binding will cause the intact probe to fluoresce. Proviruses that are positive for both fluorophore 1 and 2 are identified as intact proviruses by the assay.

Figure 3.5 Probability of fragmenting DNA between the packaging signal and env amplicons.

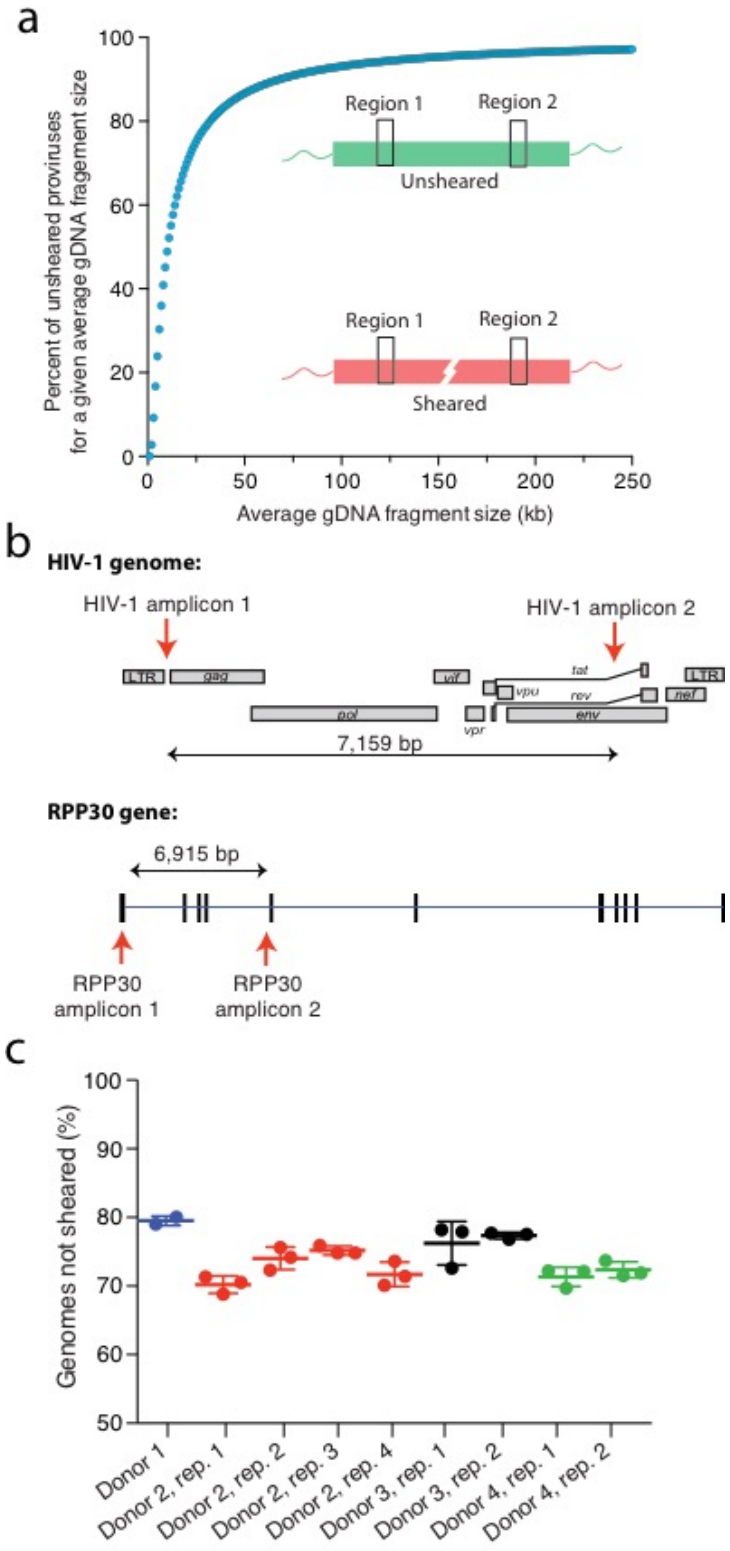

(**a**) Predicted amount of DNA shearing that will occur between two amplicons spaced 7,159 bp apart, the distance between the packaging signal and env amplicons. The amount of DNA shearing between amplicons is dependent on the average size of the genomic DNA fragments from a given DNA extraction method (x axis). Extractions producing large gDNA fragments will have less DNA shearing and ones with small gDNA fragments will have a lower percentage of unsheared proviruses. (**b**) Schematic of the two HIV-1 amplicon locations and the distance between them. The RPP30 control set of two amplicons is shown relative to the 11 exons of RPP30 (black rectangles) and introns (blue line). The distance between the RPP30 amplicons mimics the distance between the packaging signal and env amplicons. (**c**) Levels of DNA fragmentation with the QIAamp DNA extraction kit is reproducible. DNA was extracted from 9 different samples from 4 donors and was subjected to a duplex RPP30 reaction (shown in b). The percent of genomes that were not fragmented was calculated by taking the total number of double positive droplets and dividing by sum of the double positive droplets plus the average of the single positive droplet populations. Each extraction was run in 2-3 replicates on the BioRad QX100 instrument. The mean and standard deviation for each DNA extraction are shown.

Figure 3.6 Plasmids controls show specificity of the IPDA reaction.

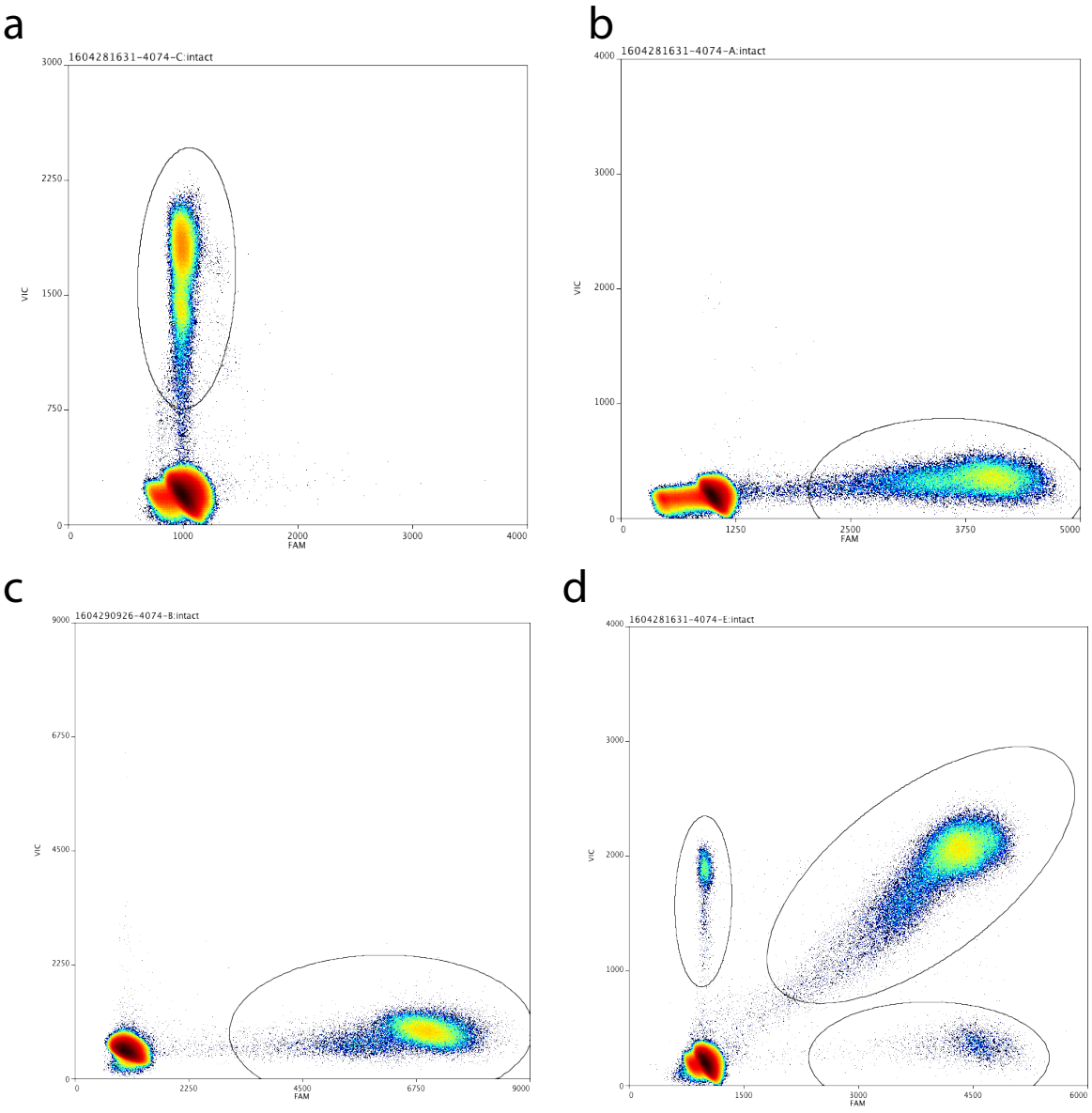

(**a**) The plasmid containing the proviral sequence CP03P22E11 which contains a 5' deletion removing the packaging signal, *gag* gene and the first part of *pol* (Bruner et al., 2016). The plasmid is single positive for the *env* amplicon (y axis). (**b**) The 4F11 plasmid containing a 3' deletion of the *env* gene (Ho et al., 2013a). The plasmid is only positive for the 5'amplicon. In the IPDA this can be a *gag* (shown here) or packaging signal amplicon (x axis). (**c**) The 19CB3 plasmid containing a full-length patient derived

hypermutated sequence (Ho et al., 2013a). The plasmid is single positive for the *gag* or packaging signal amplicon (x axis). The plasmid is hypermutated in the *env* amplicon so the intact hypermutation discriminating probe does not bind. (**d**) NL4-3 full length plasmid, double positive for both amplicons. 5% of the droplets are not double positive, likely due to small amounts of shearing of the genome or plasmid degradation. All experiments were performed on the Raindance droplet digital PCR platform.

Figure 3.7 Mixtures of plasmid controls show expected ratios in the IPDA.

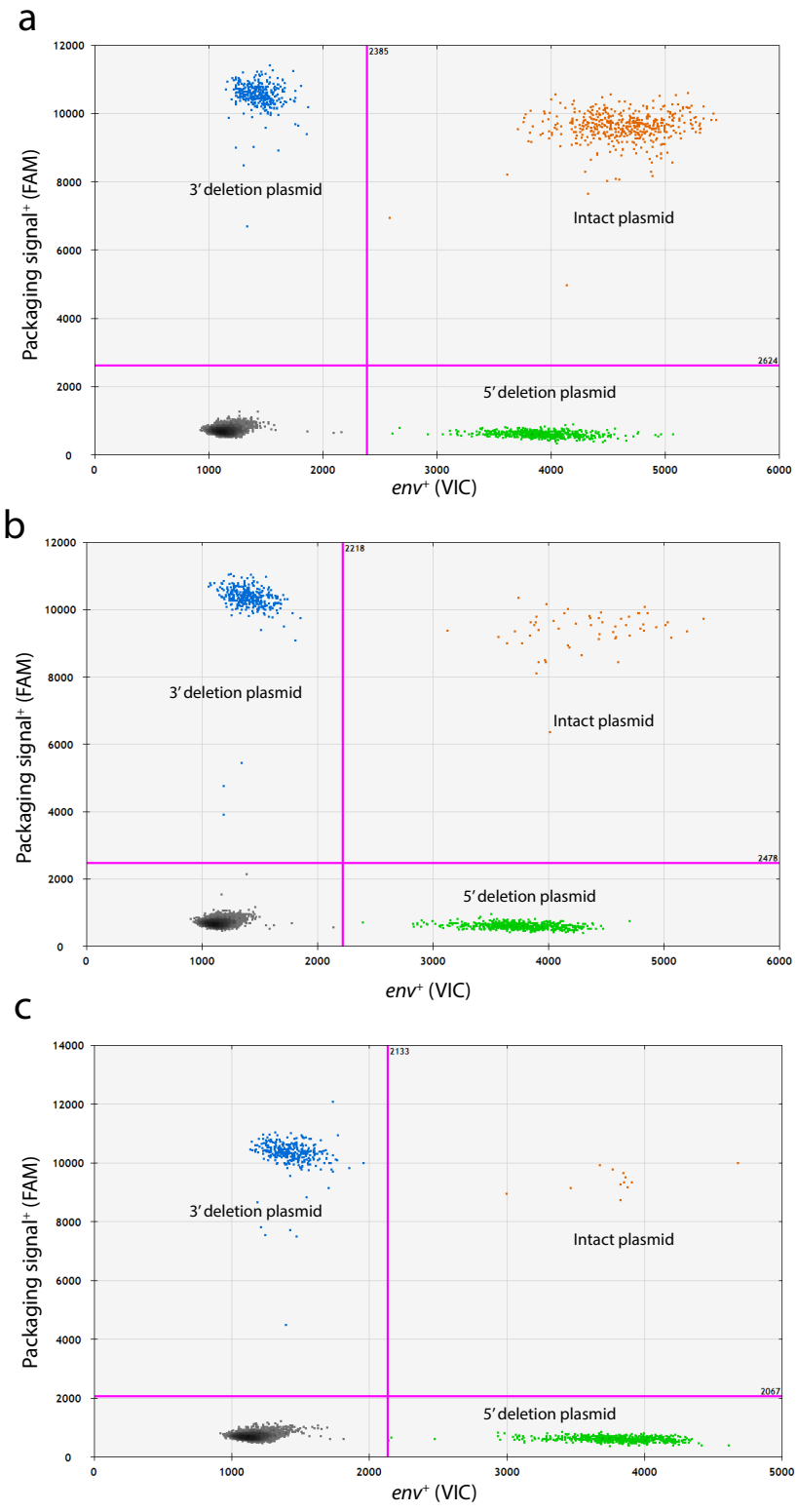

(**a**) Mixtures of 1,000 copies of a 5' deletion plasmid, 3' deletion plasmid and intact plasmid. A 1:1:1 ratio was observed between the three plasmids. See Fig. 3.6 for additional info on the origin of each plasmid. (**b**) Mixture of 1,000 copies each of a 5' deletion plasmid and 3' deletion plasmid and 100 copies of an intact plasmid. A 10:10:1 ratio was observed as expected. (**c**) Mixture of 1,000 copies each of a 5' deletion plasmid and 3' deletion plasmid and 10 copies of an intact plasmid. A 100:100:1 ratio was observed as expected. All experiments were performed on the BioRad QX100 droplet digital PCR platform.

Figure 3.8 Dilution series of HIV-1 controls shows the linearity, specificity and reproducibility of the IPDA ddPCR.

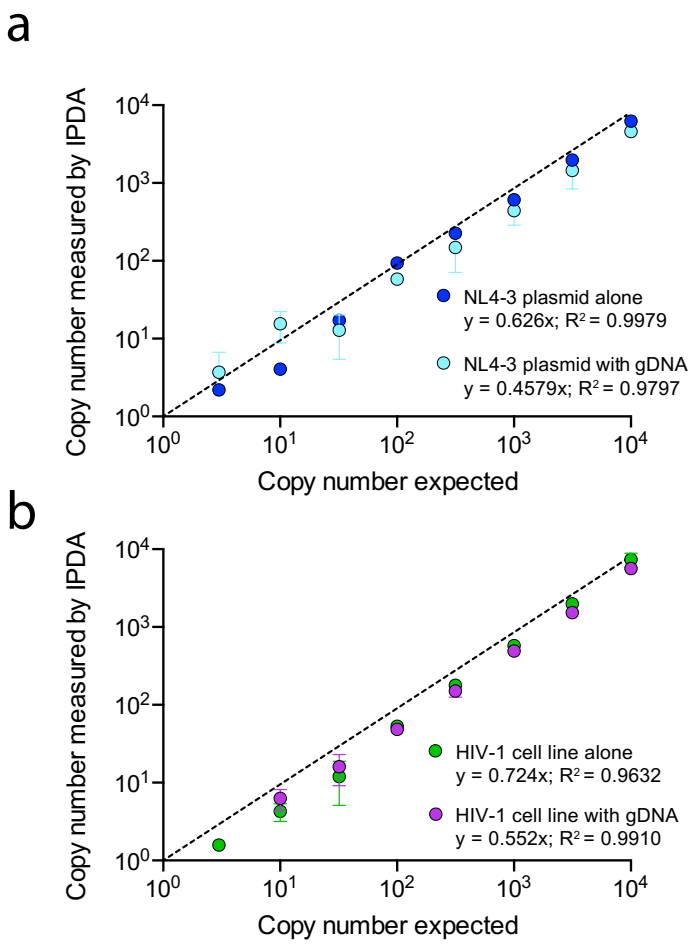

(**a**) Standard curve dilution series of NL4-3 plasmid, with (light blue) or without (dark blue) added gDNA from PBMCs or (**b**) an HIV-1 cell line (5b5) with (purple) or without (green) added gDNA. The HIV-1 cell line, 5b5, was created by infecting Jurkat cells with a single-round GFP virus and sorting for GFP^+ cells. The cell line was further characterized to verify it contained the correct HIV-1 sequence and only one HIV-1 provirus per cell. Each dilution for each condition was performed in triplicate. The average and standard deviation for each dilution are plotted. All experiments were performed on the BioRad QX100 droplet digital PCR platform.

Figure 3.9 Preliminary HIV-1 infected individual IPDA readouts correlate with full genome sequencing results.

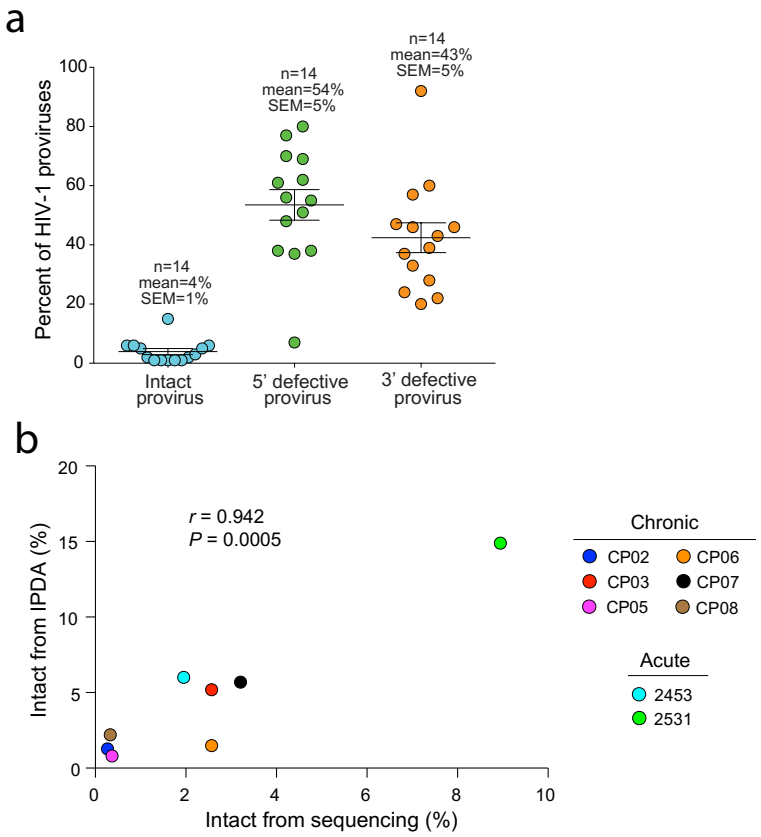

(**a**) Preliminary IPDA quantification of intact and defective proviruses from 14 HIV-1^{+} donors on ART. The percentage for each population of provirus was determined by dividing the number of droplets positive for that population by the total number of droplets positive for at least one fluorophore. Double positive droplets were defined as intact. Droplets positive for only the *env* amplicon were defined as 5' defective proviruses and droplets positive for only the packaging signal amplicon were defined as 3' defective proviruses. (**b**) Pearson correlation of IPDA results with previously obtained full-genome sequencing results from 8 HIV-1 infected individuals (Bruner et al., 2016). Six individuals initiated treatment during the chronic phase of infection and two during the acute phase of infection.

Figure 3.10 IPDA detects primarily intact proviruses whereas single region PCRs detect predominately defective proviruses in chronically treated HIV-1 infected individuals.

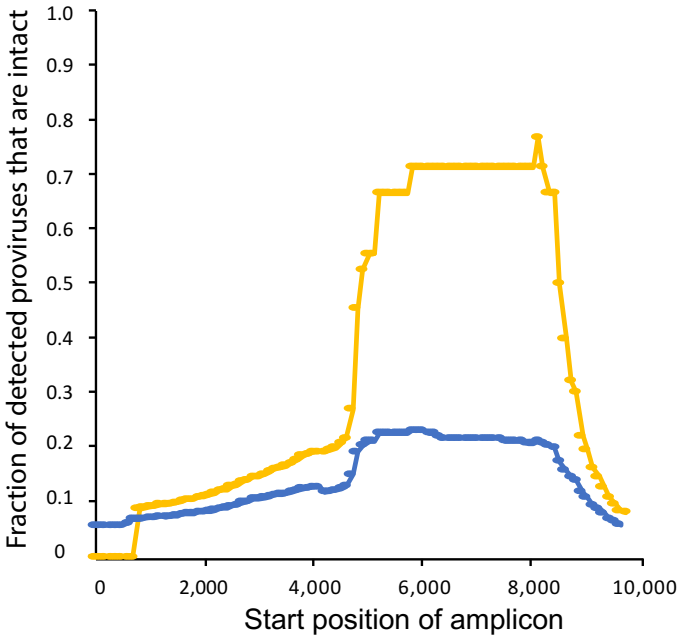

Sliding window analysis of a theoretical single region PCR at different locations in the HIV-1 genome (blue trace). The start site of the theoretical amplicons are shown in HXB2 coordinates (x axis) and the proportion of proviruses detected by each amplicon that are actually intact is shown (y axis). Sliding window analysis of a theoretical two region PCR assay with the first amplicon being the packaging signal (yellow trace). Only proviruses that are positive in both amplicons are detected as intact. Hypermutated sequences were considered not to be detected by the two region assay due to the incorporation of hypermutation discriminating probes as described in **Fig. 3.2** and **Table 3.1**. Analysis for both traces was performed on individuals from previously published cohorts initiating treatment during the chronic phase of infection (Bruner et al., 2016; Imamichi et al., 2016).

References

Archin, N.M., Liberty, A.L., Kashuba, A.D., Choudhary, S.K., Kuruc, J.D., Crooks, A.M., Parker, D.C., Anderson, E.M., Kearney, M.F., Strain, M.C., et al. (2012a). Administration of vorinostat disrupts HIV-1 latency in patients on antiretroviral therapy. Nature *487*, 482–485.

Archin, N.M., and Margolis, D.M. (2014). Emerging strategies to deplete the HIV reservoir. Curr. Opin. Infect. Dis. *27*, 29–35.

Archin, N.M., Vaidya, N.K., Kuruc, J.D., Liberty, A.L., Wiegand, A., Kearney, M.F., Cohen, M.S., Coffin, J.M., Bosch, R.J., Gay, C.L., et al. (2012b). Immediate antiviral therapy appears to restrict resting CD4+ cell HIV-1 infection without accelerating the decay of latent infection. Proc. Natl. Acad. Sci. U.S.a. *109*, 9523–9528.

Archin, N.M., Bateson, R., Tripathy, M.K., Crooks, A.M., Yang, K.-H., Dahl, N.P., Kearney, M.F., Anderson, E.M., Coffin, J.M., Strain, M.C., et al. (2014). HIV-1 Expression Within Resting CD4+ T Cells After Multiple Doses of Vorinostat. J Infect Dis jiu155.

Arnedo-Valero, M., Garcia, F., Gil, C., Guila, T., Fumero, E., Castro, P., Blanco, J.L., Miró, J.M., Pumarola, T., and Gatell, J.M. (2005). Risk of selecting de novo drug-resistance mutations during structured treatment interruptions in patients with chronic HIV infection. Clin. Infect. Dis. *41*, 883–890.

Besson, G.J., McMahon, D., Maldarelli, F., and Mellors, J.W. (2012). Short-course raltegravir intensification does not increase 2 long terminal repeat episomal HIV-1 DNA

in patients on effective antiretroviral therapy. Clin. Infect. Dis. *54*, 451–453.

Bosque, A., Famiglietti, M., Weyrich, A.S., Goulston, C., and Planelles, V. (2011). Homeostatic proliferation fails to efficiently reactivate HIV-1 latently infected central memory CD4+ T cells. PLoS Pathog *7*, e1002288.

Brady, T., Kelly, B.J., Male, F., Roth, S., Bailey, A., Malani, N., Gijsbers, R., O'Doherty, U., and Bushman, F.D. (2013). Quantitation of HIV DNA integration: effects of differential integration site distributions on Alu-PCR assays. J. Virol. Methods *189*, 53–57.

Bruner, K.M., Murray, A.J., Pollack, R.A., Soliman, M.G., Laskey, S.B., Capoferri, A.A., Lai, J., Strain, M.C., Lada, S.M., Hoh, R., et al. (2016). Defective proviruses rapidly accumulate during acute HIV-1 infection. Nat. Med. *22*, 1043–1049.

Bullen, C.K., Laird, G.M., Durand, C.M., Siliciano, J.D., and Siliciano, R.F. (2014). New ex vivo approaches distinguish effective and ineffective single agents for reversing HIV-1 latency in vivo. Nat. Med. *20*, 425–429.

Butler, S.L., Bushman, F.D., and Hansen, M.S. (2001). A quantitative assay for HIV DNA integration in vivo. Nat. Med. 1–4.

Buzón, M.J., Massanella, M., Llibre, J.M., Esteve, A., Dahl, V., Puertas, M.C., Gatell, J.M., Domingo, P., Paredes, R., Sharkey, M., et al. (2010). HIV-1 replication and immune dynamics are affected by raltegravir intensification of HAART-suppressed subjects. Nat. Med. *16*, 460–465.

Chun, T.W., Carruth, L., Finzi, D., Shen, X., DiGiuseppe, J.A., Taylor, H., Hermankova, M., Chadwick, K., Margolick, J., Quinn, T.C., et al. (1997a). Quantification of latent tissue reservoirs and total body viral load in HIV-1 infection. Nature *387*, 183–188.

Chun, T.W., Stuyver, L., Mizell, S.B., Ehler, L.A., Mican, J.A., Baseler, M., Lloyd, A.L., Nowak, M.A., and Fauci, A.S. (1997b). Presence of an inducible HIV-1 latent reservoir during highly active antiretroviral therapy. Proc. Natl. Acad. Sci. U.S.a. *94*, 13193–13197.

Chun, T.W., Murray, D., Justement, J.S., Hallahan, C.W., Moir, S., Kovacs, C., and Fauci, A.S. (2011). Relationship between residual plasma viremia and the size of HIV proviral DNA reservoirs in infected individuals receiving effective antiretroviral therapy. J Infect Dis *204*, 135–138.

Chun, T.W., Nickle, D.C., Justement, J.S., Meyers, J.H., Roby, G., Hallahan, C.W., Kottilil, S., Moir, S., Mican, J.M., Mullins, J.I., et al. (2008). Persistence of HIV in Gut-Associated Lymphoid Tissue despite Long-Term Antiretroviral Therapy. J Infect Dis *197*, 714–720.

Cillo, A.R., Sobolewski, M.D., Bosch, R.J., Fyne, E., Piatak, M., Coffin, J.M., and Mellors, J.W. (2014a). Quantification of HIV-1 latency reversal in resting CD4+ T cells from patients on suppressive antiretroviral therapy. Proc. Natl. Acad. Sci. U.S.a. *111*, 7078–7083.

Cillo, A.R., Sobolewski, M.D., Bosch, R.J., Fyne, E., Piatak, M., Coffin, J.M., and Mellors, J.W. (2014b). Quantification of HIV-1 latency reversal in resting CD4+ T cells

from patients on suppressive antiretroviral therapy. Proc. Natl. Acad. Sci. U.S.a. 201402873.

Cohn, L.B., Silva, I.T., Oliveira, T.Y., Rosales, R.A., Parrish, E.H., Learn, G.H., Hahn, B.H., Czartoski, J.L., McElrath, M.J., Lehmann, C., et al. (2015). HIV-1 integration landscape during latent and active infection. Cell *160*, 420–432.

Crooks, A.M., Bateson, R., Cope, A.B., Dahl, N.P., Griggs, M.K., Kuruc, J.D., Gay, C.L., Eron, J.J., Margolis, D.M., Bosch, R.J., et al. (2015). Precise Quantitation of the Latent HIV-1 Reservoir: Implications for Eradication Strategies. J Infect Dis *212*, 1361–1365.

Dahl, V., Peterson, J., Spudich, S., Lee, E., Shacklett, B.L., Price, R.W., and Palmer, S. (2013). Single-copy assay quantification of HIV-1 RNA in paired cerebrospinal fluid and plasma samples from elite controllers. Aids *27*, 1145–1149.

Deeks, S.G. (2012). HIV: Shock and kill. Nature *487*, 439–440.

Delviks-Frankenberry, K., Galli, A., Nikolaitchik, O., Mens, H., Pathak, V.K., and Hu, W.-S. (2011). Mechanisms and factors that influence high frequency retroviral recombination. Viruses *3*, 1650–1680.

Deng, K., Pertea, M., Rongvaux, A., Wang, L., Durand, C.M., Ghiaur, G., Lai, J., McHugh, H.L., Hao, H., Zhang, H., et al. (2015). Broad CTL response is required to clear latent HIV-1 due to dominance of escape mutations. Nature *517*, 381–385.

Durand, C.M., Ghiaur, G., Siliciano, J.D., Rabi, S.A., Eisele, E.E., Salgado, M., Shan, L., Lai, J.F., Zhang, H., Margolick, J., et al. (2012). HIV-1 DNA is detected in bone marrow

populations containing CD4+ T cells but is not found in purified CD34+ hematopoietic progenitor cells in most patients on antiretroviral therapy. J Infect Dis *205*, 1014–1018.

Eriksson, S., Graf, E.H., Siliciano, R., Dahl, V., Siliciano, J., Strain, M.C., Yukl, S.A., Lysenko, E.S., Bosch, R.J., Lai, J., et al. (2013). Comparative analysis of measures of viral reservoirs in HIV-1 eradication studies. PLoS Pathog *9*, e1003174.

Finzi, D., Blankson, J., Siliciano, J.D., Margolick, J.B., Chadwick, K., Pierson, T., Smith, K., Lisziewicz, J., Lori, F., Flexner, C., et al. (1999). Latent infection of CD4+ T cells provides a mechanism for lifelong persistence of HIV-1, even in patients on effective combination therapy. Nat. Med. *5*, 512–517.

Finzi, D., Hermankova, M., Pierson, T., Carruth, L.M., Buck, C., Chaisson, R.E., Quinn, T.C., Chadwick, K., Margolick, J., Brookmeyer, R., et al. (1997). Identification of a reservoir for HIV-1 in patients on highly active antiretroviral therapy. Science *278*, 1295–1300.

Gandhi, R.T., Coombs, R.W., Chan, E.S., Bosch, R.J., Zheng, L., Margolis, D.M., Read, S., Kallungal, B., Chang, M., Goecker, E.A., et al. (2012). No effect of raltegravir intensification on viral replication markers in the blood of HIV-1-infected patients receiving antiretroviral therapy. J. Acquir. Immune Defic. Syndr. *59*, 229–235.

Gulick, R.M., Mellors, J.W., Havlir, D., Eron, J.J., Gonzalez, C., McMahon, D., Richman, D.D., Valentine, F.T., Jonas, L., Meibohm, A., et al. (1997). Treatment with indinavir, zidovudine, and lamivudine in adults with human immunodeficiency virus infection and prior antiretroviral therapy. N. Engl. J. Med. *337*, 734–739.

Günthard, H.F., Aberg, J.A., Eron, J.J., Hoy, J.F., Telenti, A., Benson, C.A., Burger, D.M., Cahn, P., Gallant, J.E., Glesby, M.J., et al. (2014). Antiretroviral treatment of adult HIV infection: 2014 recommendations of the International Antiviral Society-USA Panel. Jama *312*, 410–425.

Hammer, S.M., Squires, K.E., Hughes, M.D., Grimes, J.M., Demeter, L.M., Currier, J.S., Eron, J.J., Feinberg, J.E., Balfour, H.H., Deyton, L.R., et al. (1997). A controlled trial of two nucleoside analogues plus indinavir in persons with human immunodeficiency virus infection and CD4 cell counts of 200 per cubic millimeter or less. AIDS Clinical Trials Group 320 Study Team. N. Engl. J. Med. *337*, 725–733.

Harper, M.S., Guo, K., Gibbert, K., Lee, E.J., Dillon, S.M., Barrett, B.S., McCarter, M.D., Hasenkrug, K.J., Dittmer, U., Wilson, C.C., et al. (2015). Interferon-α Subtypes in an Ex Vivo Model of Acute HIV-1 Infection: Expression, Potency and Effector Mechanisms. PLoS Pathog *11*, e1005254.

Hatano, H., Delwart, E.L., Norris, P.J., Lee, T.-H., Dunn-Williams, J., Hunt, P.W., Hoh, R., Stramer, S.L., Linnen, J.M., McCune, J.M., et al. (2009). Evidence for persistent low-level viremia in individuals who control human immunodeficiency virus in the absence of antiretroviral therapy. Journal of Virology *83*, 329–335.

Henrich, T.J., Gallien, S., Li, J.Z., Pereyra, F., and Kuritzkes, D.R. (2012). Low-level detection and quantitation of cellular HIV-1 DNA and 2-LTR circles using droplet digital PCR. J. Virol. Methods *186*, 68–72.

Henrich, T.J., Hanhauser, E., Marty, F.M., Sirignano, M.N., Keating, S., Lee, T.-H.,

Robles, Y.P., Davis, B.T., Li, J.Z., Heisey, A., et al. (2014). Antiretroviral-Free HIV-1 Remission and Viral Rebound After Allogeneic Stem Cell Transplantation: Report of 2 Cases. Ann. Intern. Med. *161*, 319–327.

Henrich, T.J., Hu, Z., Li, J.Z., Sciaranghella, G., Busch, M.P., Keating, S.M., Gallien, S., Lin, N.H., Giguel, F.F., Lavoie, L., et al. (2013). Long-term reduction in peripheral blood HIV type 1 reservoirs following reduced-intensity conditioning allogeneic stem cell transplantation. J Infect Dis *207*, 1694–1702.

Ho, Y.-C., Shan, L., Hosmane, N.N., Wang, J., Laskey, S.B., Rosenbloom, D.I.S., Lai, J., Blankson, J.N., Siliciano, J.D., and Siliciano, R.F. (2013a). Replication-competent noninduced proviruses in the latent reservoir increase barrier to HIV-1 cure. Cell *155*, 540–551.

Ho, Y.-C., Shan, L., Hosmane, N.N., Wang, J., Laskey, S.B., Rosenbloom, D.I.S., Lai, J., Blankson, J.N., Siliciano, J.D., and Siliciano, R.F. (2013b). Replication-competent noninduced proviruses in the latent reservoir increase barrier to HIV-1 cure. Cell *155*, 540–551.

Hütter, G., Nowak, D., Mossner, M., Ganepola, S., Müssig, A., Allers, K., Schneider, T., Hofmann, J., Kücherer, C., Blau, O., et al. (2009). Long-term control of HIV by CCR5 Delta32/Delta32 stem-cell transplantation. N. Engl. J. Med. *360*, 692–698.

Hwang, C.K., Svarovskaia, E.S., and Pathak, V.K. (2001). Dynamic copy choice: steady state between murine leukemia virus polymerase and polymerase-dependent RNase H activity determines frequency of in vivo template switching. Proc. Natl. Acad. Sci. U.S.a.

98, 12209–12214.

Imamichi, H., Dewar, R.L., Adelsberger, J.W., Rehm, C.A., O'Doherty, U., Paxinos, E.E., Fauci, A.S., and Lane, H.C. (2016). Defective HIV-1 proviruses produce novel protein-coding RNA species in HIV-infected patients on combination antiretroviral therapy. Proc. Natl. Acad. Sci. U.S.a. 201609057.

International AIDS Society Scientific Working Group on HIV Cure, Deeks, S.G., Autran, B., Berkhout, B., Benkirane, M., Cairns, S., Chomont, N., Chun, T.W., Churchill, M., Di Mascio, M., et al. (2012). Towards an HIV cure: a global scientific strategy. Nat. Rev. Immunol. *12*, 607–614.

Jain, V., Hartogensis, W., Bacchetti, P., Hunt, P.W., Hatano, H., Sinclair, E., Epling, L., Lee, T.-H., Busch, M.P., McCune, J.M., et al. (2013). Antiretroviral therapy initiated within 6 months of HIV infection is associated with lower T-cell activation and smaller HIV reservoir size. J Infect Dis *208*, 1202–1211.

Jetzt, A.E., Yu, H., Klarmann, G.J., Ron, Y., Preston, B.D., and Dougherty, J.P. (2000). High rate of recombination throughout the human immunodeficiency virus type 1 genome. Journal of Virology *74*, 1234–1240.

Jones, M., Williams, J., Gärtner, K., Phillips, R., Hurst, J., and Frater, J. (2014). Low copy target detection by Droplet Digital PCR through application of a novel open access bioinformatic pipeline, 'definetherain'. J. Virol. Methods *202*, 46–53.

Josefsson, L., Stockenstrom, von, S., Faria, N.R., Sinclair, E., Bacchetti, P., Killian, M., Epling, L., Tan, A., Ho, T., Lemey, P., et al. (2013). The HIV-1 reservoir in eight patients

on long-term suppressive antiretroviral therapy is stable with few genetic changes over time. Proc. Natl. Acad. Sci. U.S.a. *110*, E4987–E4996.

Katlama, C., Deeks, S.G., Autran, B., Martinez-Picado, J., van Lunzen, J., Rouzioux, C., Miller, M., Vella, S., Schmitz, J.E., Ahlers, J., et al. (2013). Barriers to a cure for HIV: new ways to target and eradicate HIV-1 reservoirs. Lancet *381*, 2109–2117.

Kearney, M.F., Wiegand, A., Shao, W., Coffin, J.M., Mellors, J.W., Lederman, M., Gandhi, R.T., Keele, B.F., and Li, J.Z. (2015). Origin of Rebound Plasma HIV Includes Cells with Identical Proviruses That Are Transcriptionally Active before Stopping of Antiretroviral Therapy. Journal of Virology *90*, 1369–1376.

Kieffer, T.L., Kwon, P., Nettles, R.E., Han, Y., Ray, S.C., and Siliciano, R.F. (2005). G->A Hypermutation in Protease and Reverse Transcriptase Regions of Human Immunodeficiency Virus Type 1 Residing in Resting CD4+ T Cells In Vivo. Journal of Virology *79*, 1975–1980.

Kim, M., and Siliciano, R.F. (2016). Reservoir expansion by T-cell proliferation may be another barrier to curing HIV infection. Proc. Natl. Acad. Sci. U.S.a. *113*, 1692–1694.

Kim, M., Hosmane, N.N., Bullen, C.K., Capoferri, A., Yang, H.-C., Siliciano, J.D., and Siliciano, R.F. (2014). A primary CD4(+) T cell model of HIV-1 latency established after activation through the T cell receptor and subsequent return to quiescence. Nat Protoc *9*, 2755–2770.

Laird, G.M., Eisele, E.E., Rabi, S.A., Lai, J., Chioma, S., Blankson, J.N., Siliciano, J.D., and Siliciano, R.F. (2013). Rapid Quantification of the Latent Reservoir for HIV-1 Using

a Viral Outgrowth Assay. PLoS Pathog *9*, e1003398.

Liszewski, M.K., Yu, J.J., and O'Doherty, U. (2009). Detecting HIV-1 integration by repetitive-sampling Alu-gag PCR. Methods *47*, 254–260.

Lorenzo-Redondo, R., Fryer, H.R., Bedford, T., Kim, E.-Y., Archer, J., Kosakovsky Pond, S.L., Chung, Y.-S., Penugonda, S., Chipman, J.G., Fletcher, C.V., et al. (2016). Persistent HIV-1 replication maintains the tissue reservoir during therapy. Nature *530*, 51–56.

Luebbert, J., Tweya, H., Phiri, S., Chaweza, T., Mwafilaso, J., Hosseinipour, M.C., Ramroth, H., Schnitzler, P., and Neuhann, F. (2012). Virological failure and drug resistance in patients on antiretroviral therapy after treatment interruption in Lilongwe, Malawi. Clin. Infect. Dis. *55*, 441–448.

Maldarelli, F., Wu, X., Su, L., Simonetti, F.R., Shao, W., Hill, S., Spindler, J., Ferris, A.L., Mellors, J.W., Kearney, M.F., et al. (2014). HIV latency. Specific HIV integration sites are linked to clonal expansion and persistence of infected cells. Science *345*, 179–183.

Margolis, D.M. (2014). How Might We Cure HIV? Curr Infect Dis Rep *16*, 392–395.

Markowitz, M., Evering, T.H., Garmon, D., Caskey, M., La Mar, M., Rodriguez, K., Sahi, V., Palmer, S., Prada, N., and Mohri, H. (2014). A Randomized Open-Label Study of Three- versus Five-Drug Combination Antiretroviral Therapy in Newly HIV-1 Infected Individuals. J. Acquir. Immune Defic. Syndr.

Massanella, M., Gianella, S., Lada, S.M., Richman, D.D., and Strain, M. (2015). Quantification of Total and 2-LTR (Long terminal repeat) HIV DNA, HIV RNA and Herpesvirus DNA in PBMCs. Bio-Protocol *5*, e1492.

McBride, K., Xu, Y., Bailey, M., Seddiki, N., Suzuki, K., Murray, J.M., Gao, Y., Yan, C., Cooper, D.A., Kelleher, A.D., et al. (2013). The majority of HIV type 1 DNA in circulating CD4+ T lymphocytes is present in non-gut-homing resting memory CD4+ T cells. AIDS Res. Hum. Retroviruses *29*, 1330–1339.

Mexas, A.M., Graf, E.H., Pace, M.J., Yu, J.J., Papasavvas, E., Azzoni, L., Busch, M.P., Di Mascio, M., Foulkes, A.S., Migueles, S.A., et al. (2012). Concurrent measures of total and integrated HIV DNA monitor reservoirs and ongoing replication in eradication trials. Aids *26*, 2295–2306.

O'Doherty, U., Swiggard, W.J., Jeyakumar, D., McGain, D., and Malim, M.H. (2002). A Sensitive, Quantitative Assay for Human Immunodeficiency Virus Type 1 Integration. Journal of Virology *76*, 10942–10950.

Pace, M., and Frater, J. (2014). A cure for HIV: is it in sight? Expert Rev Anti Infect Ther.

Palmer, S. (2013). Advances in detection and monitoring of plasma viremia in HIV-infected individuals receiving antiretroviral therapy. Curr Opin HIV AIDS *8*, 87–92.

Palmer, S., Wiegand, A.P., Maldarelli, F., Bazmi, H., Mican, J.M., Polis, M., Dewar, R.L., Planta, A., Liu, S., Metcalf, J.A., et al. (2003). New real-time reverse transcriptase-initiated PCR assay with single-copy sensitivity for human immunodeficiency virus type

1 RNA in plasma. J. Clin. Microbiol. *41*, 4531–4536.

Perelson, A.S., Essunger, P., Cao, Y., Vesanen, M., Hurley, A., Saksela, K., Markowitz, M., and Ho, D.D. (1997). Decay characteristics of HIV-1-infected compartments during combination therapy. Nature *387*, 188–191.

Pierson, T.C., Zhou, Y., Kieffer, T.L., Ruff, C.T., Buck, C., and Siliciano, R.F. (2002). Molecular characterization of preintegration latency in human immunodeficiency virus type 1 infection. Journal of Virology *76*, 8518–8531.

Pillai, S.K., Abdel-Mohsen, M., Guatelli, J., Skasko, M., Monto, A., Fujimoto, K., Yukl, S., Greene, W.C., Kovari, H., Rauch, A., et al. (2012). Role of retroviral restriction factors in the interferon-α-mediated suppression of HIV-1 in vivo. Proc. Natl. Acad. Sci. U.S.a. *109*, 3035–3040.

Puertas, M.C., Massanella, M., Llibre, J.M., Ballestero, M., Buzón, M.J., Ouchi, D., Esteve, A., Boix, J., Manzardo, C., Miró, J.M., et al. (2014). Intensification of a raltegravir-based regimen with maraviroc in early HIV-1 infection. Aids *28*, 325–334.

Rasmussen, T.A., Tolstrup, M., Brinkmann, C.R., Olesen, R., Erikstrup, C., Solomon, A., Winckelmann, A., Palmer, S., Dinarello, C., Buzon, M., et al. (2014a). Panobinostat, a histone deacetylase inhibitor, for latent- virus reactivation in HIV-infected patients on suppressive antiretroviral therapy: a phase 1/2, single group, clinical trial. The Lancet HIV 1–9.

Rasmussen, T.A., Tolstrup, M., Brinkmann, C.R., Olesen, R., Erikstrup, C., Solomon, A., Winckelmann, A., Palmer, S., Dinarello, C., Buzon, M., et al. (2014b). Panobinostat, a

histone deacetylase inhibitor, for latent-virus reactivation in HIV-infected patients on suppressive antiretroviral therapy: a phase 1/2, single group, clinical trial. The Lancet HIV *1*, e13–e21.

Rose, P.P., and Korber, B.T. (2000). Detecting hypermutations in viral sequences with an emphasis on G --> A hypermutation. Bioinformatics *16*, 400–401.

Rosenbloom, D.I.S., Elliott, O., Hill, A.L., Henrich, T.J., Siliciano, J.M., and Siliciano, R.F. (2015). Designing and Interpreting Limiting Dilution Assays: General Principles and Applications to the Latent Reservoir for Human Immunodeficiency Virus-1. Open Forum Infect Dis *2*, ofv123.

Routy, J.P., Boulassel, M.R., Nicolette, C.A., and Jacobson, J.M. (2012). Assessing risk of a short-term antiretroviral therapy discontinuation as a read-out of viral control in immune-based therapy. J. Med. Virol. *84*, 885–889.

Rouzioux, C., Mélard, A., and Avéttand-Fénoël, V. (2013). Quantification of Total HIV1-DNA in Peripheral Blood Mononuclear Cells. In Human Retroviruses, E. Vicenzi, and G. Poli, eds. (Totowa, NJ: Humana Press), pp. 261–270.

Ruelas, D.S., and Greene, W.C. (2013). An integrated overview of HIV-1 latency. Cell *155*, 519–529.

Sahu, G.K., Sarria, J.C., and Cloyd, M.W. (2010). Recovery of replication-competent residual HIV-1 from plasma of a patient receiving prolonged, suppressive highly active antiretroviral therapy. Journal of Virology *84*, 8348–8352.

Sanchez, G., Xu, X., Chermann, J.C., and Hirsch, I. (1997). Accumulation of defective viral genomes in peripheral blood mononuclear cells of human immunodeficiency virus type 1-infected individuals. Journal of Virology *71*, 2233–2240.

Schröder, A.R.W., Shinn, P., Chen, H., Berry, C., Ecker, J.R., and Bushman, F. (2002). HIV-1 integration in the human genome favors active genes and local hotspots. Cell *110*, 521–529.

Shirakawa, K., Chavez, L., Hakre, S., Calvanese, V., and Verdin, E. (2013). Reactivation of latent HIV by histone deacetylase inhibitors. Trends Microbiol. *21*, 277–285.

Siliciano, J.D., and Siliciano, R.F. (2005). Enhanced culture assay for detection and quantitation of latently infected, resting CD4+ T-cells carrying replication-competent virus in HIV-1-infected individuals. Methods Mol. Biol. *304*, 3–15.

Siliciano, J.D., Kajdas, J., Finzi, D., Quinn, T.C., Chadwick, K., Margolick, J.B., Kovacs, C., Gange, S.J., and Siliciano, R.F. (2003). Long-term follow-up studies confirm the stability of the latent reservoir for HIV-1 in resting CD4+ T cells. Nat. Med. *9*, 727–728.

Siliciano, R.F., and Greene, W.C. (2011). HIV latency. Cold Spring Harb Perspect Med *1*, a007096–a007096.

Silverberg, M.J., Neuhaus, J., Bower, M., Gey, D., Hatzakis, A., Henry, K., Hidalgo, J., Lourtau, L., Neaton, J.D., Tambussi, G., et al. (2007). Risk of cancers during interrupted antiretroviral therapy in the SMART study. Aids *21*, 1957–1963.

Simon-Loriere, E., and Holmes, E.C. (2011). Why do RNA viruses recombine? Nat. Rev.

Microbiol. *9*, 617–626.

Simonetti, F.R., Sobolewski, M.D., Fyne, E., Shao, W., Spindler, J., Hattori, J., Anderson, E.M., Watters, S.A., Hill, S., Wu, X., et al. (2016). Clonally expanded CD4+ T cells can produce infectious HIV-1 in vivo. Proc. Natl. Acad. Sci. U.S.a. *113*, 1883–1888.

Stacey, A.R., Norris, P.J., Qin, L., Haygreen, E.A., Taylor, E., Heitman, J., Lebedeva, M., DeCamp, A., Li, D., Grove, D., et al. (2009). Induction of a striking systemic cytokine cascade prior to peak viremia in acute human immunodeficiency virus type 1 infection, in contrast to more modest and delayed responses in acute hepatitis B and C virus infections. Journal of Virology *83*, 3719–3733.

Stopak, K., de Noronha, C., Yonemoto, W., and Greene, W.C. (2003). HIV-1 Vif blocks the antiviral activity of APOBEC3G by impairing both its translation and intracellular stability. Mol. Cell *12*, 591–601.

Strain, M.C., Lada, S.M., Luong, T., Rought, S.E., Gianella, S., Terry, V.H., Spina, C.A., Woelk, C.H., and Richman, D.D. (2013). Highly Precise Measurement of HIV DNA by Droplet Digital PCR. PLoS ONE *8*, e55943.

Strategies for Management of Antiretroviral Therapy (SMART) Study Group, El-Sadr, W.M., Lundgren, J.D., Neaton, J.D., Gordin, F., Abrams, D., Arduino, R.C., Babiker, A., Burman, W., Clumeck, N., et al. (2006). CD4+ count-guided interruption of antiretroviral treatment. N. Engl. J. Med. *355*, 2283–2296.

Søgaard, O.S., Graversen, M.E., Leth, S., Olesen, R., Brinkmann, C.R., Nissen, S.K.,

Kjaer, A.S., Schleimann, M.H., Denton, P.W., Hey-Cunningham, W.J., et al. (2015). The Depsipeptide Romidepsin Reverses HIV-1 Latency In Vivo. PLoS Pathog *11*, e1005142.

Tebas, P., Stein, D., Tang, W.W., Frank, I., Wang, S.Q., Lee, G., Spratt, S.K., Surosky, R.T., Giedlin, M.A., Nichol, G., et al. (2014). Gene editing of CCR5 in autologous CD4 T cells of persons infected with HIV. N. Engl. J. Med. *370*, 901–910.

Vandegraaff, N., Kumar, R., Burrell, C.J., and Li, P. (2001). Kinetics of human immunodeficiency virus type 1 (HIV) DNA integration in acutely infected cells as determined using a novel assay for detection of integrated HIV DNA. Journal of Virology *75*, 11253–11260.

Wagner, T.A., McLaughlin, S., Garg, K., Cheung, C.Y.K., Larsen, B.B., Styrchak, S., Huang, H.C., Edlefsen, P.T., Mullins, J.I., and Frenkel, L.M. (2014). HIV latency. Proliferation of cells with HIV integrated into cancer genes contributes to persistent infection. Science *345*, 570–573.

Wei, D.G., Chiang, V., Fyne, E., Balakrishnan, M., Barnes, T., Graupe, M., Hesselgesser, J., Irrinki, A., Murry, J.P., Stepan, G., et al. (2014). Histone deacetylase inhibitor romidepsin induces HIV expression in CD4 T cells from patients on suppressive antiretroviral therapy at concentrations achieved by clinical dosing. PLoS Pathog *10*, e1004071.

Wong, J.K., Hezareh, M., Günthard, H.F., Havlir, D.V., Ignacio, C.C., Spina, C.A., and Richman, D.D. (1997a). Recovery of replication-competent HIV despite prolonged suppression of plasma viremia. Science *278*, 1291–1295.

Wong, J.K., Hezareh, M., Günthard, H.F., Havlir, D.V., Ignacio, C.C., Spina, C.A., and Richman, D.D. (1997b). Recovery of replication-competent HIV despite prolonged suppression of plasma viremia. Science *278*, 1291–1295.

Xing, S., and Siliciano, R.F. (2013). Targeting HIV latency: pharmacologic strategies toward eradication. Drug Discov. Today *18*, 541–551.

Yarchoan, R., and Broder, S. (1987). Development of antiretroviral therapy for the acquired immunodeficiency syndrome and related disorders. A progress report. N. Engl. J. Med. *316*, 557–564.

Ylisastigui, L., Archin, N.M., Lehrman, G., Bosch, R.J., and Margolis, D.M. (2004). Coaxing HIV-1 from resting CD4 T cells: histone deacetylase inhibition allows latent viral expression. Aids *18*, 1101–1108.

Yu, H., Jetzt, A.E., Ron, Y., Preston, B.D., and Dougherty, J.P. (1998). The nature of human immunodeficiency virus type 1 strand transfers. J. Biol. Chem. *273*, 28384–28391.

Yu, Q., König, R., Pillai, S., Chiles, K., Kearney, M., Palmer, S., Richman, D., Coffin, J.M., and Landau, N.R. (2004). Single-strand specificity of APOBEC3G accounts for minus-strand deamination of the HIV genome. Nat Struct Mol Biol *11*, 435–442.

Yukl, S.A., Boritz, E., Busch, M., Bentsen, C., Chun, T.W., Douek, D., Eisele, E., Haase, A., Ho, Y.-C., Hütter, G., et al. (2013). Challenges in detecting HIV persistence during potentially curative interventions: a study of the Berlin patient. PLoS Pathog *9*, e1003347.

Yukl, S.A., Gianella, S., Sinclair, E., Epling, L., Li, Q., Duan, L., Choi, A.L.M., Girling, V., Ho, T., Li, P., et al. (2010). Differences in HIV burden and immune activation within the gut of HIV-positive patients receiving suppressive antiretroviral therapy. J Infect Dis *202*, 1553–1561.

Zhu, W., Jiao, Y., Lei, R., Hua, W., Wang, R., Ji, Y., Liu, Z., Wei, F., Zhang, T., Shi, X., et al. (2011). Rapid turnover of 2-LTR HIV-1 DNA during early stage of highly active antiretroviral therapy. PLoS ONE *6*, e21081.

Curriculum Vitae

8519 Heathrow Ct. Apt. F
Nottingham MD, 21236

KATHERINE M. BRUNER

(214) 986-0098
kbiersc1@jhmi.edu

EDUCATION

Johns Hopkins University School of Medicine — **Baltimore, MD** — **Aug. 2012 – Mar. 2017**
Ph.D. in Cellular and Molecular Medicine
Mentor: Dr. Robert Siliciano

The University of Texas at Dallas — **Dallas, TX** — **Aug. 2009 – May 2012**
Bachelor of Science in Biochemistry, GPA: 3.98, Graduated Summa Cum Laude with Major Honors, Dean's List.
Received four-year full undergraduate scholarship for all tuition and fees and a housing stipend.

RESEARCH EXPERIENCE

Laboratory of Dr. Robert Siliciano, Johns Hopkins University School of Medicine, Howard Hughes Medical Institute — **Ph.D. Thesis July 2013 – Present**
Characterized viral genomes in the HIV-1 latent reservoir in patients treated at different stages of infection using full genome sequencing methods to improve our understanding of how to assess HIV cure strategies. This work, published in *Nature Medicine*, also highlighted the inadequacies of current HIV-1 assays.

Developed a scalable, rapid multiplex digital droplet PCR (ddPCR) assay for accurately measuring replication competent virus in the latent HIV-1 reservoir for potential use in future HIV-1 clinical trials. This work resulted in a patent application (PCT/US2016/28822) and was licensed to a biotechnology startup.

Laboratory of Dr. Bruce Gnade, The University of Texas at Dallas — **June 2009 – Jan. 2012**
Collaborated with University of Texas Southwestern Medical Center urologist, Dr. Jeffrey Cadeddu, to develop a method for magnetically removing kidney stone fragments following stone fragmentation.
Awarded undergraduate research scholarship for this research in Nov. 2009 and Nov. 2011.

Green Fellow, The University of Texas Southwestern Medical Center — **Jan. 2012 – May 2012**
Awarded Green Fellowship to conduct joint research at the University of Texas Southwestern Medical Center.
Screened peptides, selected using phage display screening, in the laboratory of Dr. Kathlynn Brown to determine binding to cells containing mutations associated with non-small cell lung cancer.
Awarded first place for this research in the University of Texas at Dallas undergraduate poster competition.

NSF Texas A&M University Research Experiences for Undergraduates (REU) — **May 2011 – Aug. 2011**
Synthesized molecules that mimic protein-protein interactions for pharmaceutical and medicinal chemistry applications in the laboratory of Dr. Kevin Burgess, Rachal Professor of Chemistry.

AWARDS AND HONORS

Michael A. Shanoff Young Investigator Award, Johns Hopkins University School of Medicine	**2017**
Young Investigator Scholarship, CROI	**2016**
Keystone Symposia Travel Scholarship	**2015**
Pollard Scholar, Cellular Molecular Medicine Graduate Program	**2014**
Green Fellowship, The University of Texas Southwestern Medical Center	**2012**
First prize, The University of Texas Undergraduate Research Poster Competition	**2012**
The University of Texas at Dallas Academic Distinction Scholarship	**2009-2012**
The University of Texas at Dallas Undergraduate Research Scholarship	**2009-2010, 2011-2012**
American Chemical Society Undergraduate Award in Analytical Chemistry	**2011**
The University of Texas at Dallas STARRS Scholarship	**2009-2010**
Dean's List, The University of Texas at Dallas	**2009-2012**
Texas State President, Phi Theta Kappa College Honor Society	**2008-2009**

PUBLICATIONS

Bruner KM, Murray AJ, Pollack RA, Soliman MG, et al. Defective proviruses rapidly accumulate during acute HIV-1 infection. ***Nat Med.*** 2016 Sep;22(9):1043-9.

Bruner KM, Hosmane NN, Siliciano RF. Towards an HIV-1 cure: measuring the latent reservoir. ***Trends Microbiol.*** 2015 Apr;23(4):192-203.

Bruner KM, Murray AJ, Ho Y-C, Laird GM, Siliciano JD, Siliciano RF. A novel droplet digital PCR based assay for quantifying genetically intact HIV-1 proviruses. In preparation.

Laskey SB, Pohlmeyer CW, **Bruner KM**, Siliciano RF. Evaluating Clonal Expansion of HIV-Infected Cells: Optimization of PCR Strategies to Predict Clonality. ***PLoS Pathog.*** 2016 Aug 5;12(8):e1005689.

Hansen EC, Ransom M, Hesselberth JR , Hosmane NN , Capoferri AC , **Bruner KM**, et al. Diverse fates of uracilated HIV-1 DNA during infection of myeloid lineage cells***, eLife*** 2016 Sep 20;5. pii: e18447.

Hosmane NN, Kwon KJ, **Bruner KM**, Capoferri AA, et al. Proliferation of cells carrying replication-competent HIV-1 is a major factor in viral persistence and latent reservoir dynamics, ***JEM***, Accepted.

Pollack RA, Jones RB, Pertea M, **Bruner KM**, Martin AM et al. Cytotoxic T lymphocytes shape the landscape of HIV-1 proviruses. ***Cell Host Microbe***, Accepted.

Conference and Poster Presentations

Oral presentation, **Bruner KM**, Murray AJ, Pollack RA, Soliman MG, et al. *Rapid accumulation of defective proviruses complicates HIV-1 reservoir measurements*, Conference on Retroviruses and Opportunistic Infections (CROI). Boston, MA. Feb. 2016.
Received a young investigator scholarship to present this research at the conference.

Oral and poster presentation, **Bruner KM**, Pollack RA, Soliman MG, Murray AJ et al. *Analysis of HIV-1 genomes in the latent reservoir indicates rapid accumulation of defective proviruses.* Keystone Symposium on Mechanisms of HIV Persistence: Implications for a Cure, Boston, MA. Apr. 2015.
Received Keystone symposium travel scholarship to present this research at the conference.

Poster presentation, **Bruner KM** and Brown KC*. Biopanning of Phage Displayed Peptide Libraries for Cell-Specific Delivery to Lung Cancer Cells.* The University of Texas at Dallas Undergraduate Research Symposium, Dallas, TX. May 2012.
Received first place in undergraduate research poster competition.

Poster presentation, **Bruner KM**, Raghuraman A, Ko E, Burgess K. *Pyrrolinone-Pyrrolidine Oligomers as Universal Peptidomimetics.* Council on Undergraduate Research's Conference of Research Experiences for Undergraduate Student Scholarship. Arlington, VA. Oct. 2011.
Was selected to represent the Texas A&M REU program at this national conference. Presented poster to National Science Foundation Program Directors and met with Members of Congress and congressional staff.

Teaching, Mentoring, and Leadership

OPTIONS career advisory committee, Johns Hopkins School of Medicine **Nov. 2016 – Present**
Invited to serve on the advisory committee for a new career development program in partnership with the Cellular and Molecular Medicine graduate program and the Professional Development and Career Office.
Assist in selection of program leadership and provide input on career programming.

Graduate teaching assistant, Johns Hopkins School of Public Health **Oct. 2015 – Dec. 2015**
Teaching assistant to Dr. Dianne Griffin for Fundamental Virology course.
Designed test questions, administered and graded exams, led review sessions and held office hours.

Graduate student mentor, Johns Hopkins School of Medicine **June 2014 – Dec 2014**
Served as the primary mentor for doctoral and MD/PhD students during laboratory rotations.

Pollard Scholar, Cellular and Molecular Medicine Program **Jan. 2014 – Mar. 2014**
Selected as an upperclassman to lead weekly study sessions for students in their first year of doctoral studies.
Prepared study materials, practice exams and held review sessions for first year doctoral students.

Undergraduate teaching assistant, The University of Texas at Dallas **Aug. 2011 – Dec. 2011**
Served as a teaching assistant for a junior level biochemistry class.
Taught a weekly question and answer session for 60-80 students to reinforce concepts presented in lecture, met with students in weekly small group help sessions, proctored exams and graded assignments.

Texas State President, Phi Theta Kappa College Honor Society **May 2008 – May 2009**
Planned state-wide honors and leadership conventions for 300-500 attendees. Led team of five vice presidents to organize state-wide events and hurricane reconstruction efforts. Spoke at various college honor society induction ceremonies throughout the state.